AFIT/GEE/ENP/95D-06

MODEL OF CHLOROCARBON (CFC-12) CHEMISORPTION ON SOLID ROCKET MOTOR ALUMINA EXHAUST PARTICLES

THESIS

Gary E. Lund, Captain, USAF

AFIT/GEE/ENP/95D-06

AFIT/GEE/ENP/95D-06

MODEL OF CHLOROCARBON (CFC-12) CHEMISORPTION ON SOLID ROCKET MOTOR ALUMINA EXHAUST PARTICLES

Gary E. Lund, Captain, USAF

Approved:

Dr. Larry W. Burggraf	5 Dec 95 Date
Dr. Thomas R. Hauser	12/5/95 Date
Major Glen Perram	5 Dec 95 Date
Dr David Weeks	5 DEC 95 Date

The views expressed in this thesis are those of the author and do not reflect the official policy or position of the Department of Defense or the U.S. Government.

AFIT/GEE/ENP/95D-06

MODEL OF CHLOROCARBON (CFC-12) CHEMISORPTION ON SOLID ROCKET MOTOR ALUMINA EXHAUST PARTICLES

THESIS

Presented to the Faculty of the Graduate School of Engineering

of the Air Force Institute of Technology

Air University

In Partial Fulfillment of the

Requirements for the Degree of

Master of Science in Environmental Engineering Management

Gary E. Lund, B.S.

Captain, USAF

December 1995

Acknowledgments

I am indebted to my thesis advisor, Dr. Larry W. Burggraf for his insight and guidance during this research effort.

I would like to thank my wife and my children (Leah, Tanner, Ashley and Holley) who provided support, understanding and "occasional" interruptions during the time consuming thesis process. There were countless times when it must have seemed this effort was more important than our family. Nonetheless, they stuck with me and provided encouragement to keep at it until we can again go out to dinner, "play Batmans" and watch Saturday morning cartoons again.

Gary E. Lund

Table of Contents

List of Figures

List of Tables

Abstract

Solid Rocket Motors (SRMs) that power Titan IV rockets and Space Shuttles, exhaust large quantities of potentially ozone damaging pollutants directly into the stratosphere while in powered flight. Although SRMs discharge potentially ozone-destructive pollutants directly into the stratosphere, SRM environmental impacts have not been clearly addressed by the world community. There are no specific laws, regulations or international agreements on reduction or elimination of SRMs from use. Nonetheless, the Air Force is concerned that space launch programs may face curtailment due political and public concern over depletion of stratospheric ozone by SRM exhaust.

Studies on potential stratospheric impact of the exhaust products from aluminum/ammonium perchlorate based SRMs have focused primarily on the effect of gaseous HCl from SRMs on stratospheric ozone. After much research, the gas phase chemistry in the exhaust of a SRM has been fairly well characterized and deemed to have an insignificant impact on global ozone depletion. Until recently, the impact of heterogeneous chemistry on stratospheric ozone was believed to be relatively insignificant. However, the existence of an atmospheric heterogeneous process involving the decomposition of halocarbon source gases on alumina surfaces has recently been observed. This result provided evidence that halocarbon compounds such as CFC-12 (CF_2Cl_2) may undergo dissociative chemisorption on alumina surfaces and release reactive halogen species known to destroy ozone.

PM3, a semi-empirical quantum mechanical computational chemistry method was used to model potentially reactive sites on the surface of alumina particles. Additionally, adjacent sites were modeled to determine if the sites could be regenerated and continuously react with CFC-12 in such a manner as to catalytically release ozone depleting reactive chlorine into the stratosphere.

The findings on our limited models suggest that CFC-12 does molecularly chemisorb on reactive sites on the alumina particle surface and does not desorb at stratospheric temperatures. Dissociative chemisorption and the release of reactive chlorine was not observed, thus catalytic activity by this mechanism is not possible. Consequently, the alumina particles from SRM exhaust streams in the stratosphere do not exacerbate ozone destruction, but may rather decrease it by adsorbing and removing halocarbons as the alumina particles fall out of the stratosphere.

I. Introduction

Overview

In the early 1970's the debate about supersonic transport aircraft flying in the stratosphere established the possibility that anthropogenic air pollution, man made gasses emitted into the atmosphere, might lead to a decline in stratospheric ozone.[1] This was a profound realization. For the first time in mans existence we have learned that our actions could be destroying the stratospheric ozone layer that protects life on earth from harmful solar ultraviolet (UV) radiation.

This chapter will first introduce ozone and ozone chemistry. Next it will identify some practical and academic problems concerning the interactions of solid rocket motors and ozone, that are of interest to the Air Force. Finally, the chapter will outline the research approach and the rest of the thesis effort.

Ozone

Ozone, O_3, a gas, is the most important trace constituent of the stratosphere. Although it is present in only a few parts per million, it is responsible for shielding the earth from UV radiation that is harmful to life.[1]

Ozone production is initiated when molecular oxygen, O_2, absorbs solar ultraviolet energy (light) and breaks into oxygen atoms, O.[2]

$$O_2 + h\nu \rightarrow O + O$$

(Note: $h\nu = hc/\lambda$ where ν is frequency, h is Plank's constant and λ is wavelength and c is the speed of light. This represents the energy of light for a given wavelength, or a photon.)

These oxygen atoms then react with molecular oxygen to form ozone.

$$O + O_2 \rightarrow O_3$$

Ozone can then be broken back up into oxygen atoms and molecules by absorbing certain wavelengths of ultraviolet sunlight. In this, ozone shields the earth from these harmful wavelengths of UV light.

$$O_3 + h\nu \rightarrow O_2 + O$$

During the day, ozone and oxygen atoms coexist in a continual cycle of production and destruction. This production and destruction of ozone is greatest where the sunlight is strongest - near the equator and high in the stratosphere. Lower in the stratosphere and especially near the poles, sunlight is less intense because it passes through more air. Thus not much ozone is produced or destroyed by sunlight in these regions

Ozone Destruction

In addition to the destruction of protective ozone by UV light, we have learned that stratospheric ozone is destroyed by pollutants containing halogen, hydrogen and nitrogen.[3,1] Chlorofluorocarbons (CFCs) are halogen containing species that have been identified as the single largest anthropogenic contributor to stratospheric ozone destruction.[3,1] The halogens are fluorine (F), chlorine (Cl), bromine (Br), and iodine (I).

The troposphere is the lowest layer of the atmosphere. Any process that transports pollutants from the troposphere into the stratosphere and then transforms the pollutants into chemicals that are known to react with ozone, will be a stratospheric ozone destructive process. The mechanisms by which these chemicals attack ozone and enable the pollutants with abundances of parts per billion (ppbv=10^{-9}) in air to destroy significant ozone with abundances of per million (ppmv=10^{-6}) of air[1] will be discussed in more detail in the next chapter.

Problem Statement

Practical Problem

Solid Rocket Motors (SRMs) that power Titan IV rockets and Space Shuttles exhaust quantities of potentially ozone damaging pollutants directly into the stratosphere, while in powered flight. These exhausted pollutants come from the combustion of the SRM. The propellant for solid rocket motors currently used in the United States is a mixture commonly known as ammonium perchlorate, or AP. The three main ingredients of AP are: solid particulate oxidizer (ammonium perchlorate), solid particulate fuel (aluminum powder), and a cured elastomer (such as hydroxy-terminated polybutadiene), that binds the mix together.[4]

Typically, the SRMs of concern are the Titan IV and the Space Shuttle boosters, since they are by far the largest SRMs and they fly directly through the stratosphere. They inject 68 tons and 19 tons of ozone destroying chlorine (in the form of HCl) into the stratosphere per launch, respectively.[5] At an estimated annual launch rate of two Space Shuttles and six Titan IV, their annual percentage contribution of chlorine to the

stratosphere is estimated to be only 0.25%.[5] In 1990, the annual industrial (anthropogenic) halocarbon contribution to the stratosphere in Cl was estimated to be 300,000 tons.[6]

Although rocket exhaust emissions are extremely small compared to other anthropogenic sources, many authorities believe that every reasonable effort should be made to reduce undesirable environmental effects in future rocket propulsion systems.[7] However, until future systems can be developed with more environmentally acceptable propellants, the current system will be criticized and remain environmentally suspect. Many scientist believe that the issue of SRMs destroying the ozone layer is largely a political one.[7] Until regulators and lawmakers can be convinced by the data that SRM emissions have comparatively little impact, this will remain a political problem.[7] It has often been the case that political and public concern over the environment, even if it is not scientifically founded, can have a large impact (e.g. People were moved and homes were bulldozed in the vicinity of Love Canal, Niagara, NY even though the scientific assessment concluded that such a level of action was not necessary.[8]) Political and public pressure are a great concern for the Air Force (AF) and National Aviation and Space Administration (NASA). Both the AF and NASA have supported numerous scientific analysis and environmental studies concerning the effect of SRMs on the environment. In fact, due to governmental and public concern on this issue, the AF and NASA formed a Launch Vehicles Working Group to deal directly with the effects of SRMs on the environment. In September 1994, the Launch Vehicles Working Group held a technical interchange meeting (TIM) focusing on the impact of launch vehicles on ozone layer depletion. The

prime objective of the meeting was to establish cooperative investigations/evaluation between the AF, NASA, industry, and academia.[9]

Although SRMs discharge potentially ozone destructive pollutants directly into the stratosphere, SRMs have not been clearly addressed by the world community. There are no specific laws, regulations or international agreements on reduction or elimination of SRMs from use. Even the landmark decisions of the Montreal Protocol to eliminate the use of many man made substances that may threaten stratospheric ozone, do not address SRMs. Nonetheless, Air Force leadership is concerned that space launch programs may face curtailment due political and public concern over depletion of stratospheric ozone by SRM exhaust.[10]

Additionally, as the amount of ozone depletion attributed to substances being phased out under the Montreal Protocol declines, the global percentage of ozone depletion caused by SRMs will increase. This projected increase in the global percentage of ozone depletion due to SRMs is a concern for the AF.[10] This projected increase in percentage has lead to significant public and political pressure to develop clean propellants. Clean propellants will be discussed in next chapter.

In sum, SRMs are known to inject ozone depleting chemicals directly into the stratosphere. Although this has been determined to be small compared to other sources, there is concern by the AF and NASA that space launch programs could face curtailment.

Academic Problem

Studies on potential stratospheric impact of the exhaust products from aluminum/ammonium perchlorate based SRMs associated with Titan IV and Space Shuttle vehicles have focused primarily on the effect of gaseous HCl from SRMs on stratospheric ozone[5,6,11,12,13,14,15,16]. After much research, the gas phase chemistry in the exhaust of a SRM has been fairly well characterized and deemed not to have a significant impact on global ozone depletion.[9] As previously mentioned, the total annual addition to stratospheric chlorine from rocket launches is on the order of 0.25 percent of the global annual stratospheric chlorine source from halocarbons in the present-day atmosphere. Additionally, chlorine loading calculations predict steady-state ozone decreases to be less that 0.1% globally. This seems to be relatively insignificant. However, these computations do not include heterogeneous chemistry effects of the alumina particles. See Figure 1.

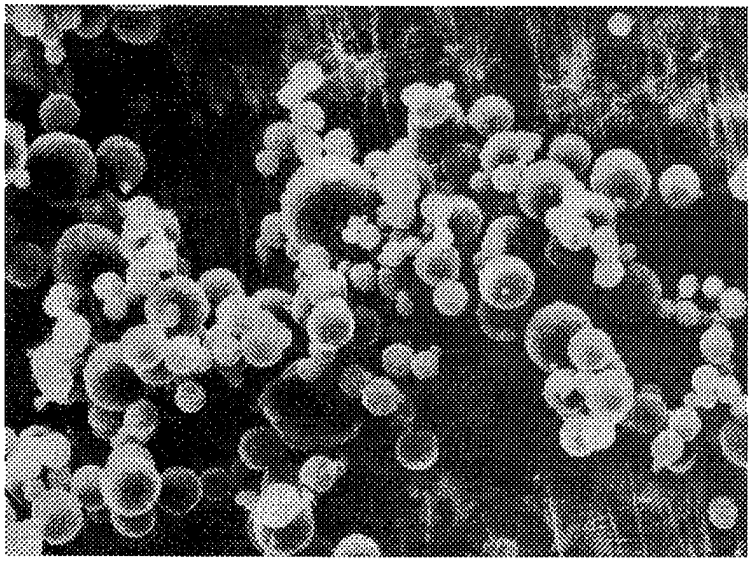

Figure 1: Alumina Particles (1-10 μm diameters) collected after Shuttle launch[17]

Until recently, the impact of heterogeneous chemistry on stratospheric ozone was also believed to be relatively insignificant.[15,14] None of these studies considered the reactivity of the alumina, Al_2O_3, surface itself.[18] This may be partly due to the limited understanding of alumina surface. Although there is a widespread interest in catalytic alumina, there is still only a limited understanding about the real nature of the surface of aluminas.[19]

Recently, in an attempt to better understand the alumina surface and its catalytic properties, much research has been done. In research by Ballinger and Yates[20], Ballinger et al.[21], and Hegde et al.[22], they found that halogenated alkanes decompose on alumina surfaces at elevated temperatures. This opened the door to understand how halogenated compounds could potentially be broken up on the alumina surfaces, releasing the halogen constituents. Taking this into consideration, Aerodyne Research began a research project funded by the United States Air Force, Space and Missile Systems Center (SMC) to investigate whether SRM exhaust alumina particles could promote the decomposition of halocarbons in the stratosphere, releasing the halogen constituents. Aerodyne found the existence of a previously unsuspected atmospheric heterogeneous process involving the decomposition of halocarbon source gases (such as CFCs) on alumina surfaces.[18] This result provided evidence that halocarbon compounds such as CFC-12 (CF_2Cl_2) undergo dissociative chemisorption on alumina surfaces and release the more reactive halogen containing species know to destroy ozone. The results were obtained under ultra high

vacuum conditions, with a reaction probability of about 10^{-5} to 10^{-4} on somewhat defective α-alumina (sapphire) surfaces at stratospheric temperatures. Aerodyne's report stated,[18]

> Calculations show that, to first order, the decomposition rates of halocarbon source gases will be markedly enhanced in the wake of an SRM exhaust plume immediately after launch. This process might release enough reactive halogen species to lead to significant ozone depletion within the wake region. Over the longer term, the magnitude of the effect depends on launch rates and on assumptions made about the chemical properties of rocket exhaust particles. *A key unresolved point is whether Al_2O_3 particle reactive surface sites can be regenerated and thus continuously react with halocarbons.* (Emphasis added)

In light of this research, the AF's and NASA's Launch Vehicles Working Group recommended that the global impact calculations should be updated to account for heterogeneous chemistry effects.[9] The most important aspect of the heterogeneous chemistry to be investigated is whether or not reactive sites on alumina surfaces could be catalytic to ozone destruction. However, if a catalytic heterogeneous chemistry effect were found, then researchers would have grossly underestimated the ozone depleting potential of alumina particles. Coupled with the fact that the stratospheric concentration of alumina particles from SRM exhaust has risen dramatically in recent years[23] it could be argued that SRMs are doing significant damage to the ozone layer. In fact, the confirmation of a catalytic cycle or a large increase in the deposition rate of alumina exhaust particles could lead to a possible environmental constraint to the Air Force's use of aluminum-loaded solid propellant launch phase rockets and strap-on boosters. The inclusion of SRMs in the Montreal Protocol or similar reduction pacts, might require the

accelerated development of clean solid fuel propulsion systems, probably involving schemes that eliminate hydrogen chloride and solid particulates from the exhaust stream.

In order for alumina surfaces to be catalytic to ozone destruction, four steps are necessary. The first step is the chemisorption of halocarbons on reactive sites on the alumina surface. The second step is the decomposition of the halocarbons on the surface. The third step is the desorption of the decomposition products, thus freeing up the bonding sites on the surface to react again. The fourth step is the desorbed halogen reacting with and destroying ozone.

The purpose of our research is to assess alumina surfaces and to determine if halocarbon compounds can catalytically decompose on these surfaces and release reactive halogen species.

Approach

We will use semi-empirical quantum mechanical computational chemistry methods to calculate potentially reactive sites with the aim of describing the chemisorption and surface reactivity process. In order to accomplish this, we first will establish a basic premise that we will work towards. The premise is that we believe adjacent, rather than isolated, reactive moieties constitute the catalytically active sites on the alumina surface.[24] For instance, in order for CFC-12 to react with an alumina particle, there have to be some sites on the alumina surface that are reactive to the CFC-12. Additionally, we believe that it will take more than one reactive site to react with CFC-12 and free up chlorine, which

could go on to destroy ozone. Finally, there must be a process whereby those sites are again made reactive if the process is to be catalytic.

The modeling effort will involve work in two areas:

1. Calculations of alumina oxide cluster structures and reaction mechanisms for halocarbons. Aluminum oxide clusters having structures corresponding to those which have been implicated in catalytic reactions will be calculated. We will examine correlation's between cluster structure and the reactivity of the Lewis acid/base or Brϕnstead acid/base sites. Furthermore, the effect on surface reactivity of the proximity of the acid and base sites to one another will be studied.

2. Description of reactions which may promote release of halogen species from the alumina surface and the implication of adjacent electron donor and electron acceptor sites in the type of catalytic reactions of interest.

The objectives of the modeling effort are to create a framework for understanding and predicting reactivity of molecular aluminates to larger structures. We will model aluminum oxide clusters (small groups of aluminum oxide molecules within an alumina particle) that are analogous to defective alumina surfaces.

To be effective, the modeling effort will have some specific constraints:

1. CFC-12 will be the only halocarbon studied.

2. Only chlorine and carbon bonding from CFC-12 to alumina will be studied. Potential fluorine bonds from CFC-12 to alumina will not be studied.

Features of aluminum chemistry will be made evident from semi-empirical calculations. Semi-empirical methods combine molecular quantum mechanical calculations with experimentally derived parameters to provide a relatively quick and fairly accurate representation of the chemistry being studied. The semi-empirical method that we will employ is the Parametric Model Number 3 (PM3).[25] We will use this method to flesh out the most likely chemical pathways that could lead to catalytic activity.

Outline

Chapter I has introduced the topic of ozone and ozone layer destruction as well as provided some background information. It also discussed some practical and academic problems dealing with the AF and NASA's current use of ammonium perchlorate SRMs. Finally, it suggested an approach to understanding whether or not alumina particles are catalytic to halocarbon destruction through semi-empirical quantum mechanical modeling. Chapter II will discuss in more detail the stratospheric ozone cycles, ozone destruction by chlorine, SRMs and potential replacements, and the current knowledge regarding O_3 destruction from SRMs. Chapter III will review theoretical computational chemistry methods and the approach in detail. Chapter VI will analyze the model output and results. Chapter V will review the conclusions and make recommendations.

II. Background

Overview

In order to understand and appreciate the approach taken in this research effort it is first necessary to understand important facts about chemical and physical environment surrounding the research. This chapter will review the stratosphere and chemical and physical processes that are important to ozone cycles. Also, several proposed solid propellants as well as the current propellant will be discussed in order to understand how solid propellants are involved in stratospheric ozone cycles. Finally, the subject of heterogeneous chemistry will be reviewed as it pertains to SRM alumina particles, catalysis and ozone destruction.

Stratospheric Ozone Cycles

The stratosphere extends from about 10 to 15 km above the surface of the Earth to about 50 km.[2] Between it and the surface of the Earth is the troposphere. The density of air falls off exponentially with height throughout the troposphere and stratosphere, a factor of 1/e each 7 km, thus 90% of the air is in the troposphere, and only 10% is in the stratosphere.[1] In the troposphere temperatures decrease with height, but in the stratosphere temperatures increase with height. This increase is caused by the absorption of ultraviolet sunlight by ozone in the stratosphere.[2]

Ozone is produced when molecular oxygen absorbs solar ultraviolet energy and breaks into oxygen atoms.[2] These oxygen atoms then react with molecular oxygen in a three body recombination process to form ozone, where M represents the third body.[2]

$$O_2 + h\nu \rightarrow 2O \qquad \lambda < 242 \text{ nm} \qquad (1)$$

$$O + O_2 + M \leftrightarrow O_3 + M \qquad (2)$$

Ozone itself is broken back into oxygen atoms and molecules by sunlight that is less energetic than the ultraviolet sunlight that breaks up molecular oxygen. This photochemical destruction is known as the Oxygen Cycle:[26]

$$O_3 + h\nu \rightarrow O + O_2 \qquad 240 \text{ nm} < \lambda < 320 \text{ nm} \qquad (3)$$

$$O_3 + O \rightarrow 2O_2 \qquad (4)$$

Ozone is continually being generated and destroyed in the stratosphere, and its concentration at any given time is dependent on the solar flux, the temperature, and the relative concentrations of dozens of different chemical species. The only important source of ozone in the stratosphere according to current theories is the photolysis of molecular oxygen as seen in equations (1) and (2).[27,2]

The production and destruction of ozone by ultraviolet light is greatest where the sunlight is strongest - near the equator and high in the stratosphere. Lower in the stratosphere, especially near the poles, sunlight is less intense because it passes through more air. In these regions, not much ozone is produced or destroyed by sunlight.

Nevertheless substantial ozone exists in the lower stratosphere near the poles. Air from the ozone-producing regions in the tropical stratosphere is forced by the dynamics of the atmosphere to flow downward toward the lower stratosphere near the polar regions.[1] This flow of ozone is as critical in establishing the amount of ozone in a given location.

The other factor that determines the amount of ozone in a given location is the chemical loss, in addition to the losses already mentioned in equations (3) and (4). The destruction of ozone by sunlight results in an oxygen atom that, in the absence of any other chemical to react with simply and exclusively reforms ozone giving off heat.[1] However, a small but significant set of ozone depleting gases are transported from the troposphere into the stratosphere, or directly injected into the stratosphere. Some of these gases are carried by warm tropical air rising into the stratosphere. Others are injected by volcanoes or by anthropogenic activities such as high flying aircraft, rockets and space shuttles or nuclear explosion.

Presently, most of the gases that cause chemical loss of stratospheric ozone enter the stratosphere through the tropics. They survive in the troposphere long enough to enter the stratosphere because: 1) They are not very soluble in water and thus not absorbed into clouds or rained out 2) They are only weakly attacked by the UV sunlight that manages to pass through the ozone layer, and 3) They are very stable and react either slowly or not at all with other gases in the troposphere. Once in the stratosphere they can be decomposed by stronger UV light, or are attacked by reactive gases created by that light. In these forms, they react with a number of other gases, including ozone and atomic oxygen. The primary gases that enter the stratosphere and affect ozone are water vapor, methane (CH_4), nitrous oxide (NO), and halogen-containing carbon compounds. All of these, except water have significant anthropogenic components, and all except water have increasing global abundances.[1]

The chlorine, hydrogen and nitrogen cycles shown below are examples of chemical loss.[26]

Photochemical Destruction

Oxygen Cycle

$O_3 + h\nu \rightarrow O + O_2$ (3)

$O_3 + O \rightarrow 2O_2$ (4)

Chlorine Cycle

$Cl + O_3 \rightarrow ClO + O_2$ (5)

$ClO + O \rightarrow Cl + O_2$ (6)

Hydrogen Cycle

$H + O_3 \rightarrow OH + O_2$ (7)

$OH + O \rightarrow H + O_2$ (8)

$OH + O_3 \rightarrow HO_2 + O_2$ (9)

$HO_2 + O \rightarrow OH + O_2$ (10)

Nitrogen Cycle

$NO + O_3 \rightarrow NO_2 + O_2$ (11)

$NO_2 + O \rightarrow NO + O_2$ (12)

$NO_2 + h\nu \rightarrow NO + O$ (13)

Alternate Cl Cycle[28]

$Cl + O_3 \rightarrow ClO + O_2$ (5)

$Cl + O_3 \rightarrow ClO + O_2$ (5)

$ClO + ClO + M \rightarrow Cl_2O_2$ (5a)

$Cl_2O_2 + h\nu \rightarrow Cl + ClO_2$ (5b)

$ClO_2 + M \rightarrow Cl + O_2 + M$ (5c)

Net: $O_3 + O_3 \rightarrow O_2 + O_2 + O_2$ (5d)

Note that chlorine, hydrogen, and nitrogen are all catalytic and regenerate ozone destroying species, thus many ozone molecules may be destroyed by a single molecule or reactive atomic radical (see eq. (5)-(5d)). Note that these cycles are interrelated (for example, eq. (14)-(17)) so changes in the relative concentrations of species in one cycle may affect those in another cycle.[29]

$$OH + O_3 \rightarrow HO_2 + O_2 \qquad (14)$$

$$ClO + HO_2 \rightarrow HOCl + O_2 \qquad (15)$$

$$HOCl + h\nu \rightarrow OH + Cl \qquad (16)$$

$$Cl + O_3 \rightarrow ClO + O_2 \qquad (17)$$

Reactive nitrogen compounds are derived from the decomposition of nitrous oxide, and reactive hydrogen compounds are derived from the decomposition of methane and water vapor. The reactive nitrogen catalytic cycle is the primary ozone destroying cycle throughout the stratosphere, not because the reactions are faster than for the other cycles (they are slower), but because the abundances of the reactive nitrogen gases are many times greater than the abundances of either reactive chlorine, or reactive hydrogen.[1] However, at present, nitrous oxide, which is partially natural in origin, is increasing at a much slower rate than CFCs.[3]

Chlorine Destruction of Ozone

The chlorine cycle (eq. (5,a-d)-(6)), represents the halogen of greatest importance in ozone destruction. As mentioned in Chapter I the annual industrial halocarbon

contribution to the stratosphere in Cl was estimated to be 300,000 tons in 1990.[6] Chlorine is by far the most abundant halogen species in the stratosphere. The vast majority of this chlorine is from CFCs. "The CFCs (-11, -12, and -113) and carbon tetrachloride (CCl_4) compose 70 percent of the anthropogenic organochlorine loading of the troposphere (CFC-12, 28 percent; CFC-11, 23 percent; CCl_4, 13 percent; CFC-113, 6 percent)."[30] They are inert in the troposphere but photodissociate in the stratosphere and hence are a major source of stratospheric reactive chlorine.[30] The CFCs are used as refrigerants, foam blowing agents and solvents.[30,1] CCl_4 is used in the production of CFCs.[30] The chemical structure of the most abundant CFCs in the stratosphere are as follows[31]:

CFC-11: $CFCl_3$

CFC-12: CF_2Cl_2

CFC-113: $CFCl_2CF_2Cl$

Chlorine atoms are produced when CFCs absorb ultraviolet sunlight or undergo chemical reaction followed by more sunlight. These chlorine atoms are unreactive with the major components of air, but react with ozone to from chlorine monoxide (ClO). If chlorine monoxide were stable, chlorine could have little effect on the stratospheric ozone abundance. Chlorine monoxide is not stable. Some of the oxygen atoms react with chlorine monoxide to form chlorine atoms and molecular oxygen. Thus both the oxygen atoms and the ozone produced from the initial breakdown of molecular oxygen by ultraviolet sunlight are reformed into molecular oxygen by the catalytic action of reactive chlorine chemicals. Each chlorine atom that enters the stratosphere will go through this

catalytic cycle 100,000 times before it is returned to the troposphere.[1] In this way small amounts of chlorine can destroy much greater amounts of ozone.

The following six steps show how, a typical chlorofluorocarbon, CFC-12, is involved in the ozone destruction process:

Step 1: Rapid mixing in the troposphere. CFC-12 is unreactive and not affected

Step 2: CFC-12 diffuses into the stratosphere (CFC-12 atmospheric lifetime ~ 110 yrs.[2])

Step 3: Ultraviolet sunlight breaks a C-Cl bond an releases Cl

Step 4: Catalytic destruction of ozone $Cl + O_3 \rightarrow ClO + O_2$

$$ClO + O \rightarrow Cl + O_2$$

Step 5: Chlorine exchange with less reactive forms: $Cl + H \leftrightarrow HCl$

$$ClO + NO_2 \leftrightarrow ClONO_2$$

Step 6: Diffusion of HCl back into the troposphere

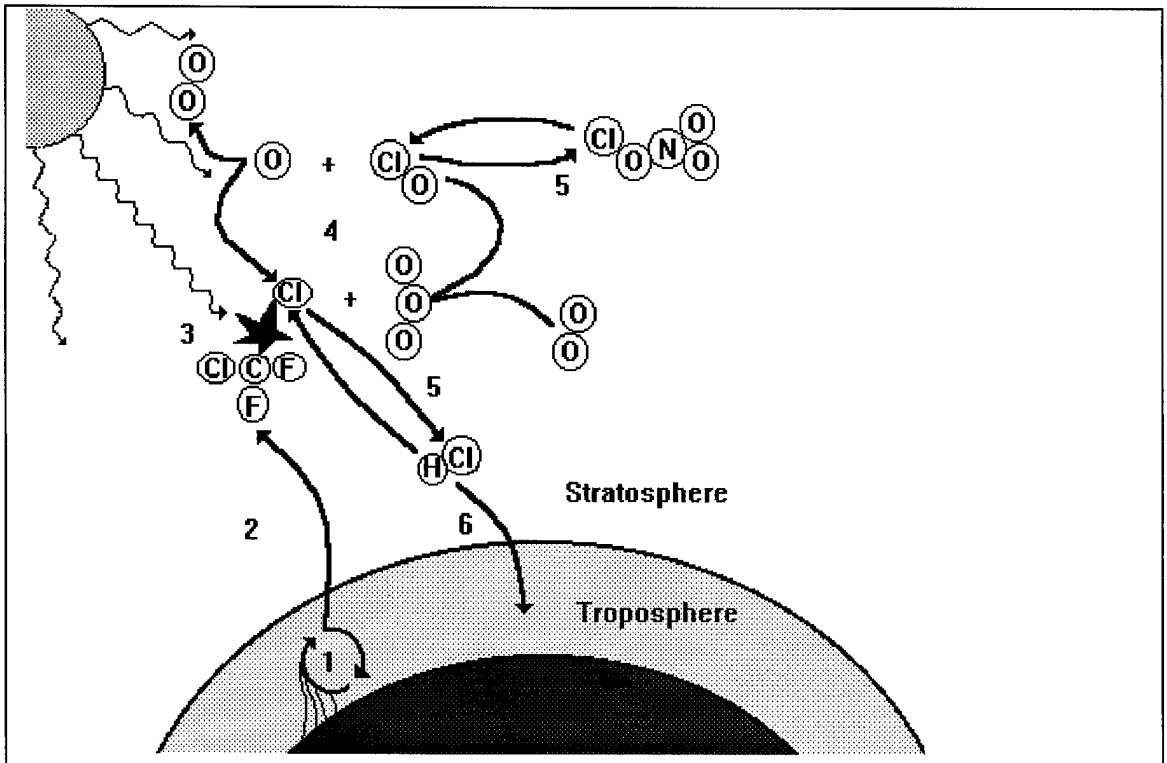

Figure 2: A schematic for how chlorine from CFCs cycle through the atmosphere. Steps 1 through 6 indicate the rapid mixing in the troposphere, diffusion into the stratosphere, chlorine release from CFCs by ultraviolet sunlight, catalytic destruction of ozone, chlorine exchange with less-reactive forms, and diffusion of HCl back into the troposphere.[1]

The entire circuit in figure 2 takes a few decades. Brune, from The Pennsylvania State University, Department of Meteorology, stated that,[1]

> However, since only one-tenth of the CFCs are in the stratosphere and exposed to ultraviolet sunlight at any given time (since only 10% of the air is in the stratosphere), the average time for chlorine in CFCs to complete this circuit is about a century. The chlorine in a CFC molecule released into the troposphere today will very likely still be in the atmosphere a century from now.

Chlorine also undergoes other reactions in the stratosphere, especially with the activated products of nitrous oxide and methane. These reactions tend to convert chlorine

into chemicals that are much less reactive with atomic oxygen and ozone than with chlorine atoms and chlorine monoxide. In the lower stratosphere, more than 98% of the chlorine is in these 'reservoir' forms, primarily HCl and $ClONO_2$.[1] Higher in the stratosphere, above 35 km, ~ 40% of chlorine is in the reactive forms, like ClO.

At present, stratospheric chlorine, from CFCs, are expected to increase 50% no matter what actions are taken to curb the production and use of CFCs.[1] The first step towards elimination of CFCs was made in 1989 with the ratification of the Montreal Protocol by more than thirty nations. Only considering gas phase chemistry, it is estimated that with the Montreal Protocol in effect, the maximum loss in global ozone will be ~ 3%.[1] However, a 'no controls' scenario where CFC and halon release rates, based on a 2.8% increase in CFCs and halons up to the year 2050 would lead to a 30% decrease in global total column ozone by 2050 and that would have unimaginable effects on the behavior of the stratosphere and on the life on the surface below it.[1] Even with the Montreal Protocol the total abundance of chlorine in the stratosphere is likely to almost triple between 1985 to 2050,[31] and that is enough to convince many that CFC and halon production must be curbed rapidly and globally.

Propellants

The impact that environmental regulations can have on a product and its manufacturing process is becoming increasingly important. For example, President Bush's announcement to phase out CFC production by 1995, and the AF's decision to eliminate the purchase of chlorinated solvents at all Air Force owned or operated facilities by July 1992, illustrate the far reaching influence that environmental issues can have.[26]

A report issued by the American Institute of Aeronautics and Astronautics (AIAA) in October 1991 concluded that the use of rockets with the current production propellants has a very minor impact on the environment.[13] However, in spite of the technical evidence of a very minor environmental impact, if substances emitted during the manufacture or use of rockets are regulated, restricted or banned, alternate process or new fuel formulations may be required. Hawkins and Wilkerson have asserted that HCl as an emission product appears technically to have very little environmental impact, but has been attacked in the press as a harmful to the environment,[32] and may be subjected to stringent emission regulations in the future.[7]

From what is currently known, there are no rocket propellants, liquid oxygen/liquid hydrogen systems included, which are completely benign to the environment.[26] The testing and launching of rockets represents only a part of their impact. A more complete assessment would include the entire 'cradle-to-grave' impact. Hawkins and Wilkerson have discussed the environmental issues involved in the production, use, and disposal for rocket propellants. They state that 'only a cradle-to-grave, system-wide view of environmental regulatory compliance will allow future propulsion systems to be cost effective and viable.[7] They conclude that although the rocket industry contributes only one-tenth of one percent of hazardous waste in the U.S., it is not exempt from either environmental regulations or public scrutiny.[7]

In order to make a rational decision about which rocket fuel to use for a propulsion system, a detailed cost/benefit analysis must be performed. Changing from a conventional fuel to an alternate on the basis of environmental impact does not mean

simply pouring the new propellant into a rocket chamber in place of the old fuel. One must also consider the impact to system performance, hazards, reliability, cost, operability, material availability, and long term system stability, and decide whether or not the expected improved environmental impact is worth the price.[26]

The next three sections will discuss the current three best options for a more environmentally acceptable propellant for solid rocket motors. The options are neutralized, scavenged or reduced chlorine propellants.

Neutralized

In neutralized propellants, magnesium is used in the place of aluminum as the metal fuel. All other ingredients remain essentially the same. Approximately 70% of the formulation by weight is AP, 12-14% is polymeric binder, and 16-18% is magnesium.[26]

As the propellant burns, the magnesium is oxidized to from magnesium oxide (eq. (18)). Upon contact with water, the magnesium oxide forms magnesium hydroxide (eq. (19)). This is a very basic material and reacts readily with HCl to form magnesium chloride and water (eq. (20)).

$$Mg + O \rightarrow MgO \qquad (18)$$

$$MgO + H_2O \rightarrow Mg(HO)_2 \qquad (19)$$

$$Mg(OH)_2 + 2HCl \rightarrow MgCl_2 + H_2O \qquad (20)$$

In the lab and in small scale motors, neutralization does occur and water is an essential component of the mechanism. The water comes from the after burning of

molecular hydrogen, the major molar exhaust product, which is believed to be sufficient for complete neutralization. It is believed that the deposition of water-soluble magnesium chloride should not be a significant environmental concern, since both Mg^{2+} and Cl^- ions are very common in nature.[26] Unfortunately, in an unconfined open air test of a 2000 lb. motor, full neutralization did not occur. The exhaust cloud appeared to disperse more quickly than the neutralization reaction and thus approximately only half of the HCl was neutralized.[33]

The specific impulse (Isp), a measure of thrust/mass propellant, of the neutralized propellant is close to that of conventional aluminized propellants (281.8 vs 285.3), but the density is significantly lower (0.0591 vs 0.0641 lb/in^3).[26] Thus, the magnesium base propellant would not work for a retrofit into current systems due to the larger volume of propellant necessary, but might be a candidate for a new system that took into account these properties.

The cost would be about the same as conventional motors since the materials are essentially the same. An additional processing concern is that the magnesium stay as dry as possible. An extensive hazards characterization has been performed on this propellant under the Solid Propulsion Integration and Verification (SPIV) program, and has shown it to be Class 1.3 similar to the Space Shuttle and Peacekeeper Stage I propellants.[34] A Class 1.3 propellant has a low detonability.[33]

Scavenged

In scavenged propellants, sodium nitrate is used in place of about 1/2 of the ammonium perchlorate. As the propellant burns in the rocket chamber, the sodium ions

scavenge most of the chloride ions, forming NaCl, thus preventing the chloride ions from forming HCl.[26] Laboratory measurements and theoretical calculations indicate that HCl emissions are reduced by over an order of magnitude from conventional propellants.[35,36] To date an accurate quantification of the acid reducing capability of the scavenged propellants during an open air test has not yet been made.[33]

The sodium nitrate system has a lower specific impulse than the full AP system. Some of the Isp can be regained if an energetic nitramine, such as cyclotetramethylene tetramine (HMX), is used, but attaining Space Shuttle Isp with a sodium nitrate alone is not realistic.[26] HMX is a Class 1.1 and is more highly detonable. Nevertheless, because sodium nitrate has a greater density than AP, a scavenged propellant appears to be practical in smaller volumes like boosters/first stage applications.[26] The loss in specific impulse can be compensated by the fact that a greater mass of propellant can be used in the motor. Furthermore, it appears that essentially the same overall performance as the Space Shuttle can be achieved in a scavenged propellant by a combination of the addition of HMX and a higher solids loading. For example, a scavenged propellant formulated at 90% solids and 15% HMX has a total performance (Isp x density$^{0.6}$) of 54.94 compared with the Space Shuttle's 54.87.[26]

Processing techniques are expected to be about the same as conventional, with about the same waste generation. Material cost are slightly higher if HMX is used. Manufacturing cost could be slightly higher due to the larger number of a materials used. A complete hazards characterization has not been done yet, but initial tests show the hazards of the scavenged propellants to be about the same as a conventional Class 1.3

composite propellants.[26] Although HMX is a Class 1.1, it can be used in amounts up to 15% without making the mixture excessively detonable.[26] Of the proposed alternate solid propellants, the neutralized and scavenged propellants are the most mature.

Reduced Chlorine

Reduced Chlorine Propellants, contain little or no chlorine. Currently, these systems are receiving the most interest. The most simple method to produce reduced chlorine propellants is to replace the ammonium perchlorate oxidizer with a nonchlorine oxidizer.

For Class 1.3 composite propellants, ammonium nitrate (AN) has been extensively studied. More recently, the more energetic hydroxyl ammonium nitrate (HAN) has been used in conjunction with AN to form a eutectic mixture which is a liquid at room temperature.[26] This liquid oxidizer has then been mixed with polyvinyl alcohol and aluminum (if desired) to form a gel propellant.[37,38] Other potential oxidizers such as ammonium dinitramide (ADN) are under preliminary investigation on the lab scale. Since, the replacement of AP by AN results in a substantial performance loss, systems are being investigated to make the binding and plasticising agents more energetic and thus contribute to the Isp.

AN presents other challenges in addition to lower performance capability. Studies to date have shown little ballistic or mechanical property tailorability, the burn rate is low, and burn rate slope is high.[26] Processing is generally more difficult than AP propellants, and AN has a number of crystalline phase transitions in the temperature range normally associated with propellant cure and storage requirements. Since the different phases have

different densities, AN must be stabilized by an additive in order to maintain its integrity.[26] Additionally, AN is more moisture sensitive than AP. While none of these difficulties appears insurmountable, they do represent a significant challenge to propellant designers. AN propellants have been static tested in at least 70 lb. motors.

Energetic polymers and placticizers (binders) have been considered for some time in connection with improving the performance of AN oxidized propellants. Among those polymers considered are glycidyl azide polymer (GAP),[39] polygylcidyl nitrate (PGN), polyoxetanes, and polynitramines. Some of these materials are available in large enough quantities to be considered for production propellants. GAP is commercially available. A GAP/AN propellant has already been tested at Edwards AFB in a 70 lb. motor. PGN and the polyoxetanes are available in pilot plant quantities.

Nitrate ester plasticizers have been used in AN propellant formulations. If the propellant is to remain class 1.3, only limited amounts of the less energetic nitrate esters such as triethlene glycol dinitrate (TEGDN), diethylene glycol dinatrate (DEGDN) and n-butyl-2-nitraoethyl-nitramine (BuNENA) can be used.[40] These propellants show some promise, but are not mature enough to know if they are viable for production motors.[26]

HAN/AN gel propellants exhibit greatly improved strain capability over conventional class 1.3 composite propellants.[41,42] A HAN/AN propellant has been tested in a an 800 lb. motor at Edwards AFB.[26] The processing and gel mechanisms of the HAN/AN gel propellant are considerably different than conventional propellants. Gel propellants have the potential to significantly reduce propellant waste streams. Both the

specific impulse and the density of the HAN/AN propellants are lower than conventional Shuttle propellant, so motors could not likely be retrofit with them.

Cost, reliability, operability, hazards, aging characteristics, and material availability all remain open issues with the Class 1.3 AN and HAN/AN systems.[26] They are considerably less mature than the scavenged and neutralized propellants. While ADN looks promising on paper, it is currently no more than a laboratory curiosity with potential.[26] Its practical use in rocket motors is at least several years distant.

If the Class 1.3 requirement does not apply, conventional high energy, Class 1.1 propellants can be used in order to reduce the HCl in the exhaust. These generally consists of polyethylene or polyester binders, plasticized with nitrate esters. HMX is used as the main solid oxidizer, with only 8-10% AP present for ballistic tailoring. [26]

If Class 1.1 propellants are acceptable for the rocket motor of interest, many proven options for reducing the exhaust HCl and the chlorine burden exist. Nitrate ester/polyether (NEPE) propellants using HMX as the solid oxidizer have been developed and used for years in submarine launched ballistic missiles such as C-4 and D-5, and in tactical minimum smoke applications. These propellants, when aluminized, outperform the conventional class 1.3 composite propellants and are easily processed. They typically cost more than Class 1.3 propellants, because of the price of the nitrate esters and the HMX. [26] Their major perceived drawback is their hazardous properties since they are more highly detonable than the Class 1.3 systems currently in use. This could impact operability for space launch systems. Despite the potential for detonation, motors loaded

with Class 1.1 propellants enjoy a very good safety record in the field; however, none of the current space launch vehicles use this family of propellants. [26]

In summary, there are several approaches to reducing the HCl content of the exhaust plume. The most mature are the conventional high energy Class 1.1 propellants, which have been in production for many years, but are viewed as being more hazardous than the class 1.3 propellants. For the class 1.3 propellants, the neutralized and scavenged propellants are the most mature, having been made in full scale mixes, and characterized extensively. The AN propellants, both gel and conventional, are not as mature, and have more technical challenges to overcome. The sodium nitrate and high energy propellants have the potential of reducing HCl in the exhaust by about an order of magnitude to 1-3%, while the nonchlorine and neutralized propellants may eliminate it entirely.[26]

Current System

It is not likely that a more environmentally acceptable propellant will be available soon. The cost to research, test and implement new propellants, and potentially whole new systems (if retrofitting the existing systems is not feasible), is estimated to be in billions of dollars and tens of years.[43] Thus, the current ammonium perchlorate propellant formulation in SRMs is likely to be in place for quite some time yet. In the interim, it is important to further investigate the impact of the current system on the environment. The scope of this research will only address the ozone destruction concerns on the environment.

As discussed previously, the most common propellant used in solid rocket motors is ammonium percholorate. AP contains three main ingredients: solid particulate oxidizer

(ammonium perchlorate), solid particulate fuel (aluminum powder), and a cured elastomer (such as hydroxy-terminated polybutadiene), that binds the mix together.[4] Upon ignition, SRMs exhaust large quantities of gases and particulates into the atmosphere. In its scientific assessment of ozone depletion for 1991 to the World Meterological Organization, Jackman et al stated that "[t]he major chemical effluents [of SRMs] . . . that can potentially perturb stratospheric ozone include chlorine compounds (HCl), nitrogen compounds (NO_x), and hydrogen compounds (H_2 and H_20)".[5] Additionally, they indicated that other exhaust compounds such as aluminum oxide (Al_20_3), could lead to ozone destruction, either by direct reaction with ozone or by providing a surface for heterogeneous processes that could lead to ozone destruction.[44]

The effects of SRM emissions on stratospheric ozone have been widely investigated by Prather et al.[6], Pyle[45], and many others. Generally, whenever the issue of stratospheric ozone and chemical propulsion has been raised, the focus has been on the effects of chlorine emissions.[46] As a consequence, propellant development efforts addressing stratospheric ozone have been aimed at reducing or eliminating chlorine from the systems by means such as neutralized, scavenged or reduced chlorine systems previously discussed. According to Prather et al., "[b]ased on our current state of understanding of stratospheric chemistry, of the species emitted during rocket motor operations, chlorine does appear to be the most significant contributor to ozone removal on a global scale although this contribution is extremely small."[6] According to Jackman et al., the total annual addition to stratospheric chlorine from rocket launches in on the order of 0.25 percent of the global annual stratospheric chlorine source from halocarbons is the

present day atmosphere.[5] Chlorine loading calculations result in steady-state ozone decreases computed to be less and 0.1% globally.[5] However, these computations do not include heterogeneous chemistry effects, i.e. Al_2O_3 particles.[5] At the Technical Interchange Meeting of the Launch Vehicles Working group, it was recommended to update the global impact calculations with heterogeneous chemistry effects.[9]

Heterogeneous Chemistry

A heterogeneous chemical process is one that involves more than one phase of matter. For example, hydrogen chloride *gas* could react with *solid* ice crystals and liberate chlorine molecules. When discussing heterogeneous chemistry with regards to SRMs, what is really being considered is the potential chemistry that takes place between alumina (Al_2O_3) particles and the gases of the exhaust plume or those found in the atmosphere. Alumina particles is a more encompassing term for all possible forms of aluminum oxide (see figure 1).

Until recently, the impact of heterogeneous chemistry on stratospheric ozone was believed to be relatively insignificant.[15,14] Even the WMO assessment concluded that the long term global effects of Al_20_3 is likely to be negligible. None of these studies considered the reactivity of the alumina, Al_2O_3, surface itself.[18] This may be partly due to the limited understanding of alumina surface. "Despite widespread interest in catalytic alumina . . . there is still only a limited understanding about the real nature of the surface of aluminas."[19]

According to Zolensky et al. [1989], the stratospheric concentration of alumina particles from SRM exhaust has risen dramatically in recent years. Because of the increase of alumina particles in the stratosphere and new research, some feel the impact of SRM exhaust particles on ozone has come under scrutiny.[18] Furthermore, Robinson et al. have suggested the possibility of a previously unsuspected heterogeneous process involving alumina particles from SRMs and halocarbon gases that could prove to be catalytic and destroy more ozone than previously suspected.[18]

Alumina

While it is not known at this time what effect aluminum oxide or other metal particulates may have on the stratosphere, solid ice has been implicated in the catalytic destruction of ozone in the Antarctic.[47] Some measurement work has shown correlations between ozone depletions and large increases in the stratospheric aerosol content due to volcanic activity.[26] Brasseur et al. have performed model calculations on the effects of stratospheric aerosols on the ozone levels of predicted future atmospheres and report that the natural background stratospheric aerosol content of 0.5 $\mu m^2/cm^3$ will be responsible for a 1-2% future decrease in total global ozone.[48] According to Bennett, the integrated surface area of particulates from El Chichon and background aerosols greatly exceed that of the anticipated launches of nine Shuttle and six Titan IV rockets per year and that the effect of rockets would be extremely small in comparison.[26] Additionally Bennett asserts that, since most of the aluminum oxide particles that have been captured were aspherical and solid rocket exhaust particles are typically spherical, the bulk of the particles were attributed to space debris reentry.[26]

Particle Properties

Al_2O_3 particles from SRMs are virtually all spherical and generally range is size from 0.1 μm to 10 μm.[49] Aluminum oxide particles in the exhaust of solid propellant rocket motors are found to occur in at least two different major phases, alpha and gamma. The majority, 64% to 93% by mass, of the particles collected Dill et al. were found to be gamma phase.[50] The general indication is the smaller particles tend to be gamma phase, and the larger ones tend to be alpha phase. This is consistent with the observation that gamma phase is produced by rapid temperature quenching of the liquid. The abundance of the gamma phase is also of interest to atmospheric scientist because it is an efficient catalyst for many surface reactions. Thermophysical properties of alpha and gamma Al_2O_3 are given in Table 1.

Table 1: Thermophysical properties of alpha and gamma Al_2O_3[50]

Property	*Alpha (α)*	*Gamma (γ)*
Crystal Structure	Hexagonal	Cubic
Density (g/cm^3 at 298 K)	3.98	3.5
Heat of Formation (kcal/mol at 298.15 K)	-400.4	-396
Heat Capacity, C (cal/g-mole K at 298.15 K)	18.889	19.773
Melting Point, K	2324	----

Gamma (γ) phase has stronger Lewis acid sites than alpha (α) and should therefore react more readily.[18] A Lewis acid site is an electron pair accepting site. The more a potential bonding site 'wants' electrons, the stronger the acidity or the more reactive the site will be. This is most likely because gamma alumina is widely believed to have defect spinel lattices.[51] The literature consensus is that the defects in the lattice structure produce abnormal bonding conditions in surface that expose reactive cations. The reactive cations

are synonymous with reactive sites and therefore Lewis acid sites. This argument is supported by Peri's work. "Active sites on γ-alumina have also been identified with cation defects arising from its presumed defect spinel structure, with such defects which have captured protons, or with aluminum ions abnormally exposed as a result of surface dehydration."[51]

In summary, Al_2O_3 particles are mostly γ-phase, which are generally believed to be the more reactive phase. This is most likely due to gamma's defected spinel structure which exposes reactive sites on the surface of the particle. Thus, we believe that defected γ-alumina surfaces will provide the potential reactive surface for catalytic destruction of CFCs and the release of reactive, ozone destroying Cl.

Catalysis

The confirmation of a catalytic cycle or a large increase in the deposition rate of alumina exhaust particles could lead to a possible environmental constraint to the Air Force's use of aluminum-loaded solid propellant launch phase rockets and strap-on boosters.

Catalysis is a process whereby a 'catalyst' increases the rate of reaction or allows the reaction to occur more easily. The rate of reaction is typically increased by lowering or removing the barriers to activation for the given reaction. (See Figure 3). Normally, the 'catalyst' is chemically unchanged after the reaction is finished.[52] For example in equations 5a-5c, Cl acts as a catalyst. It is part of the reactions but remains when the reactions are finished. This can be seen by the net result in equation 5d which

increases the reaction probability and thus the reaction rate.

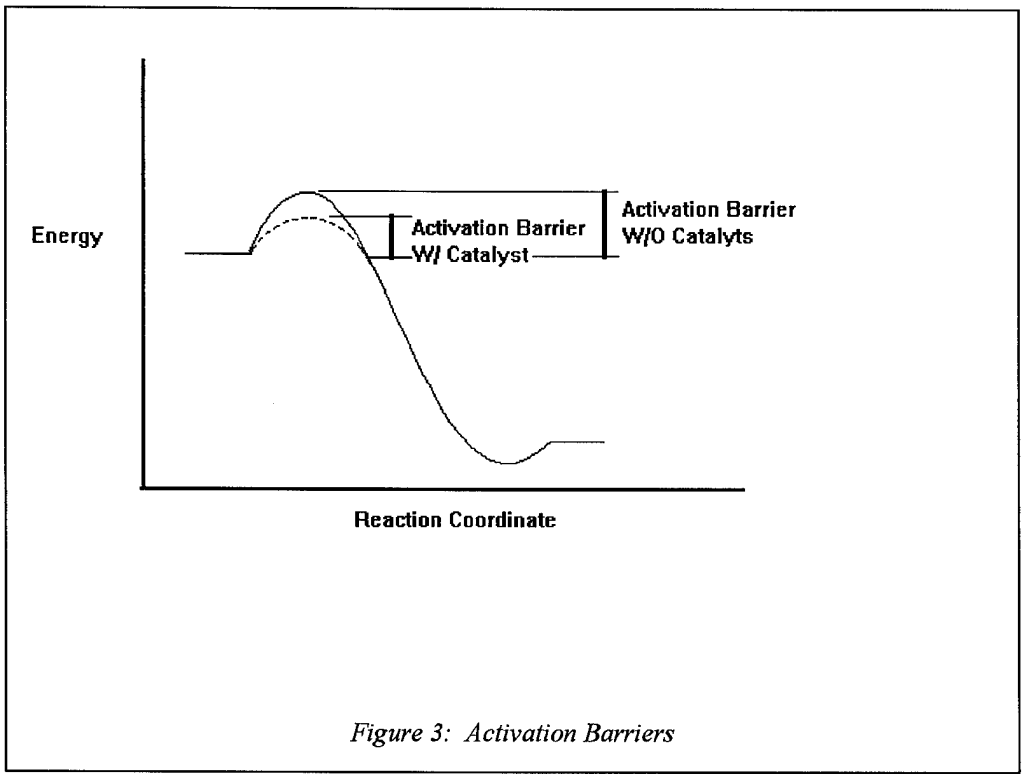

Figure 3: Activation Barriers

We believe that defected γ-alumina surfaces provides potential pathways for the destruction of CFCs and the release of reactive, ozone destroying Cl. This pathway may be catalytic.

Summary

The only significant way in which ozone is produced is by the combination of monatomic and molecular oxygen; however, ozone may be destroyed by both photo and chemical means. A chemical of great importance to ozone destruction is chlorine. Because the current solid propellant uses significant amounts of chlorine, concern over current and proposed propellants centers around chlorine. However, little concern has been given to alumina particles and the potential ozone destructive heterogeneous

chemistry associated with the particles. We believe that alumina particle heterogeneous chemistry may play an important role in the breakdown and release of reactive chlorine from CFCs. The next chapter will detail the approaches employed to research this hypothesis.

III. Approach

Overview

> The more progress physical sciences make, the more they tend to enter the domain of mathematics, which is a kind of centre to which they all converge. We may even judge the degree of perfection a science has arrived by the facility with which it may be submitted to calculation [Adolphe Quetelet 1796-1874].

Adolphe Quetelet's words turned out to be prophetic with regard to chemistry and physics when, in 1925 Schrodinger formulated his famous equation upon which quantum mechanics is based.[53] With the solution to this differential equation in hand, in principle, one could quantitatively predict most, if not all chemical phenomena using only Plank's constant, the velocity of light, and the masses and charges of nuclei and the electron.[66] This meant, experimentally useful properties could now be calculated without doing physical experiments. Quantities that were once difficult, or impossible, to obtain experimentally could now be obtained by solving a differential equation. However, solving the Schrodinger equation involves extremely complex mathematics which are completely solvable only for the isolated hydrogen atom. Even after massive mathematical approximations, the computations necessary to calculate interesting molecular properties for any system of chemical interest were far too complicated to do by hand.[53]

This chapter will discuss the modeling methods and the approach used to research the pertinent alumina particle heterogeneous chemistry. The chapter will first review modeling methods that were chosen for this reasearch and then detail how they were employed. After reviewing the modeling methods, the approach for developing small

molecular clusters from which chemistry can be predicted on larger, more realistic structures will be outlined.

Modeling Methods

Computational chemistry is becoming an ever more popular method with which to study chemical reactions. Many forms of chemical modeling have existed ever since Schrodinger developed his wave equation; however, the speed and accuracy of the modeling vary widely within the methods and molecular systems being modeled. We have chosen to use semi-empirical calculation methods to model the chemistry of interest for this research effort. Semi-empirical methods were chosen for their balance between the speed necessary to accomplish the expected number of calculation during the allotted research time and the accuracy necessary to produce believable results. Semi-empirical methods are based on ab initio theoretical calculations; however, many simplifying approximations are made which are compensated by parameters obtained from experimental methods. The following sections will explain ab initio and semi-empirical methods in greater detail.

Ab initio

The term ab initio, Latin for "from the beginning," implies a rigorous, nonparametrized molecular orbital method derived from first principles, namely the Schrodinger equation (eq. 18). This gives ab initio methods an automatic claim to respectability in that they are nominally fundamental, basing their predictions on a small number of fundamental constants such as the speed of light, the charge on an electron, and Planck's constant.[66]

The goal of ab initio calculations is to get the best possible solution to the Schrodinger partial differential equation (eq. 18):

$$H\Psi = E\Psi \qquad (18)$$

where H is a differentiating operator representing the total energy of the molecule called the Hamiltonian. E is the value of the energy of the state of the molecule relative to a state where all of its nuclei and electrons are infinitely separated and at rest. Ψ is the wavefunction which can be represented by a mathematical function dependent on the Cartesian and spin coordinates of all the particles in the molecule. All information about the molecule, i.e. bond orders, dipole moments, valencies, etc., is contained within the wavefunction.[53] The square of the wavefunction, Ψ^2, gives the probability of finding any of the molecule's particles in any given volume of Cartesian space. In principle, all properties of a molecular state can be calculated from its wavefunction and its associated energy.[53] Ab initio calculations make use of the approximations of molecular orbital theory to get the best possible wavefunction, Hamiltonian and energy.

The Hamiltonian, like any energy expression, is composed of both kinetic and potential parts:

$$H = T + V \qquad (19)$$

where T, the kinetic energy operator, is dependent on the velocity and mass of all the particle and V, the potential energy operator, is dependent on the electric charge and distance between particles. When the Hamiltonian operator is applied to the wavefunction, Ψ, the result is the wavefunction times the actual value for the energy, E.

E is known as the eigenvalue of the operator and Ψ is the eigenfunction. The Schrodinger equation for any molecule will have several solutions corresponding to different states of the molecule. The lowest energy state is the ground state.

Ab initio methods have an accuracy comparable with experiments for heats of formation and are at least as accurate as experiments for the determination of molecular geometries.[66] They are also versatile enough to allow transition states and excited states to be calculated. The only drawback to high level ab initio work is the cost in terms of computer resources, which normally require supercomputers and large blocks of time to run for all but the smallest systems.[53,66]

Semi-empirical

Soon after ab initio molecular orbital theory was developed, it became obvious that it was impractical to use for all but small systems. Even after the advent of supercomputers, the computer time required to sufficiently study a system with over ten second row elements is far too great for all but the most fortunate and well-funded research groups. In response to this problem, several molecular orbital (MO) based methods have been formulated which use experimentally derived parameters to approximate values explicitly calculated with ab initio methods. These fall under the category of semi-empirical methods.

Two of the earliest and crudest semi-empirical methods treated only planar conjugated molecules. The Huckel Molecular Orbital (HMO) method, developed in the

early 1930's by E. Huckel, treated only π-electrons assuming they were the greatest contributors to the total electronic energy.[53] The HMO method is relatively simple and uses only matrix algebra. The parameters used are all relative to a carbon atom, which is given a value of 1 in all cases. Although the HMO method is a crude approximation, it gives surprisingly good qualitative results for MO's, bond orders, atomic charges and other molecular properties.[53] Roald Hoffman formulated an Extended Huckel MO (EHMO) method in 1963 which includes σ-electrons in the calculation, allowing any type of system to be computed.[54] It is still used extensively today for extremely large systems which are too big for more accurate semi-empirical techniques.[55] The Pariser-Parr-Pople (PPP) method[56], developed in 1953, also treats only π-electron conjugated systems and still finds uses today in the study of nonlinear optical phenomena in molecules.[53]

The techniques listed above fall into the category of qualitative MO theory, and although they provide vast quantities of useful qualitative information, they are not quantitatively accurate enough in their calculation of energies, geometries and other properties to satisfy most computational chemistry problems. The roadblock to quick, accurate MO computations is the enormous amount of computer time required to evaluate the thousands to hundreds of thousands of electron repulsion and exchange integrals, sometimes referred to as differential overlap (DO) integrals.[53] One solution is to neglect the integrals that have little impact on the final energy and find approximate values for the other integrals so they don't need to be explicitly evaluated. This is how the most popular semi-empirical MO methods work, hence the name 'approximate MO theory' is sometimes used for describing these techniques.

The first two of the these methods use the neglect of differential overlap (NDO) approximation where some or all of the differential overlap (repulsion and exchange integrals) between different atomic orbitals (AOs) centered on atoms are neglected. [53] They also explicitly treat only valence electrons, assuming a stable or frozen core of inner electrons which does not change much during the course of the computation. The complete neglect of differential overlap (CNDO) method, developed in 1964, neglects all differential overlap between repulsion and exchange integrals.[57] Only the one electron resonance integrals, are retained and parameterized values are input for them.[53] This means that the orbital around the atoms are treated as spheres. The intermediate neglect of differential overlap (INDO) method[58], formulated in 1966, differs from CNDO in that exchange integrals between electrons on the same atom need not be equal, but can depend on the orbitals involved.[59] CNDO and INDO give nearly the same results for closed-shell systems, but INDO is far superior in calculating electron spin density in radicals. [53]

Although CNDO and INDO were more accurate than previous semi-empirical attempts, they did not give the desired accuracy, so their inventor J. A. Pople, abandoned further work in semi-empirical methods and continued advancing ab initio theory. A significant problem with CNDO and INDO was that they had been parameterized to reproduce the results of available ab initio calculations on diatomics and other small molecules.[53] The best ab initio computations in the mid-1960's were minimal basis set (STO-3G) runs which are recognized today as not being especially accurate. When CNDO and INDO results were not as accurate as STO-3G, semi-empirical methods were marked deemed only marginally useful or abandoned. A different approach to semi-

empirical MO theory, taken by Dewar, has resulted in the three most popular semi-empirical techniques in use today. Instead of giving the overlap integrals values to reproduce energies and geometries from ab initio calculations, Dewar's techniques are parameterized to reproduce experimental data.[60] This gives much better and more usable results than previous semi-empirical methods. The first such approach was the modified intermediate neglect of differential overlap (MINDO/3) method, developed in 1975.[61] MINDO/3 is basically the INDO method described previously except all included integrals are approximated to reproduce molecular geometries and heats of formation. MINDO/3 is parameterized by atom pairs, i.e. in order to have parameters for a compound with Li-N bonds must be available. A "*" in Figure 4 denotes the bond pairs for which MINDO/3 is parameterized. Although MINDO/3 is not perfect, its strong points and shortcomings

Table 2: Available MINDO/3 parameters[62]

	H	B	C	N	O	F	Si	P	S	Cl
H	*	*	*	*	*	*	*	*	*	*
B	*	*	*	*	*	*				
C	*	*	*	*	*	*	*	*	*	*
N	*	*	*	*	*	*			*	*
O	*	*	*	*	*	*				
F	*	*	*	*	*	*				
Si	*		*							
P	*		*		*	*		*		*
S	*		*	*	*				*	*
Cl	*		*	*				*	*	*

are extremely well documented.[63] It was a breakthrough in computational chemistry. Now, fairly accurate energies and optimized geometries could be obtained quickly for a 50-atom molecule[60], something unthinkable with ab initio calculations.

MINDO/3 does as good a job at calculating energies and geometries as an INDO-based formalism. To improve the results, all one-centered electron repulsion integrals must be included in the calculation. It has been shown that it is not correct to neglect repulsion integrals involving overlap if the overlap is between two AOs of the same atom.[60] The inclusion of all the electron repulsion and exchange integrals between AOs on the same atom and neglect of those between AOs on different atoms is known as the neglect of diatomic differential overlap (NDDO) approximation.[58] Dewar and Thiel used the NDDO approximation for formulate the modified neglect of diatomic differential overlap (MNDO) semi-empirical Hamiltonian in 1977.[64] It is parameterized to reproduce experimental ionization potentials, dipole moments, and heats of formation and was developed to avoid the weakness of MINDO/3.

MNDO handles most problems better than MINDO/3 with the notable exceptions of treating carbocations and silanes.[53] It handles the effects of lone-pair electron repulsion much better than MINDO/3.[64] MNDO calculations usually take 1.5 times longer than corresponding MINDO/3 computations but the improvement in results are often worth the extra time. A significant advantage of MNDO over MINDO/3 is that it works for a larger range of compounds because it uses and atom-by-atom parameterization instead of bonded atom pairs.[53] I.e., to have parameters for a compound with a Li-N bond pair, experimental data on nitrogen-containing compounds and lithium-containing compounds are needed not compounds with Li-N bonds which may be hard to come by. MNDO presently handles any molecule containing H, Li, B, C, N, O, F, Na, Al, Si, P, S, Cl, K, Cr, Ge, Br, Sn, I, Hg, and Pb.[62]

A brief word on semi-empirical parameters is appropriate here. When the 'overlap' integrals, are approximated several different parameters are used for each integral. Guesses at these parameters are made and calculations are run on several compounds for which there is experimental data. The calculated values are compared to the experimental numbers and a mean error is calculated for the set of compounds. The parameters are then adjusted and the calculations run again, the values compared and the parameters adjusted. The procedure is repeated until the mean error over the set of compounds is below a deemed acceptable value and the 'optimized' parameters are input into the computer program.[53]

One of the most significant problems with MNDO (and MINDO/3) is its tendency to overestimate repulsions between atoms when they are near their van der Waals radius distance apart. This leads to energies that are too positive for crowded molecules and too negative for four-numbered rings, and the failure to reproduce hydrogen bonds.[53] Dewar and Thiele recognized this problem, but it was not successfully corrected until 1985 with the introduction of the Austin Model 1 (AM1) Hamiltonian.[65] AM1 is basically the MNDO method with the core-core repulsion terms 'softened up.' The core (nucleus and inner non-valence electrons) repulsion function was modified from MNDO to AM1, then a new set of parameters was made to make the new method self consistent. AM1 reproduces heats of formation, dipole moments, and ionizations potentials better than MNDO or MINDO/3 in most cases.[53]

AM1 is an improvement over MNDO, even though it uses the same basic approximation. It deals with hydrogen bonds properly, produces accurate predictions of

activation barriers for many reactions, and predicts heats of formation for molecules with and error that is about 40 percent smaller than with MNDO.[59] Problems still exists with AM1. Treatment of phosphorus-oxygen bonds is inaccurate, nitro compounds are still too positive in energy, and the peroxide bond, for example, is still too short.[59] Elements available in AM1 are: H, Li, B, C, N, O, F, Na, Al, Si, P, S, Cl, K, Ti, Zn, Ge, Br, Rb, Sn, I, Hg, Pb.[62]

In an attempt to improve the accuracy of the MNDO method yet again, J. J. P. Stewart developed the Parametric Method Number 3 (PM3).[66] PM3 is a reparameterization of AM1, which is based on the neglect of diatomic differential overlap (NDDO) approximation.[59] NDDO retains all one-center differential overlap terms when Coulomb and exchange integrals are computed. PM3 differs from AM1 only in the values of the parameters. The parameters for PM3 where derived by comparing a much larger number and wider variety of experimental versus computed molecular properties. In many cases, PM3 is an improvement over AM1.[66] Typically, nonbonded interactions are less repulsive in PM3 than in AM1. Elements available in PM3 are: H, Li, Be, C, N, O, F, Na, Mg, Al, Si, P, S, Cl, K, Zn, Ga, Ge, As, Se, Br, Rb, Cd, In, Sn, Sb, Te, I, Hg, Ti, Pb, Bi.[62]

For the research effort we choose to use PM3 as based on the strength of the NDDO methods described above. Additionally, due to the more comprehensive parameters used in PM3, we believe that PM3 will be more apt to give accurate results for the chemistry that we are investigating. Finally, in comparing the different NDDO methods, average errors in ionization potentials and average errors in dipole moments

between the different compounds containing Al and/or Cl showed PM3 to have the smallest average error in each case.[66]

Develop Small Clusters

Since PM3 was selected as the method of choice for this research, the next step was to begin making calculations. The calculations consist of three basic steps: 1) select the atoms that will make up the molecule, 2) arrange the atoms in an approximate molecular geometry, and 3) allow the software to optimize the geometry and perform energy and vibrational spectra determinations as needed. Once the calculations have been made, results ranging from heats of formation, and molecular geometry to infrared (IR) vibrational spectra can be read graphically from the screen and/or from data in log files.

The chemistry that we endeavored to model through PM3 semi-empirical calculations was that of: 1) an add-atom or add-molecule chemisorbing on the surface of an aluminum and oxygen molecule, 2) the add-molecule dissociating on the surface, 3) thermal desorption of dissociated add-molecule products and, 4) the potential catalytic activity of a given site. The add-atoms to be used were fluoride (F^-) and chloride (Cl^-) ions. The add molecules to be used were hydroxide (OH^-), water (H_2O), and CFC-12 (CCl_2F_2). We chose to use CFC-12 as the representative chlorofluorocarbon because time would not permit the modeling of all CFCs and CFC-12 is the most abundant CFC in the stratosphere.[3]

With the understanding of the calculational capability of PM3 in hand, we began to develop small molecules of aluminum and oxygen that might represent a very small section

of an Al_2O_3 particle. We called these molecules 'clusters' because we wanted to develop clusters of reactive sites. We hoped that reactive sites would react in the same manner as defected sites on the surface of γ-alumina particles react.

Our initial work was based on developing very small clusters of approximately two to fifteen atoms each that would expend no more than a few hours per calculation. With this approach we could become familiar with the types of molecules we could build and the potential chemistry and trends that we might expect on larger clusters without completely expending the research time available. However, at this stage we would only model individual reactive sites due to the size limitations. On the larger clusters we will model adjacent reactive sites. Recall our basic premise that we believe adjacent, rather than isolated, reactive moieties constitute the catalytically active sites on the alumina surface.[24]

In summary, we hoped that by characterizing small clusters, we could save time and point the way to the pertinent chemistry to be performed on larger clusters. The clusters developed are discussed in the following sections.

Geometry

The first clusters were developed with the aim of finding a geometry that would provide a surface for reaction, representative of an Al_2O_3 particle surface, with at least one central Al atom to represent the remaining internal bulk of the particle. Each geometry investigated was allowed to have a charge as predicted by standard oxidation states found on the Periodic Table of Elements. For example: Al_2O_3 is a neutral molecule, (2*(+3) + 3*(-2) = 0), but Al_3O_4 has a charge = +1, (3*(+3) + 4*(-2) = +1). The goal was to

construct the desired cluster while limiting the number of atoms to the fewest possible so that subsequent calculations would take no more than a couple of hours each.

O-H Vibrational Trends

The next clusters developed were based on determining the trends in O-H vibrations on Al_2O_3 clusters. The vibrational frequency of the H atom on the O atom is an experimental measurement of how tightly the H is bonded to the O. This in turn is affected by how strongly the O is bonded to the Al. The Al is an electron pair acceptor and thus acts as a Lewis acid site. The vibrational frequency, then, will help to characterize the Lewis acidity of the Al atom under the given conditions. We also decided to record the Al-O bond distances to see how they would vary as the Lewis acidity varied, as predicted by the O-H vibrations.

The two different O-H vibrational methods used to investigate Lewis acid trends are discussed below.

$Al(OH)_x$

The first method was to have a single Al atom surround by varying amounts of OH^- groups. The clusters were developed with the following chemical formula: $Al(OH)_x$, where x = 1-6. See figure 4, for an example of $Al(OH)_4$.

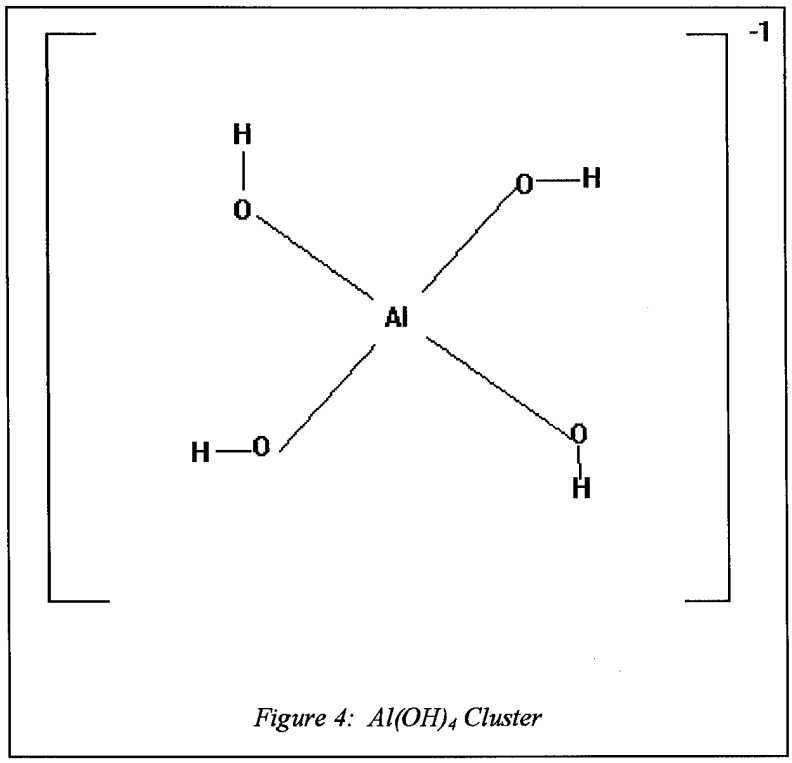

Figure 4: $Al(OH)_4$ Cluster

The charges were allowed to vary as described in the geometry section, i.e., $Al(OH)_6$ had a charge of -3 while Al(OH) had a charge of +2. Six O-H vibrational frequencies were obtained for the $Al(OH)_6$ cluster, with its six OH-groups, while one was obtained for the Al(OH), with only one OH-group. Additionally, six Al-O bond distances were recorded.

Al-Coordination

This method varies from the previous method in that only one OH group was coordinated to the oxygen as the total Al coordination increased from three to six (see figure 5). Lesser total Al coordination was not investigated because we do not believe they are representative of bonding sites found on alumina particles. The chemical formulas were as follows: three coordinate - $[Al_2O_2*OH]^{+1}$, four coordinate -

$[Al_2O_3*OH]^{-1}$, five coordinate - $[Al_3O_4*OH]$, and six coordinate - $[Al_3O_5*OH]^{+2}$. Again, the molecular charge was allowed to vary. However, we desired to keep the charge from becoming excessively negative as additional O^{-2} were added to the clusters, so an additional Al^{+3} was added to the five and six coordinate clusters. One O-H vibrational frequency and one Al-O bond distance was obtained from each calculation.

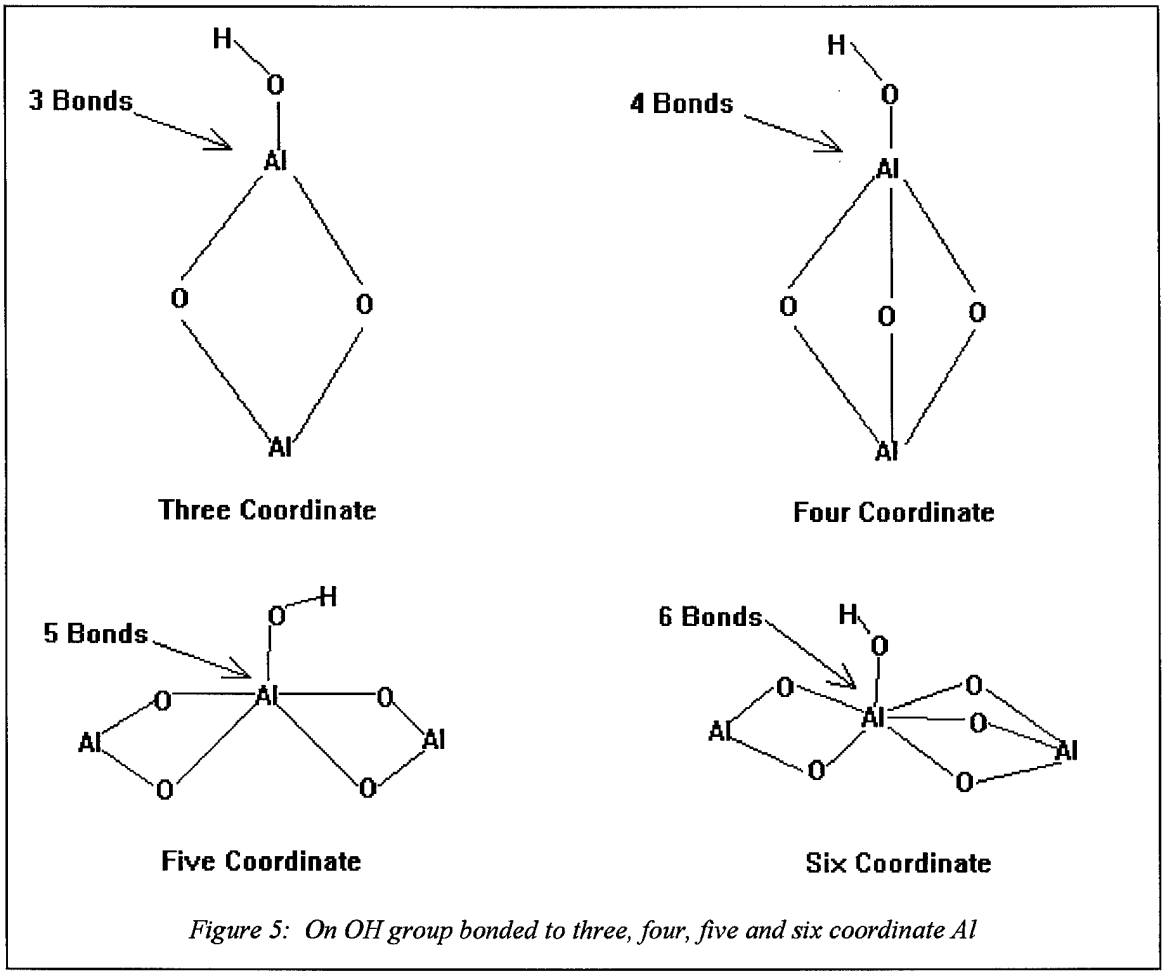

Figure 5: On OH group bonded to three, four, five and six coordinate Al

Bond Order Conservation

The bond distances and the O-H vibrations from the previous two sections appeared to directly correlate to each other and to Lewis acidity (see the results in the

next chapter). Since bond distance is related to bond order, the next idea we investigated through cluster model calculations was that of bond order conservation. We hoped that further investigation of bond order conservation would help us to better characterize the Lewis acidity of bonding sites.

The bond order of a covalent bond between two atoms is the number of effective bonding electron pairs shared between the two atoms. The repulsion due to electrons in antibonding orbitals cancels the attraction due to bonding electrons. Therefore, to find bond order, the number of electrons in antibonding orbitals must be subtracted from the number of electrons in bonding orbitals and the difference divided by two.[52] In general, as bond order increases, the strength of a bond increases and the length of the bond decreases.

Clusters were developed based on AlO groups with H_2O as the add-molecule to which the bonding distances were measured. Water was chosen as the add-molecule because it was a non-charged species and therefore would not change the characteristics of the Lewis site by donating or removing electrons as a charged species might. The chemical formula of the clusters were as follows: $Al_xO_x*H_2O$ where x = 1 - 5. The charge on the cluster was maintained at zero in each case since an Al_2O_3 particle is not believed to be charged. Additionally, water was chosen as the add-molecule because it is a charge neutral species. See figure 6 for a typical cluster: $Al_3O_3*H_2O$.

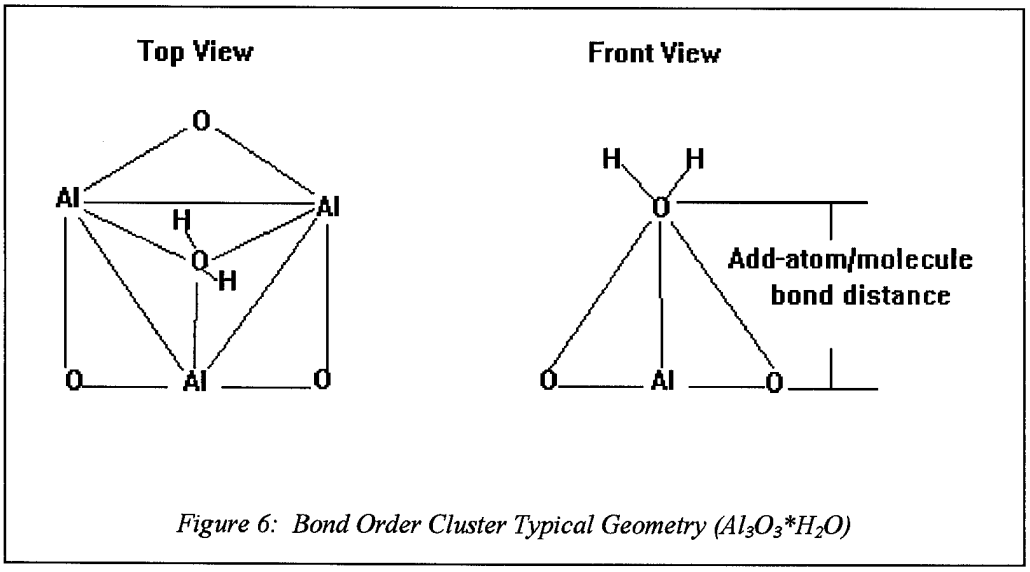

Figure 6: Bond Order Cluster Typical Geometry ($Al_3O_3*H_2O$)

Once the geometries were optimized, the single and multi-center bond distances were measured. Since the bond distances are a measure of bond order and thus bond strength, this method was used to characterize different bonding sites. The bond distances and heats of adsorption for each cluster were then compared against the Shustorovich bond order conservation model[67] for relevance.

Shustorovich Bond Order Conservation Model

The Shustorovich Bond Order Conservation Model is a Bond Order Conservation (BOC) model for homogeneous atomic surfaces. Approximating atomic adsorption bond energy is relatively straight forward using the simple Shustorovich approach. Shustorovich's approach is based on the Morse potential (eq. 20). The two-center bond order χ is described by

$$\chi = e^{-(d-do)/a} \qquad (20)$$

where d relates to the internuclear bond distance and a is an empirical constant. The total energy is represented by a Morse potential

$$E(\chi) = Q_o(\chi^2 - 2\chi) \qquad (21)$$

where Q_o is the equilibrium bond energy and d_o is the equilibrium bond distance when $\chi = 1$, by definition.[67] To make calculations for coordination of an add-atom to a metal surface in an n-fold coordination site (M_nA coordination) Shustorovich made four assumptions: [67]

1. Each two-center bonding interaction is described by the Morse potential (eq. 20-21).
2. The two-center bonding interactions, MA are additive.
3. The total bond order of M_nA is conserved and normalized to unity.
4. Only nearest neighbor bonding is considered.

From this set of postulates it follows that the bond energy for atomic adsorption in an n-fold coordination site is

$$Q_n = Q_o(2 - 1/n) \qquad (22)$$

where Q_o is the two-center M-A bond energy for an A atom coordinated to a single metal atom (on-top coordination) in the adsorption-adjusted metal lattice. [67]

Although a from (eq. 20) is an empirical constant, it can be estimated from (eq. 23),

$$a = (\cos \psi_n/\omega_n)(2Q_n/\mu) \qquad (23)$$

where ψ_n is the angle between the M-A vector and the surface normal and μ is the mass of the add-atom and ω_n is the vibrational frequency of the add-atom.[67]

Finally, it important to note that the minimum total energy, E, is equal to the maximum bond energy, so

$$E_n = -Q_n \qquad (24)$$

Thus, as total energy (a described by the heat of formation) becomes more negative, the add-atom bond energy or Lewis acidity increases.

Single Bridged

Similar in structure to the clusters used in the bond order determinations are the single bridged structures. These structures are again composed of Al and O in a single planar ring, alternating the Al and O so that a single O bridges between each Al. This allowed us to keep the structures bivalent as additional Al-O groups were added to the clusters. The Al-Al distances were lightly restrained to 2.57 angstroms (a typical Al-Al, PM3 optimized bond distance) in order to induce a symmetrical structure. The chemical structure is Al_xO_x where x = 2 - 4.

Add atoms/molecules were then bonded to the planar base structure. The add-atoms/molecules used were: fluoride (F^-), chloride (Cl^-), hydroxide (OH^-) and water (H_2O). The base structure alone kept a neutral charge but when and add-atom/molecule was applied, that charge was applied to the whole structure. For example $[Al_3O_3*F]^-$ has a negative charge. See figure 7 for an example of a single bridged cluster (Al_3O_3) with an add atom (F^-).

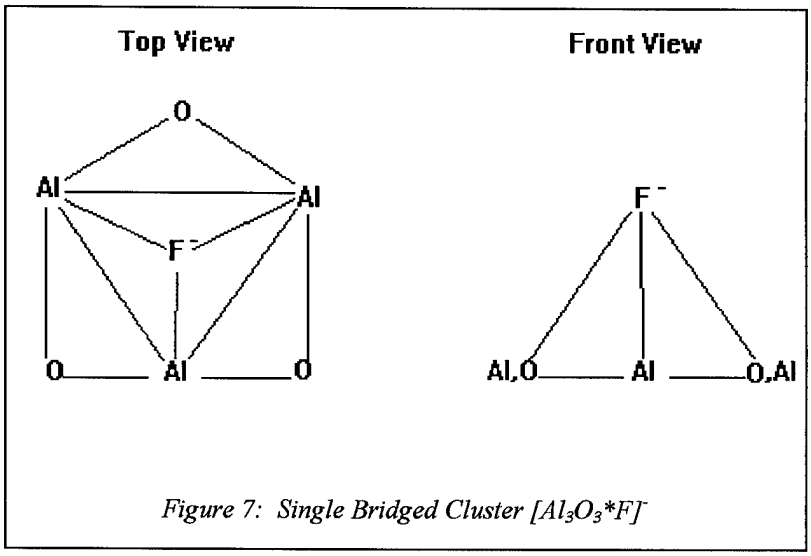

*Figure 7: Single Bridged Cluster [Al_3O_3*F]*

The single bridging cluster were developed to help characterize the bonding characteristics of each cluster and the trends between them. The single bridging structure allowed for the characterizations to be made while maintaining a total Al-O coordination of three for each structure when add-atoms/molecules were applied. The relevant information extracted from each cluster optimization calculation was the heats of formation, bond lengths and O-H vibrational frequencies where applicable.

Double Bridged

The next successful series of clusters calculated was the double bridged structures. These structures were the same as the single bridged except that two oxygens bridged between each Al in the ring and each Al was maintained tetravalent as Al-O_2 groups were added Additionally, the second bridging O was maintained below the ring plane while the first bridging O was restrained to be in the planar ring of Al and O. See figure 8 for an example of Al_4O_8*F^-. The chemical structure was $Al_xO_{(2x)}$ where x = 2 - 4. Again, the

same add-atoms/molecules were applied in the same manner as in the single bridged clusters.

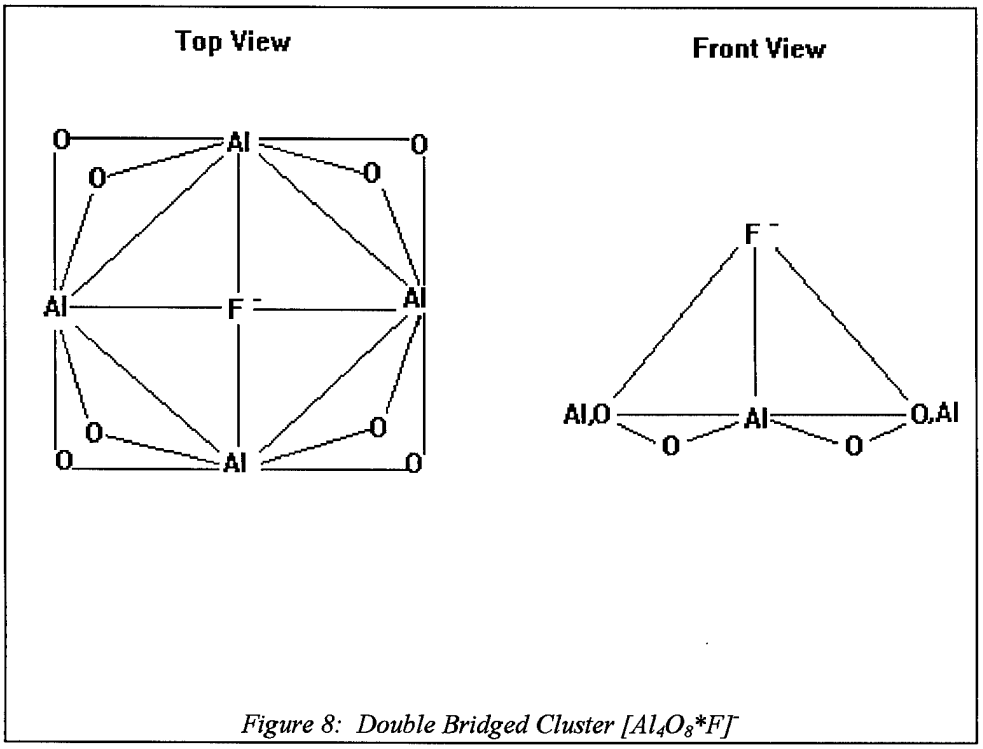

*Figure 8: Double Bridged Cluster [Al_4O_8*F]$^-$*

The 'top' of the ring surface was maintained planar to simulate a planar bonding site on a larger Al_2O_3 particle. The Al coordination in this case was five when add-atoms/molecules were applied. Heats of formation, bonding distances and OH vibrational frequencies were obtained from the optimized calculations. It was desirable to obtain a series of clusters where the total Al coordination was maintained at four. However, these structures did not produce similar geometries between the clusters as the numbers of Al and O was increased. Thus it was believed that the results would not be consistent with each other due to the widely varying geometries.

Increasing Oxygen Coordination

The final series of small clusters developed, tested the reactions of a single Al bonding site to increasing O coordination. The chemical structure is Al_2O_x, where x = 1 - 5. Add-atoms/molecules of fluoride (F^-), chloride (Cl^-), hydroxide (OH^-),water (H_2O) and CFC-12 (CCl_2F_2) were applied to the structure in the same manner as in the previous series of clusters. See figure 9.

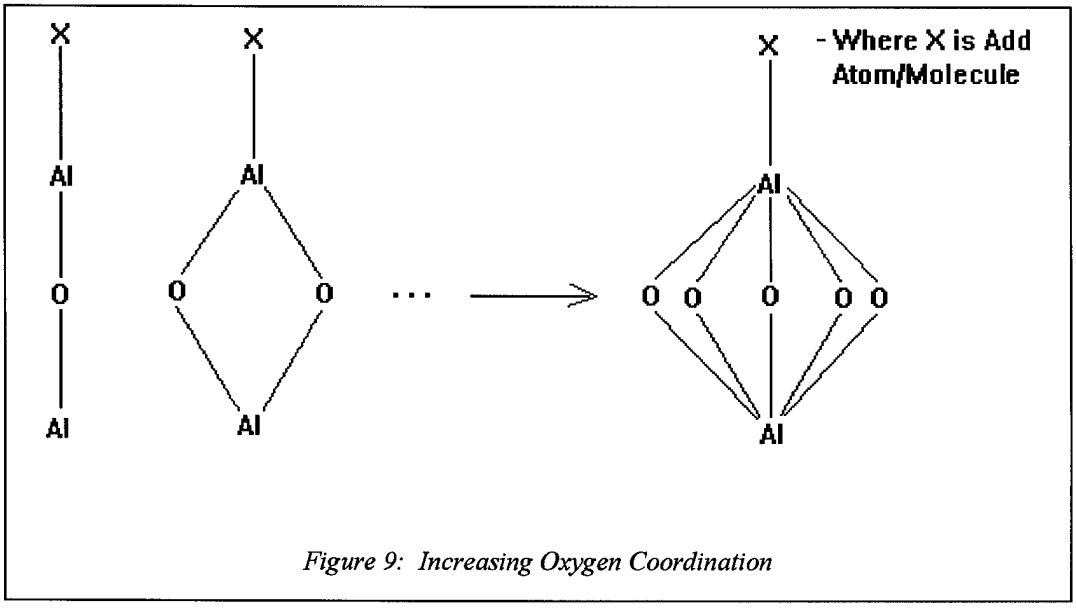

Figure 9: Increasing Oxygen Coordination

The relevant information extracted from each cluster optimization calculation included the heats of formation/adsorption, bond lengths and O-H vibrational frequencies where applicable. Additionally, the CFC-12 was stepped down onto each bonding site from a distance of approximately 4 angstroms to a distance of approximately 1 angstrom. This was done by restraining the bonding distance and optimizing the CFC-12 with respect to the bonding site. The heats of formation and bonding distance from each optimization allowed for the development of reaction pathways for each structure.

Develop Large Clusters

Based on the experience of previous researchers[68] and lessons learned from developing the small clusters, larger clusters that were expected to be more representative of actual reactive bonding sites on Al_2O_3 particles. These were developed with strong Lewis acid sites located next to base sites. Again, recall our basic premise as discussed in Chapter II; we believe that adjacent acid/base sites are the reactive bonding sites that are potentially catalytic.[24] For example, as a CFC approaches an alumina particle, the negative 'end' of the CFC will be attracted towards a Lewis acid site while the positive 'end' of the CFC will be attracted towards a base site. This will strain the bonds in the CFC and increase the likelihood of surface dissociation. Recall that dissociation of the CFC is necessary to desorb a reactive halocarbon and free up the Lewis acid site on the surface. We believe then, that adjacent acid/base sites will be the ones most likely to chemisorb the CFC-12, dissociate the Cl(s), desorb the Cl(s), thus freeing up the site to react again.

Two types of clusters were developed having two central, adjacent three or four coordinated aluminums each. These central bonding sites were joined by a single or double oxygens, respectively and capped on either end by six coordinated aluminums. See figures 10 and 11.

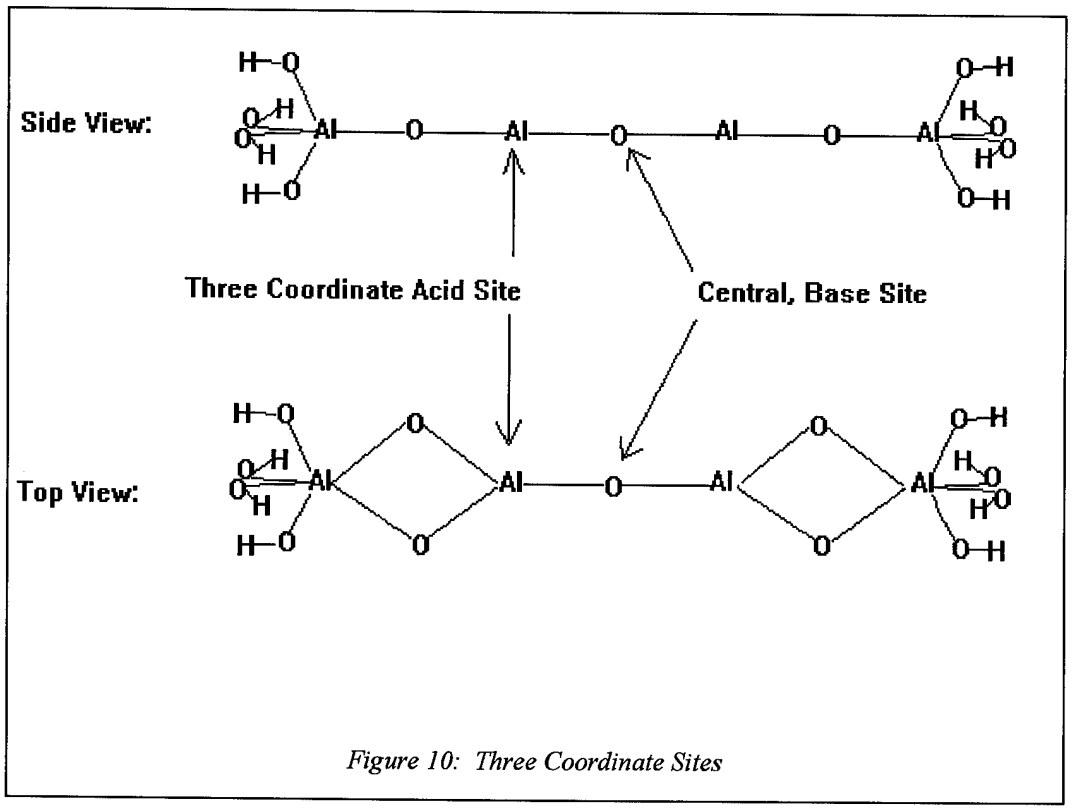

Figure 10: Three Coordinate Sites

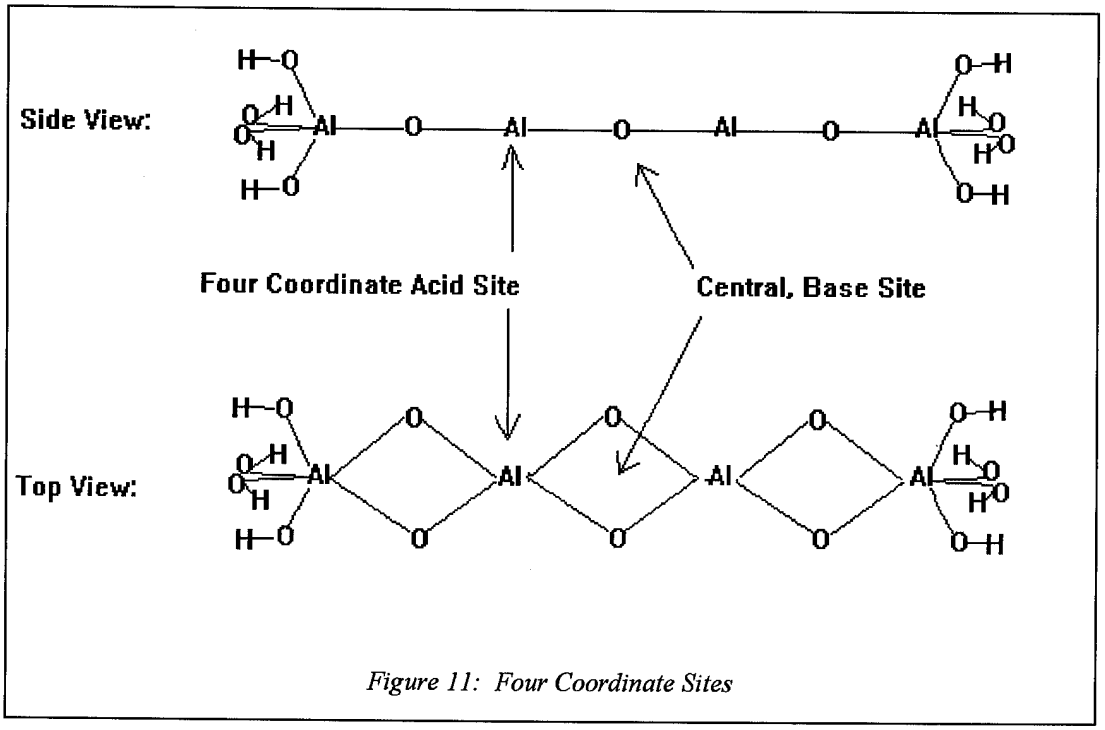

Figure 11: Four Coordinate Sites

Three Coordinate Sites

This cluster, as seen in figure 10, is intended to model a reactive bonding site on the surface of an Al_2O_3 particle. This cluster was optimized without restraints and was charge neutral. The resulting cluster was known as the three coordinate surface on which further calculations were made. The optimized geometry of this surface was then manually restrained to remain essentially fixed as it would be if it were on the surface of an Al_2O_3 particle.

The initial calculations made with the three coordinate surface were made by allowing CFC-12 to bond to the surface in three different orientations. The first orientation was with one Al-Cl bond. The second orientation was with one Al-Cl bond and one O-C bond. The third orientation was with two Al-Cl bonds (see figure 12). These clusters provided heats of formation/adsorption essential in determining chemisorption. The CFC-12 was then broken up on the surface, dissociating one Cl then both Cls, and re-optimized. The results are recorded in the next chapter.

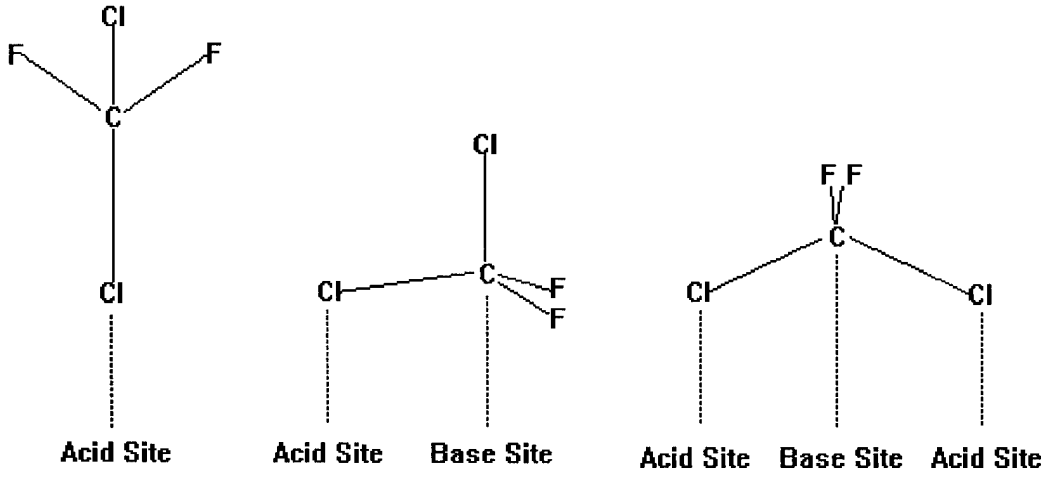

Figure 12: Bonding Orientations

The next calculations made were with HCl bonding to the surface. The first calculation made was to determine if HCl would chemisorb with the Cl bonding to an acidic Al site and the H bonding to the basic, central O site. The H and the Cl were then dissociated and allowed to move freely as the cluster was re-optimized. This calculation would allow for comparisons between the chemisorbed molecule and the chemisorbed dissociated atoms. A second dissociated H and Cl calculation was made where the Cl was induced to react with one of the OH groups from the adjacent six OH coordinated Al. The results of this calculation were used to determine whether or not HOCl would desorb from the surface. Finally, a reaction pathway was mapped out for HCl chemisorption by freezing the three coordinate surface with an H bonded to the central O, and stepping in the Cl on an adjacent acidic Al site, from 4 to 1.5 angstroms.

The last optimization made with the three coordinate surface was to place an OH^- on one of the acidic Al sites. It was hoped that obtaining the heat of formation and vibrational frequency for this structure would help to characterize its acid strength.

Four Coordinate Sites

The four coordinate sites cluster was essentially the same as the three coordinate except that there were two central bridging oxygen atoms instead of one. This structure increases the total coordination of each acid site from three to four. In the optimization of this 'base surface,' the geometry between the aluminums and bridging oxygens was restrained in order to keep the atoms approximately in the same plane. This was necessary in order to present a planar and symmetrical bonding surface that was consistent with that of the three coordinated cluster (see figure 11). Upon obtaining the optimized geometry, this 'base surface' was restrained to maintain that approximate geometry as if it were a reactive site on an Al_2O_3 particle surface. This was done the same way as it was for the three coordinate clusters.

With the optimized four coordinate cluster, calculations were made to model chemisorption, dissociation and desorption of CFC-12 and HCl, on this cluster. CFC-12 was first investigated by allowing CFC-12 to bond to the cluster in the exact same orientations as it did on the three coordinate cluster (see figure 12). Calculations were then made with CFC-12 dissociated into CF_2 bound to the central oxygens and one Cl bound to each of the four coordinate acidic Al sites on either side of the central oxygens. Finally, calculations were made with $CClF_2^+$ and CF_2^{+2} removed from the cluster. Note that this left a charge of -1 and -2 respectively, on the clusters.

HCl was then investigated for chemisorption, dissociation, and desorption in the same manner as it was for the three coordinate cluster. First HCl was allowed to chemisorb on the cluster such that the Cl bonded to one of the acid Al sites and the H bonded to the central oxygens. Then, the H-Cl bond was broken and the cluster was re-optimized, in order to obtain energies for HCl dissociation. Finally, several attempts were made to map out the reaction pathway for HCl chemisorption the same way it was done with the three coordinate cluster. However, these structures would not optimize so the and the reaction path was not mapped out.

The last optimization made with the four coordinate surface was to place an OH^- on one of the acidic Al sites. It was hoped that obtaining the heat of formation and vibrational frequency for this structure would help to characterize its acid strength.

Summary

"Modern methods and modern computers have allowed researchers whose knowledge of quantum mechanics is minimal to easily and confidently carry out theoretical chemistry research programs."[66] James J. P. Stewart fairly accurately described this research effort, except that it was not easy, nonetheless, using PM3 was not particularly difficult. PM3 allowed us to somewhat confidently model the chemisorption, dissociation, desorption and catalytic possibilities of add-atoms/molecules on the small and then larger aluminum and oxygen clusters. The result obtained in each enlightening and/or successful step in this process will be discussed in the next chapter.

IV. Results

Overview

The presentation of the results, with some interpretation, closely follows the structure of the approach chapter. Some of the methodologies are reiterated to further clarify to the reader how the results were obtained, thus increasing understanding. The results are presented in tabular, graphical and written form in the following sections.

Small Clusters

Geometry

The goals of this approach were to develop a structure with at least one central Al atom to represent the bulk of a larger particle and to use few atoms so that calculations would take less than a few hours to compute for each cluster. The results of the geometry calculations are largely negative, in that a cluster or clusters were not developed that met the stated goals.

Most of the clusters developed twisted up on themselves during optimization and did not provide an internal Al bulk atom. Additionally, many optimized cluster geometries forced a three coordinate O bonding condition that we did not believed to represent reality. We believe that oxygen is normally bonded to two, not three other atoms, thus these clusters were eliminated. However, when the clusters were built and optimized, it was determined that a minimum of five Al atoms and eight O atoms were necessary to build a structure that provided an internal Al and a potential surface for bonding that did not force a three coordinate O bonding condition. Moreover, structures this large and

larger required a minimum a three hours to calculate, and this was determined to be to long to complete the remaining work. Thus, the approach was modified by first applying the methods in the following sections to smaller clusters to characterize the geometries and bonding conditions that could potentially exist and help point the way to building larger, more representative clusters.

O-H Vibrational Trends

The O-H vibrational trends were tested as described in the previous chapter. The results were as follows:

$Al(OH)_x$

In this analysis the aluminum remained constant at one while the number of OH-groups increased from one to six The O-H vibrations and Al-O bond distance results are shown in Table 3.

Table 3: O-H Vibrations and Al-O bond distances on $Al(OH)_x$

Cluster	Charge	ν, (1/cm), d, (10^{-10}m)	ν, (1/cm), d, (10^{-10}m)	ν, (1/cm), d, (10^{-10}m)	ν, (1/cm), d, (10^{-10}m)	ν, (1/cm), d, (10^{-10}m)	ν, (1/cm), d, (10^{-10}m)	Average, ν, (1/cm), d, (10^{-10}m)
$Al(OH)_6$	-3	3948, 2.571	3940, 1.947	3935, 1.920	3931, 1.911	3920, 1.898	3789, 1.885	3911, 2.022
$Al(OH)_5$	-2	3968, 1.879	3955, 1.865	3955, 1.865	3951, 1.860	3848, 1.847		3935, 1.863
$Al(OH)_4$	-1	3980, 1.795	3980, 1.795	3980, 1.794	3980, 1.794			3980, 1.795
$Al(OH)_3$	0	4006, 1.732	3998, 1.729	3983, 1.728				3996, 1.730
$Al(OH)_2$	1	3991, 1.659	3988, 1.658					3990, 1.659
Al(OH)	2	3838, 1.592						3838, 1.592

The larger the wavenumber, ν, the smaller the frequency and the more energy there is in the bond, and thus the stronger bonding condition. Thus, base on the average values in Table 3 and plotted in Figure 13, it can be seen that the strongest bonding of O to H peaks when the Al is in the three coordinate condition. It is progressively weaker with higher or lower coordination, with the single coordinate Al having the weakest O-H bond.

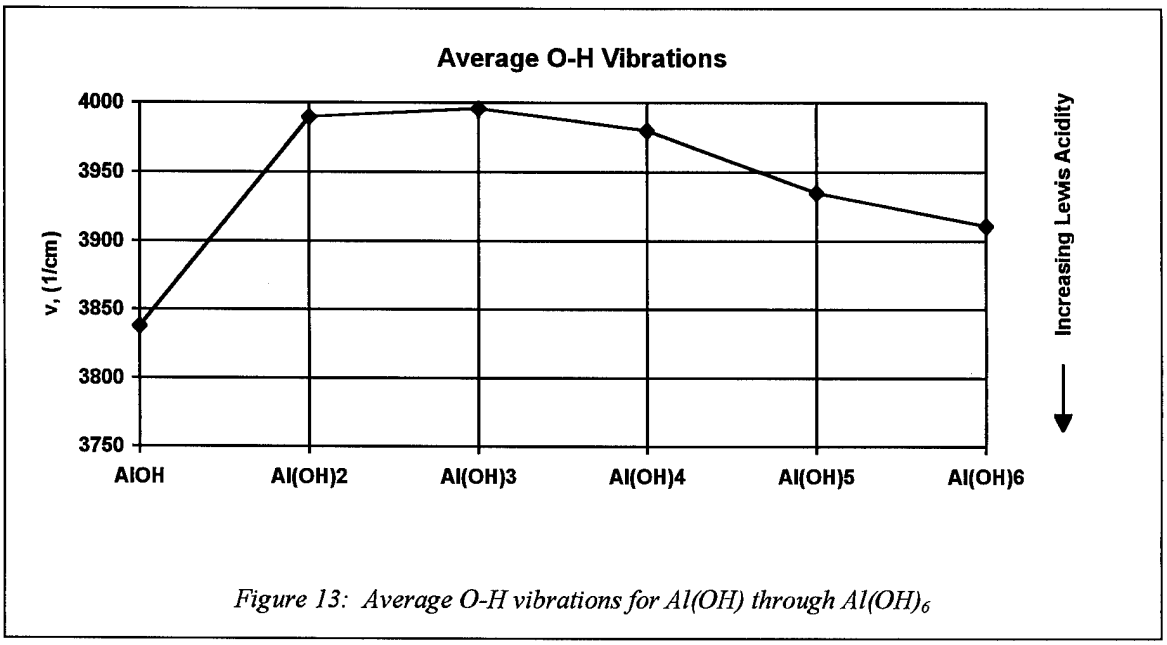

Figure 13: Average O-H vibrations for Al(OH) through $Al(OH)_6$

However, what is of greater concern is the strength of the Al bond to the O because the Al-O bond is what characterizes the Lewis acidity of the Al-site. The bond strength, or the willingness to accept electron pairs is known as the Lewis acidity or Lewis acid strength.

The Al-O bond is the conjugate of the previous O-H results. That is, the stronger the O-H bond the weaker the Al-O bond and the weaker the O-H bond, the stronger the

Al-O bond. Thus, from the above analysis, the Lewis acidity of the Al site increases in the following order of hydroxide coordination: three, two, four, five, six, and one hydroxide coordinate Al, where the one coordinate is the strongest Lewis acid and the three coordinate is the weakest (see Figure 13). This analysis suggest that a three hydroxide coordinated Al is most electrically satisfied and more or less coordination than this leads to increased bonding opportunities.

Assuming bond order conservation, the average Al-O bond distance increases from Al(OH) through $Al(OH)_6$ (see Figure 14). This suggests that the average Al-O bonding condition weakens with each additional OH-group added to the aluminum. This seems reasonable since each additional OH has to share the same Al, which has a finite bonding capability. Thus as the Al is shared among more OH-groups, each individual Al-O bond is weaker and the bond distances increase.

The previous result is not in harmony with the results of the O-H vibrations and our belief that lower O-H vibrations indicate higher Lewis acidity on the aluminum. We believe that using the average values does not necessarily provide clear results because of the variability of the results within each cluster. Although we designed each cluster such that each OH-group attached to the Al would be equal, that was not the result obtained in each case. For example, $Al(OH)_6$ has six OH-groups and the O-H vibrations vary from 3789 to 3984 1/cm and the Al-O bond distances vary from 1.885 to 2.571 Angstroms. On the other hand, each O-H vibration and Al-O bond distance are virtually identical on $Al(OH)_4$.

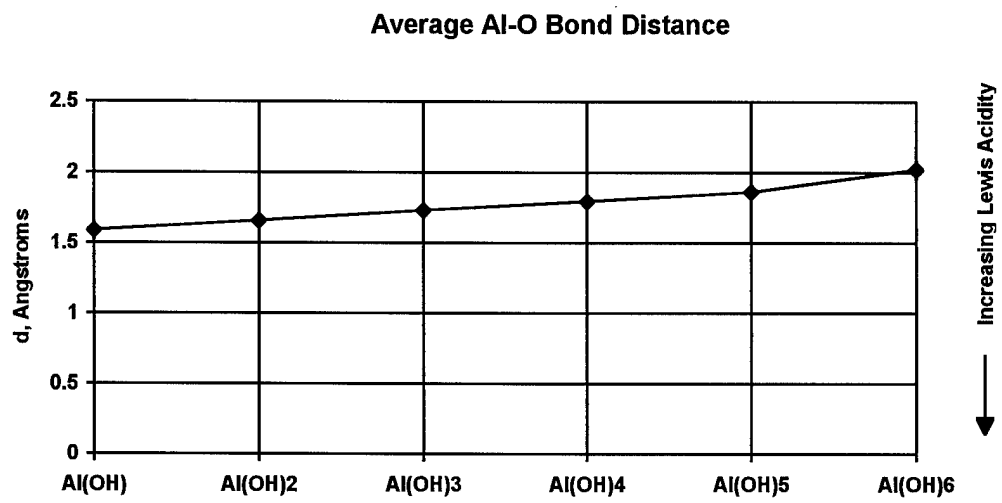

Figure 14: Average Bond Distance for Al(OH) through $Al(OH)_6$

We did notice that the O-H vibrations and Al-O bond distances did directly correspond within each cluster (i.e. the largest vibration goes with the largest distance and the smallest vibration goes with the smallest distance). So, perhaps the vibrations and distances compare bonding sites within each cluster but not across clusters (see Figure 15).

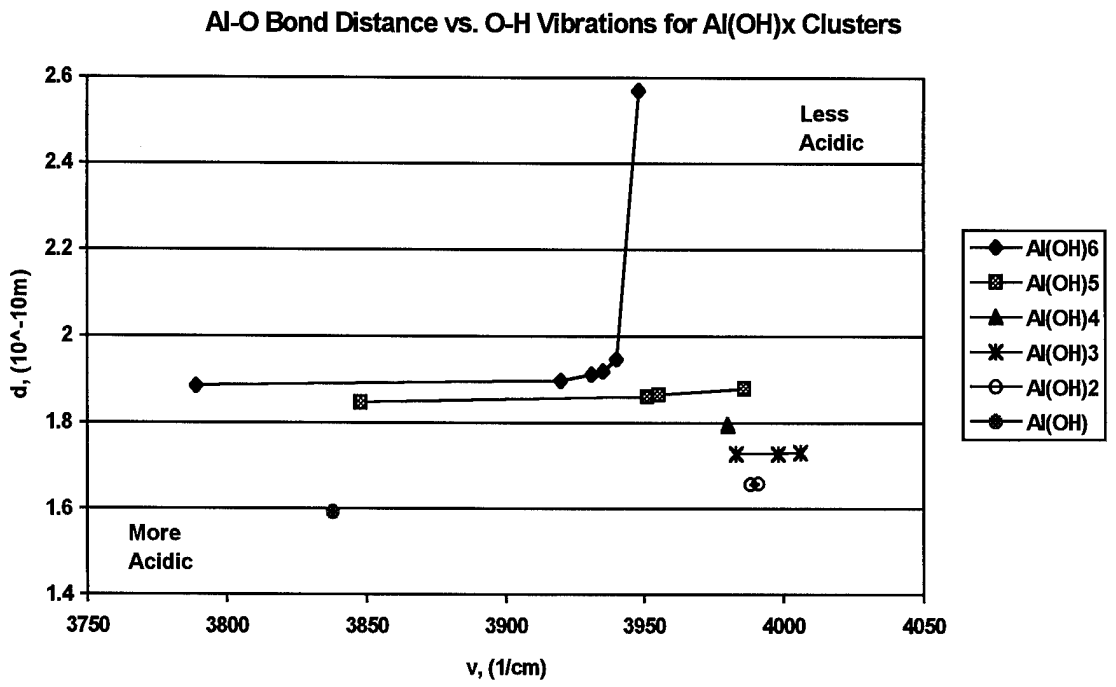

Figure 15: $Al(OH)_x$ acidity trends as determined by O-H vibrations and Al-O bond distances

Figure 15 demonstrates the O-H vibration and Al-O bond distance variability within each cluster and the differences between clusters. With the exception of the endpoints in $Al(OH)_6$, we see that the Al-O distances remain fairly constant across the clusters while the O-H vibrations tend to vary more. Note that it is understood that the fewer the number of OH-groups, the smaller the variability is likely to be. From Figure 15, we also see the same increasing bond distance trend with increasing OH-groups that we had seen in Figure 14.

In summary, O-H vibrations and Al-O bond distances are indicators of Lewis acidity. However, in this case we were only able to apply vibration comparisons within a cluster while bond distances appeared to apply within and across clusters.

Al-Coordination

In this analysis the number of aluminums increased as well as the number of oxygens. Additionally, just one OH-group was attached to the Al site that was being investigated. By investigating just one OH-group, instead of the average of many OH groups, we hoped to have more directly comparable results (see Table 4).

Table 4: O-H vibrations and Al-O bond distances on three to six coordinate Al

Cluster	**Charge**	**ν, (1/cm)**	**d, (10^{-10}m)**
3-Coord	1	3974	1.700
4-Coord	-1	3963	1.783
5-Coord	0	4000	1.781
6-Coord	-2	3973	1.839

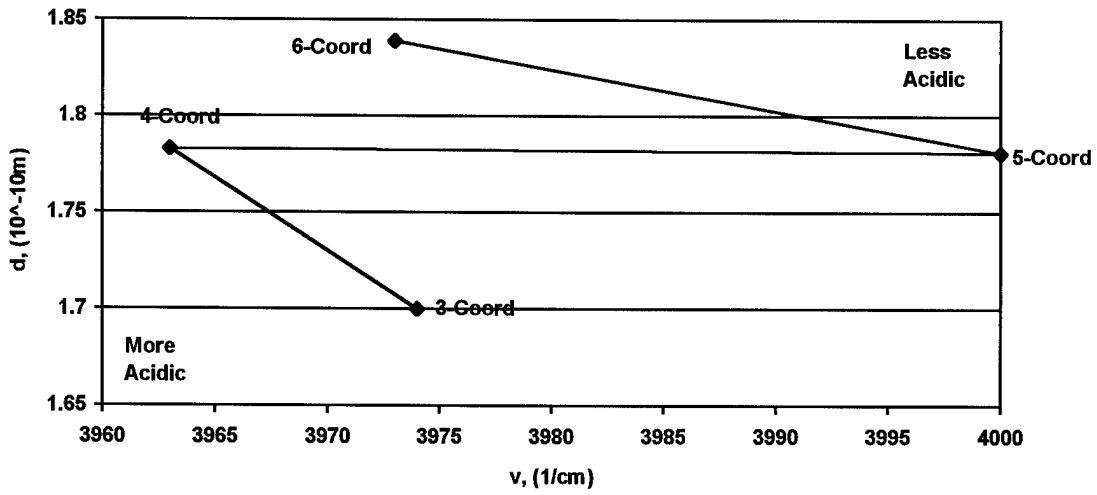

Figure 16: Lewis acidity as measured by O-H vibrations and Al-O bond distance for Al-coordination clusters

This analysis produced vibrations that were much closer to each other than the previous analysis. This time, the vibrations predict the Lewis acid strength of the Al bonding site to increase as follows: five, three, six, and four coordinate. Thus, this analysis predicts the four hydroxide coordinate Al to be the strongest bonding site. However, if the Lewis acidity were based on Al-O bond distance, the acidity would increase as follows: six, four, five and three coordinate (see Figure 16). Although we hoped to eliminate some confusion by investigating only one OH-group instead of varying numbers of OH-groups on a give Lewis acid site, we nonetheless introduced another form of variability in the cluster itself. When we increased the coordination on the central Al atom from four to five, we also added another Al atom to the structure (see Figure 5).

This was done in order to keep the charge on the cluster from becoming excessively negative as O^{-2} atoms were added. However, this had the effect of changing the structure of the cluster significantly. Thus, we feel that it is not necessarily appropriate to compare the results from this series of calculations. Nonetheless, Figure 16 does appear to show that as coordination increases to the bonding site, the bond Al-O bond distance generally increases and the Lewis acidity therefore decreases. This is same trend that we observed with the $Al(OH)_x$ clusters.

Bond Order Conservation

The $Al(OH)_x$ and Al-Coordination clusters demonstrated that bond distances changed in response to Lewis acidity and bond strength. This occurrence led us to believe that we were observing a bond order conservation phenomenon. That is why we proceeded to investigate bond order conservation through the Shustorovich bond order conservation model. Recall that the add-molecule chosen for this comparison was H_2O.

The values from the PM3 calculations for bond lengths and heats of adsorption are plotted against the values predicted by the Shustorovich bond order conservation model for the given approach as described in the previous chapter. The values often differ significantly, but the trends are of greater concern. See figures 17 and 18 below. The complete Shustorovich bond order calculations can be found in appendix A.

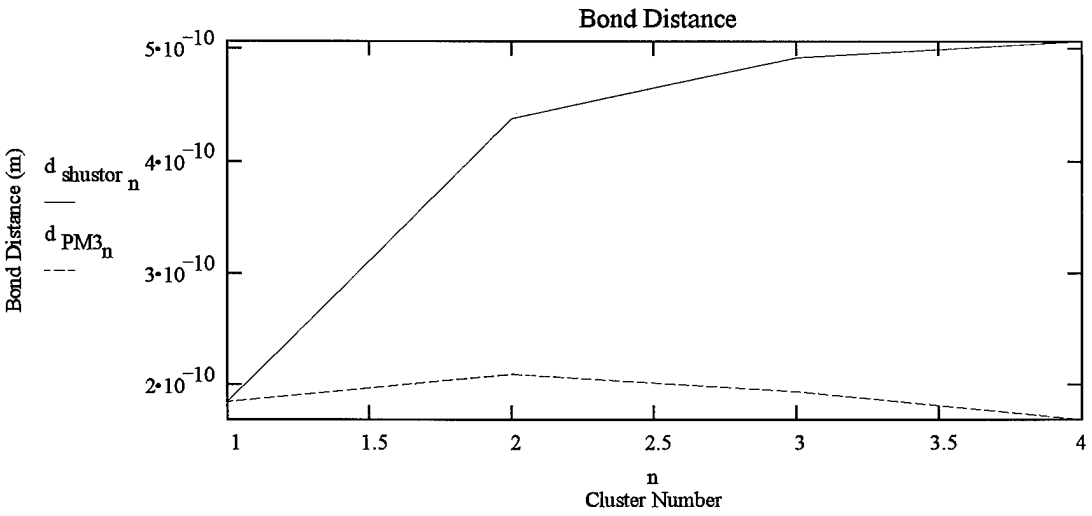

Figure 17: Bond order: Shustorovich predictions vs. PM3 calculations for bond distances. Cluster number: 1=AlOH_2O, 2=Al_2O_2*H_2O, 3=Al_3O_3*H_2O, and 4=Al_4O_4*H_2O*

The Shustorovich calculations predict that the bond distance will increase significantly and then level out. This would indicate that the bonds get continually weaker across the series as Al coordination to the O in the water add-molecule is increased. This result was not anticipated. We expected the bond distances to decrease as Al coordination to the water increased. On the other hand, the PM3 calculations show that bond distance gets somewhat larger on the two Al coordinate bonding condition and then gets smaller on the three and four coordinate bonding conditions. This indicates that the bonds get a little weaker on the number two cluster but then get stronger on the three and four molecule. The strongest bonding condition from the PM3 results is the number four cluster or the Al_4O_4.

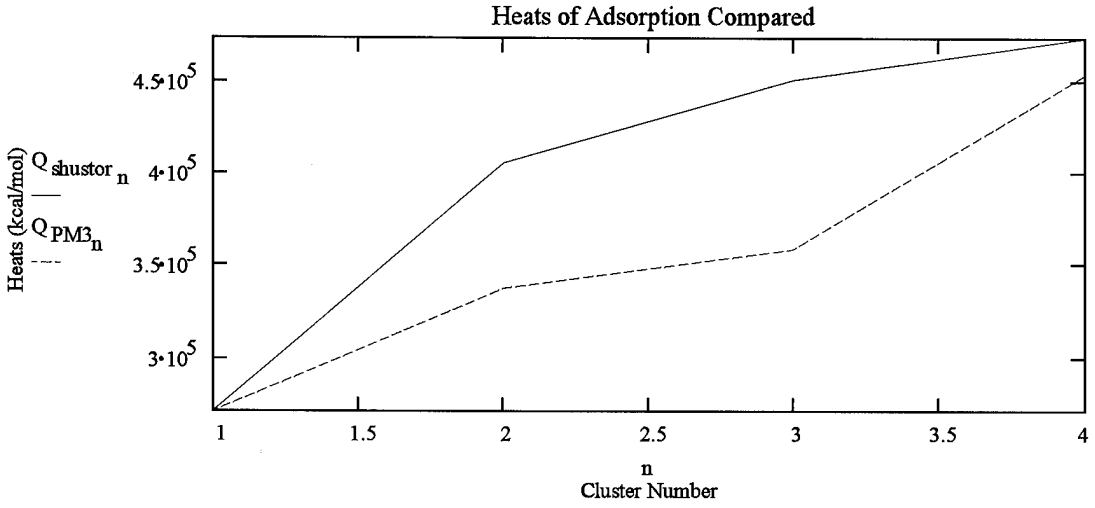

Figure 18: Bond order: Shustorovich predictions vs. PM3 calculations for heats of formation. Cluster number: 1=AlOH_2O, 2=Al_2O_2*H_2O, 3=Al_3O_3*H_2O, and 4=Al_4O_4*H_2O*

The heats of adsorption between the Shustorovich and the PM3 calculations show similar trends, that is, the heat of adsorption increases as the number of Al coordination increases for both the Shustorovich prediction and the PM3 calculations. This is a trend that we expected. We expected the energy in the bonds, bonding the water to the surface would increase with increasing Al coordination.

The results do not show good correlation between the PM3 calculated values and the Shustorovich predicted values. The trends, however, offer greater insight into how the bonding conditions of the molecules change as the molecular structure changes. We believe that the reason the Shustorovich model predicts increasing bonding distances is that Shustorovich's model was intended for use on a metal with and add-atom and we applied his model to a different situation: a metal-oxide with an add-molecule.

Additionally, Benzinger pointed out that Shustorovich is a good approximation when repulsive terms for chemisorption bonding are negligible.[69] However, water, a dipolar molecule, has both attractive (O^{-2}) and repulsive ($2H^{+}$) characteristics. Also, the metal-oxide surface has attractive and repulsive characteristics due the positive Al ions and negative O ions. Thus, we believe the repulsive terms that are not accounted for in the Shustorovich model is one reason that Shustorovich does not correspond better to the PM3 calculations. Another reason that for the differences is that Shustorovich based his theoretical predictions on an add-atom that would be attracted to the positive metal ions of the surface. We however attempted to bond the H^{+} part of the water molecule to the metal ions. Normally, H^{+} would attempt to bond to the electron donating oxygen atoms. Thus, we forced an unnatural condition and should not expect good results. Finally, the Shustorovich model is a simple bond order conservation model whereas PM3 is more sophisticated. Had time permitted, it would have been informative to see how Cl^{-} as an add-atom, would have affected the results of the Shustorovich model. Perhaps better yet would have been to add repulsive terms to Shustorovich's model and then compare them against PM3.

The heat of adsorption trends predicted by the Shustorovich model will be evaluated in the remaining calculations in hope that it will help characterize the strength of the bonding conditions. Also, the bond order conservation idea of decreasing bond length with increasing bond strength will be evaluated. Note that this is not what our application of Shustorovich predicted, but rather typical bond order theory predicts. Thus, as we

discuss BOC in the following results, what we intend to show is that bond energy increases with decreasing bond distances and increasing (negative) heats of adsorption.

Single Bridged

The single bridging oxygen cluster result for three clusters with four different add-atom/molecules are shown in Table 5. Recall that the Al-O coordination is constant within the base clusters. Each Al in the base clusters is bivalent. Also note that the 'SQ' in Al_4O_4SQ denotes that the base structure was square rather than rectangular or diamond shaped. The square shape was maintained in order to keep the clusters as symmetrical as possible so that each Al in the base cluster was essentially equivalent. Note that AlO was not investigated. We believe that an exposed Al atom with only one coordinating O on the surface of an alumina particle is a very unlikely occurrence.

Table 5: Single Bridged Heats of Adsorption and Bonding Distances.

Heats of Adsorption are in kcal/mol and bond distances are in Angstroms.

Name	HF Base	HF X-	HF w/X-	Delta HF	Bond Distance
OH-:					
Al2O2	-171.220	-33.20	-299.011	-94.591	1.384
Al3O3	-245.502	-33.20	-402.896	-124.194	1.222
Al4O4SQ	-298.340	-33.20	-488.980	-157.440	0.904
Cl-:					
Al2O2	-171.220	-55.90	-292.386	-65.266	2.122
Al3O3	-245.502	-55.90	-404.661	-103.259	1.950
Al4O4SQ	-298.340	-55.90	-495.733	-141.493	1.650
F-:					
Al2O2	-171.220	-61.00	-307.363	-75.143	1.381
Al3O3	-245.502	-61.00	-421.867	-115.365	1.493
Al4O4SQ	-298.340	-61.00	-494.820	-135.480	1.459
H2O:					
Al2O2	-171.220	-57.753	-251.702	-22.729	2.087
Al3O3	-245.502	-57.753	-331.014	-27.759	1.931
Al4O4SQ	-298.340	-57.753	-402.610	-46.517	1.670

The results show that the 'Delta HF' or changes in heats of adsorption for the total cluster become more negative in each case as the add-atom/molecule is added to the base cluster. This indicates that the new structure formed is a lower energy structure than when the base and add-atom/molecule were separate. Thus, bonding of the add-atom/molecule is indicated in each ease. See Figure 19.

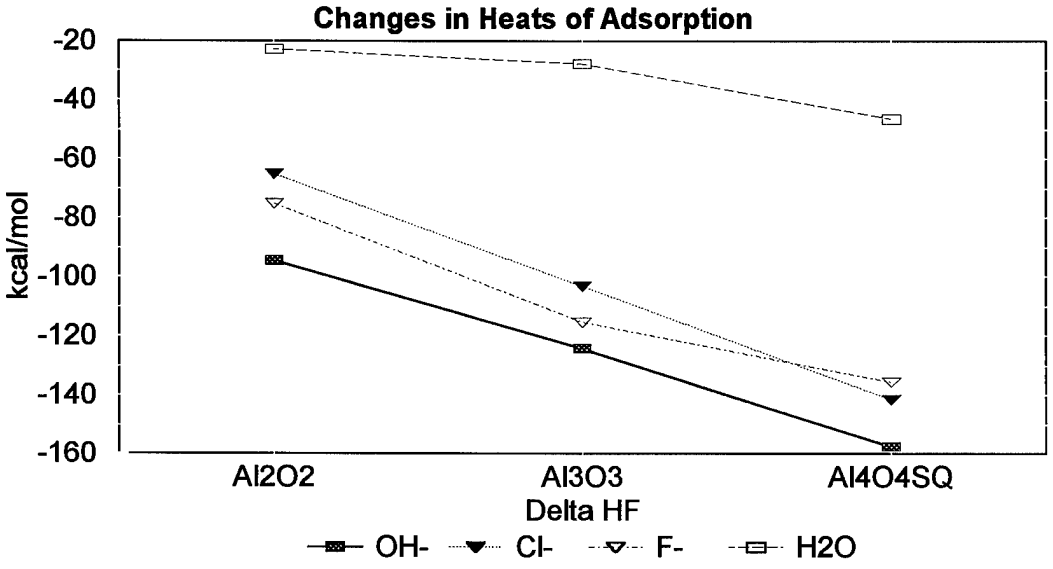

Figure 19: Single bridged changes in heats of adsorption with add-atoms/molecules.

The bond distances decrease across the different base clusters for each add-atom/molecule, with the exception of the fluoride ion which showed a slight increase in bond distance. See Figure 20. The decrease in bond distance tends to indicate an stronger bonding condition, assuming BOC.

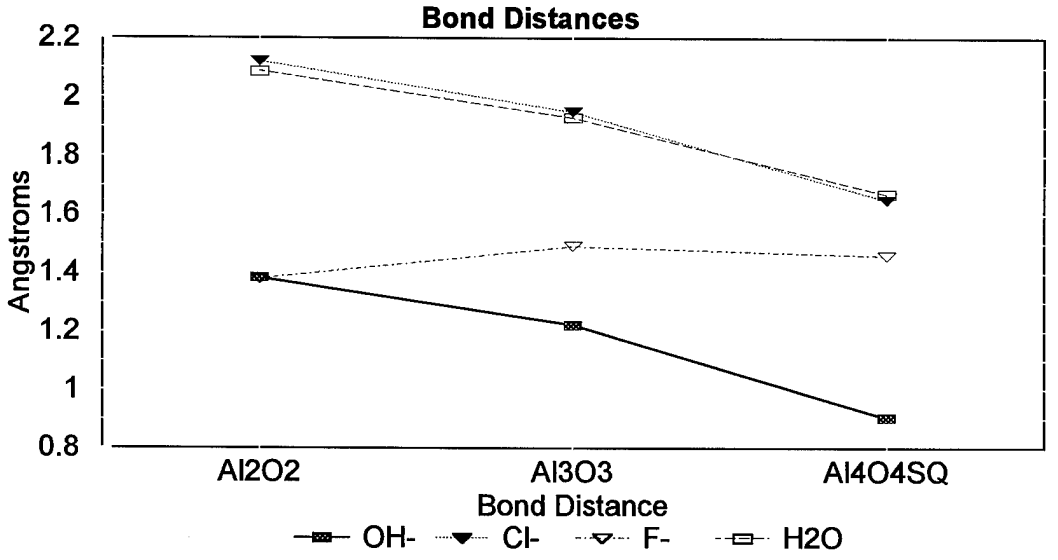

Figure 20: Single bridged changes in bond distances for different add-atoms/molecules

From the from both the heat of adsorption and bond distance results we can conclude that Al_4O_4 provides for the strongest bonding conditions. This agrees with our application of BOC for increasing bond energy with increasing Al coordination to the add-atom/molecule. However, remember from the previous chapter (eq. 24) that $E_n = -Q_n$, where E_n is bond energy and Q_n is total energy. So, as the heats of adsorption become more negative, the bond energy increases.

Double Bridged

The double bridging oxygen cluster result for three clusters with four different add-atom/molecules are shown below in Table 6. Recall that the Al-O coordination is constant within the base clusters. Each Al in the base clusters is tetravalent. Also note that the overall trends are similar to that of the single bridged. Even the values of the

changes in the heats of adsorption brought on by bonding are very similar. The one exception is H_2O, which formed higher energy structures than the single bridged method.

Table 6: Double Bridged Heats of Adsorption and Bonding Distances.

Heats of adsorption are in kcal/mol and bond distances are in Angstroms.

Name	HF Base	HF X-	HF w/X-	Delta HF	Bond Distance
OH-:					
Al2O4	-171.220	-33.20	-291.364	-86.944	1.383
Al3O6	-245.502	-33.20	-394.368	-115.666	1.267
Al4O8	-298.340	-33.20	-499.496	-167.956	0.860
Cl-:					
Al2O4	-171.220	-55.90	-289.005	-61.885	2.192
Al3O6	-245.502	-55.90	-397.350	-95.948	1.972
Al4O8	-298.340	-55.90	-515.200	-160.960	1.607
F-:					
Al2O4	-171.220	-61.00	-307.789	-75.569	1.632
Al3O6	-245.502	-61.00	-414.178	-107.676	1.321
Al4O8	-298.340	-61.00	-511.059	-151.719	0.786
H2O:					
Al2O4	-171.220	-57.753	-198.471	30.502	1.749
Al3O6	-245.502	-57.753	-314.874	-11.619	1.943
Al4O8	-298.340	-57.753	-389.313	-33.220	1.657

The results show that the 'Delta HF' or changes in heats of adsorption for the total cluster decrease in each case as the add-atom/molecule is added to the base cluster, with one exception: H_2O on Al_2O_4. This required an energy input of 30.5 kcal/mol to form the new structure. Otherwise, the decrease in heat of adsorption indicates that the new structure formed is a lower energy structure than when the base and add-atom/molecule were separate. Thus, bonding of the add-atom/molecule is indicated. See Figure 21.

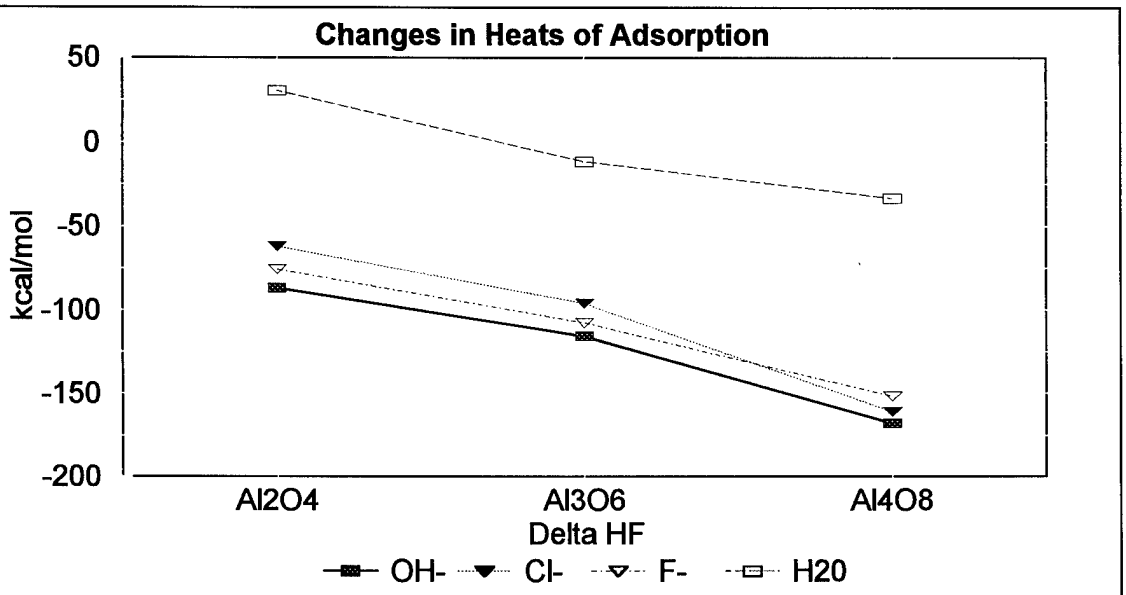

Figure 21: Double bridged changes in heats of formations with add-atoms/molecules.

The bond distances decrease across the different base clusters for each add-atom/molecule, with the exception of the fluoride ion which showed a slight increase in bond distance. See Figure 22. The decrease in bond distance tends to indicate a stronger bonding condition.

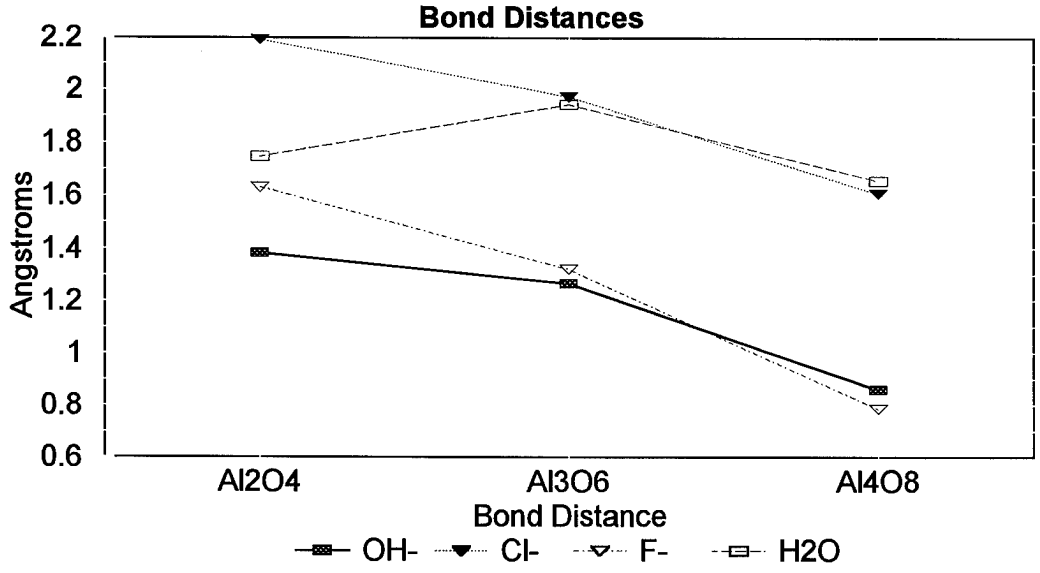

Figure 22: Double bridged changes in bond distances for different add-atoms/molecules

Again, both the heats of adsorption and bond distances show the same trend of increasing bond strength or Lewis acidity with increasing Al coordination to the add-atom/molecule. Also, the heat of adsorption trend is consistent with the BOC prediction as mentioned in the previous section. Thus, from the results we conclude that Al_4O_8 provides for the strongest bonding conditions or that as Al coordination to the add-atom/molecule increases, bond strength and Lewis acidity increases.

Increasing Oxygen Coordination

The affects of increasing the oxygen coordination on an aluminum bonding site was studied and the result are presented below. Table 7 presents tabular data for heats of formation, bond distances, and O-H vibrational results. Figures 23, 24 and 25 graphically display the results for heats of adsorption, bond distances, and O-H vibrations,

respectively. Following these results are the reaction pathway determinations for CFC-12 chemisorption on each of the five oxygen coordination clusters. See Figures 26-30.

Table 7: Heat of adsorption, bond distance and O-H vibrational results for increasing oxygen coordination. Heats of adsorption in kcal/mol, bond distances in Angstroms and vibrations in 1/cm.

Name	HF Base	HF X-	HF w/X-	Delta HF	Bond Distance	Vibration (1/cm)
OH-:						
Al-O-Al	-7.90	-33.20	-205.845	-164.744	1.739	3961
Al-O2-Al	-171.22	-33.20	-270.833	-66.413	1.715	4218
Al-O3-Al	-176.85	-33.20	-274.762	-64.713	1.723	4220
Al-O4-Al	-155.42	-33.20	-309.405	-120.785	1.774	3970
Al-O5-Al	-43.15	-33.20	-155.36	-79.011	1.764	3975
Cl-:						
Al-O-Al	-7.90	-55.90	-183.92	-120.121	2.048	
Al-O2-Al	-171.22	-55.90	-263.579	-36.459	2.265	
Al-O3-Al	-176.85	-55.90	-296.012	-63.263	2.272	
Al-O4-Al	-155.42	-55.90	-284.415	-73.095	2.279	
Al-O5-Al	-43.15	-55.90	-135.16	-36.110	2.322	
F-:						
Al-O-Al	-7.90	-61.00	-230.54	-161.641	1.672	
Al-O2-Al	-171.22	-61.00	-309.164	-76.944	1.681	
Al-O3-Al	-176.85	-61.00	-317.722	-79.873	1.684	
Al-O4-Al	-155.42	-61.00	-338.785	-122.365	1.678	
Al-O5-Al	-43.15	-61.00	-178.98	-74.834	1.678	
H2O:						
Al-O-Al	-7.90	-57.75	-143.85	-78.198	1.839	
Al-O2-Al	-171.22	-57.75	-241.65	-12.680	2.391	
Al-O3-Al	-176.85	-57.75	-223.94	10.653	1.875	
Al-O4-Al	-155.42	-57.75	-228.65	-15.485	2.475	
Al-O5-Al	-43.15	-57.75	-101.18	-0.276	2.475	

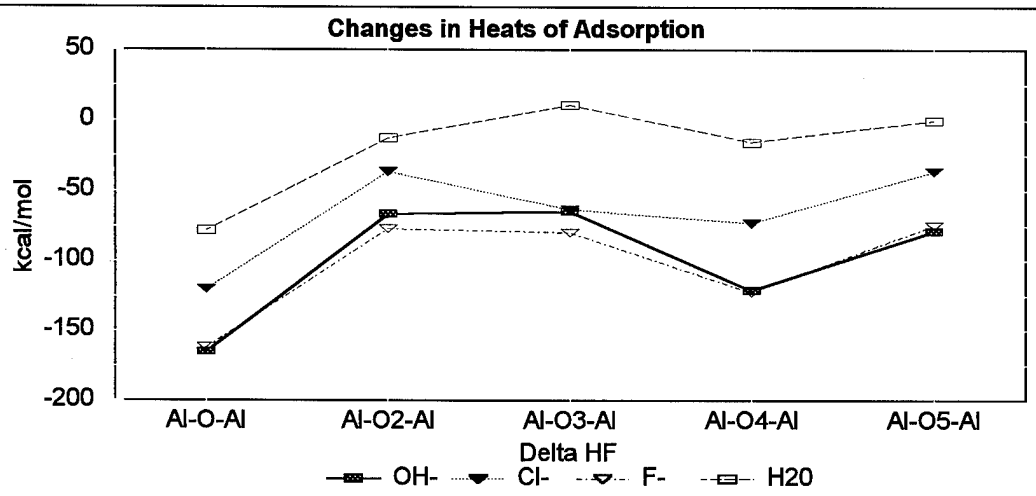

Figure 23: Changes in heats of adsorption as oxygen coordination varies

The results show, across each add-atom/molecule, that the lowest energy clusters are the one and four oxygen coordinated sites, respectively. This indicates that these two clusters represent sites where the Lewis acidity is the greatest.

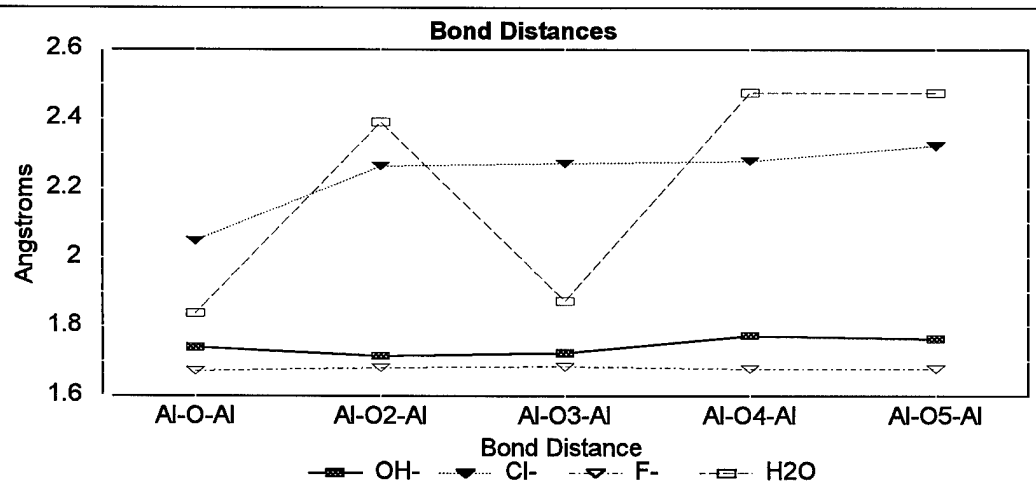

Figure 24: Changes in bond distances as oxygen coordination varies

The change is bond distance (thus bond order) is quite varied for each add-atom/molecule. The bond distance remains relatively unchanged for F^- and OH^- indicating the bond strength remains approximately constant across the series. H_2O however, varies greatly across the series. The results for H_2O indicate that the single and the triple oxygen coordinated site have the shortest and thus strongest bonding conditions. Cl^- indicates that the single oxygen coordinated site is by far the most acidic site when compared to the remaining coordination sites in the series.

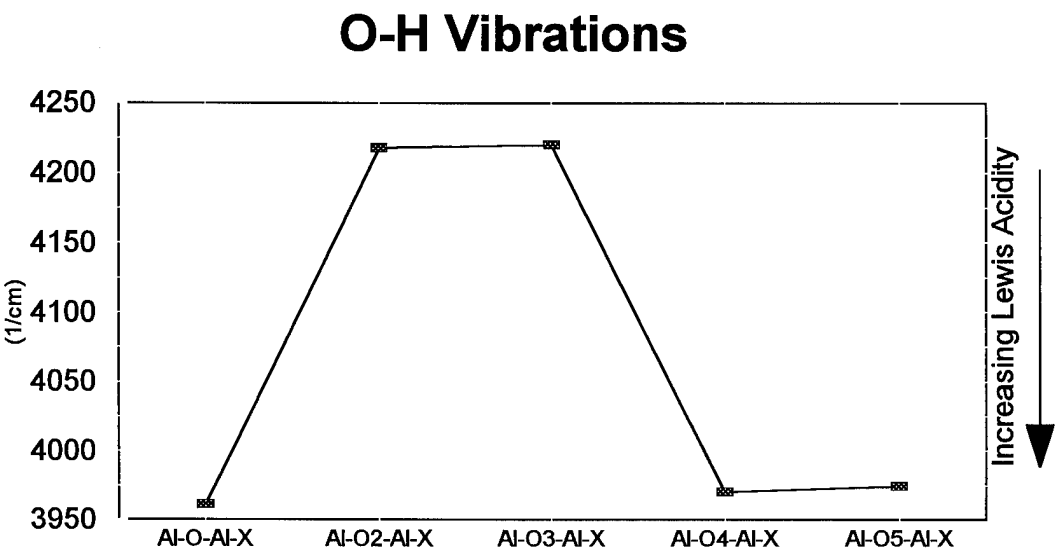

Figure 25: Changes in O-H vibrations as oxygen coordination varies for an OH-group add-molecule

As discussed previously, the higher the wavenumber, the weaker the Al bonding site or the lower the Lewis acidity. This result directly correlates with the results from the heats of adsorption. That is, the O-H vibrational results show that the one and four oxygen coordinated sites are the strongest Lewis acid sites.

Figures 26-30 are intended to show how the energy changes as CFC-12 approaches and chemisorbs on the Lewis acid site of a base cluster, in a pseudo-reaction path format. Unfortunately, the reaction path curves were not as smooth as they could have been. In several instances, the PM3 optimization produced data points which varied greatly from the data points to either side. Upon further investigation, the data points that fell on the expected reaction path curve appeared to show an ionic bonding condition between the anions and cations, that is the anions had large negative charges and the cations had large positive charges. However, the data points that were not on the anticipated curve appeared to be more covalently bonded. That is, the respective negative and positive charges were very small, indicating a covalent or sharing of electrons condition. The 'covalent' points are indicated in Figures 26-30, where appropriate. Also note that the lowest data point on each curve was the value obtained when the base cluster and CFC-12 were optimized, free of bond distance restraints.

In every case examined, the initial part of the semi-empirical optimization appeared to calculate the geometries correctly as the CFC-12 was restrained closer and closer to the surface. No 'covalent' bonding conditions appeared to exist. However, when the restraints were removed and the energies were calculated for the optimized structure, seemingly random 'covalent' point(s) would occur. We believe this to be a deficiency in the semi-empirical result and not representative of the chemisorption process. Thus, in determining the barriers to chemisorption and desorption, the 'covalent' data points were not considered.

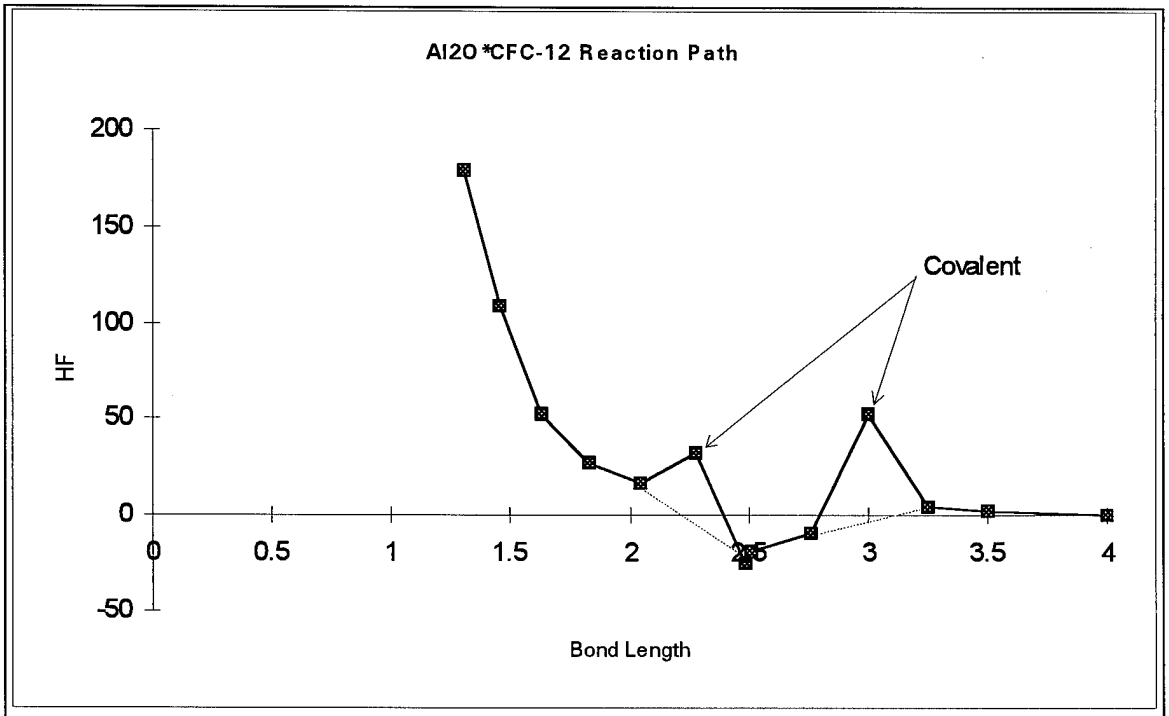

Figure 26: Reaction path for CFC-12 chemisorption on Al_2O

Ignoring the 'covalent' points, the barrier to chemisorption is approximately 3.9 kcal/mol. After crossing this barrier, the CFC-12 falls into a well approximately 28.3 kcal/mol deep. Thus, the CFC-12 is effectively chemisorbed on the surface and would require approximately 28.3 kcal/mol to molecularly desorb from the surface.

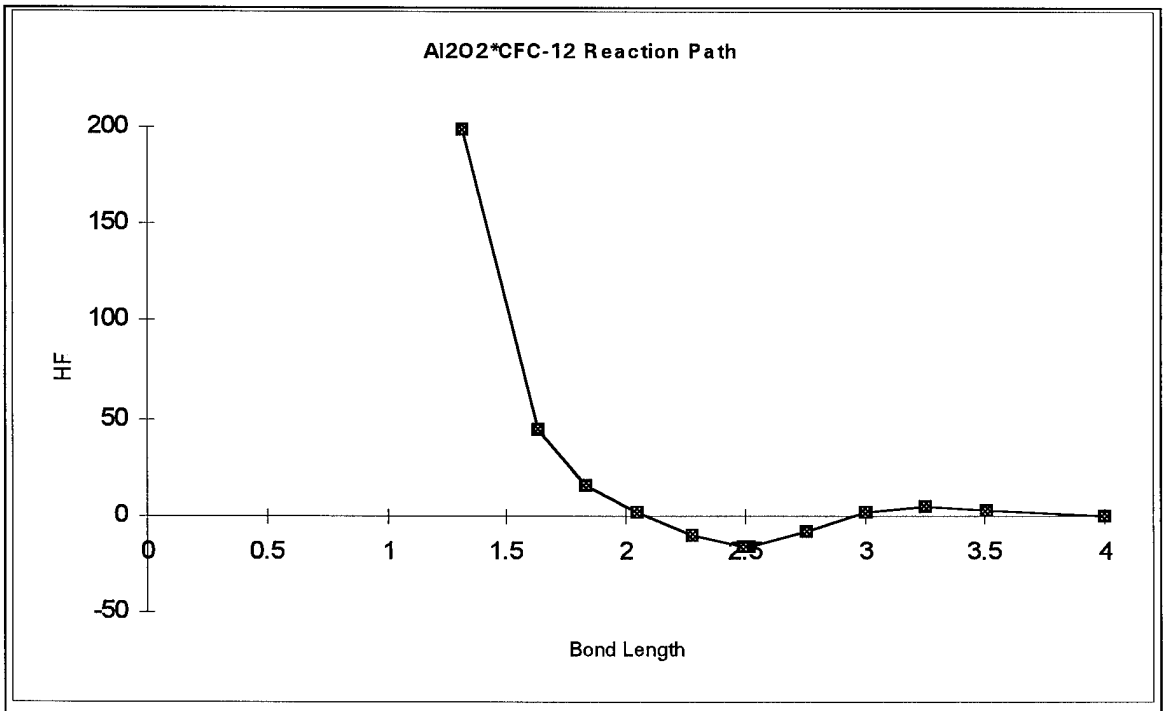

Figure 27: Reaction path for CFC-12 chemisorption on Al_2O_2

In modeling the reaction path for CFC-12 on Al_2O_2, no 'covalent' points were encountered. The barrier to chemisorption was approximate 4.4 kcal/mol and the chemisorbed 'well' was 20.9 kcal/mol deep.

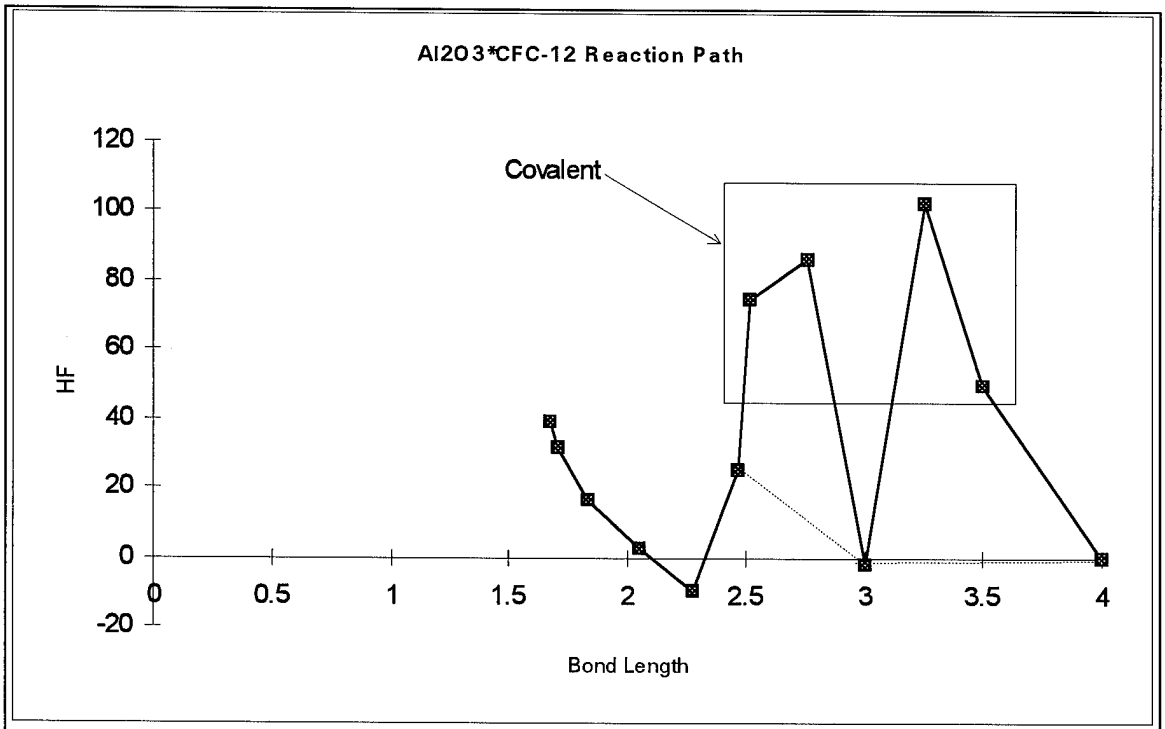

Figure 28: Reaction path for CFC-12 chemisorption on Al_2O_3

From Figure 28, one can see that a significant number of 'covalent' points appeared, such that an accurate determination of chemisorption and the respective barriers were not determined. However, we believe that trend from the previous two clusters, indicate that chemisorption most likely occurred.

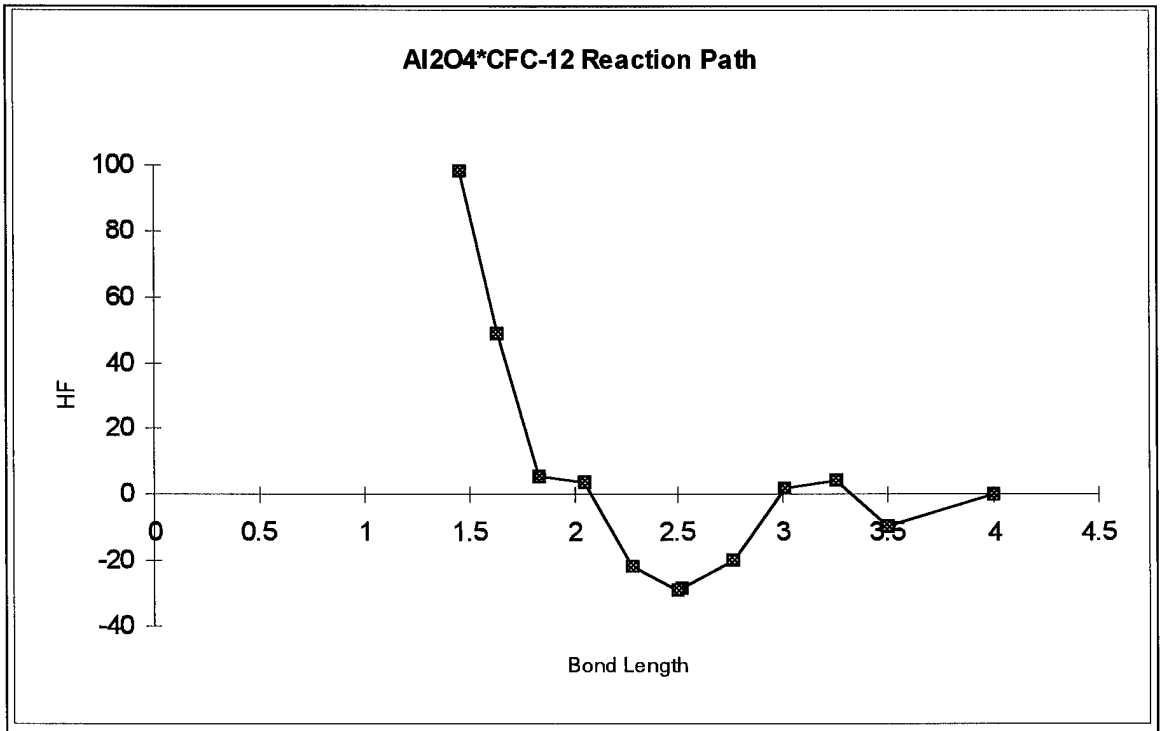

Figure 29: Reaction path for CFC-12 chemisorption on Al_2O_4

No mysterious 'covalent' points manifested themselves in the reaction path calculations for CFC-12 on Al_2O_4. The approximate barrier to chemisorption was 4.4 kcal/mole and the chemisorbed 'well' was approximately 33.4 kcal/mol deep.

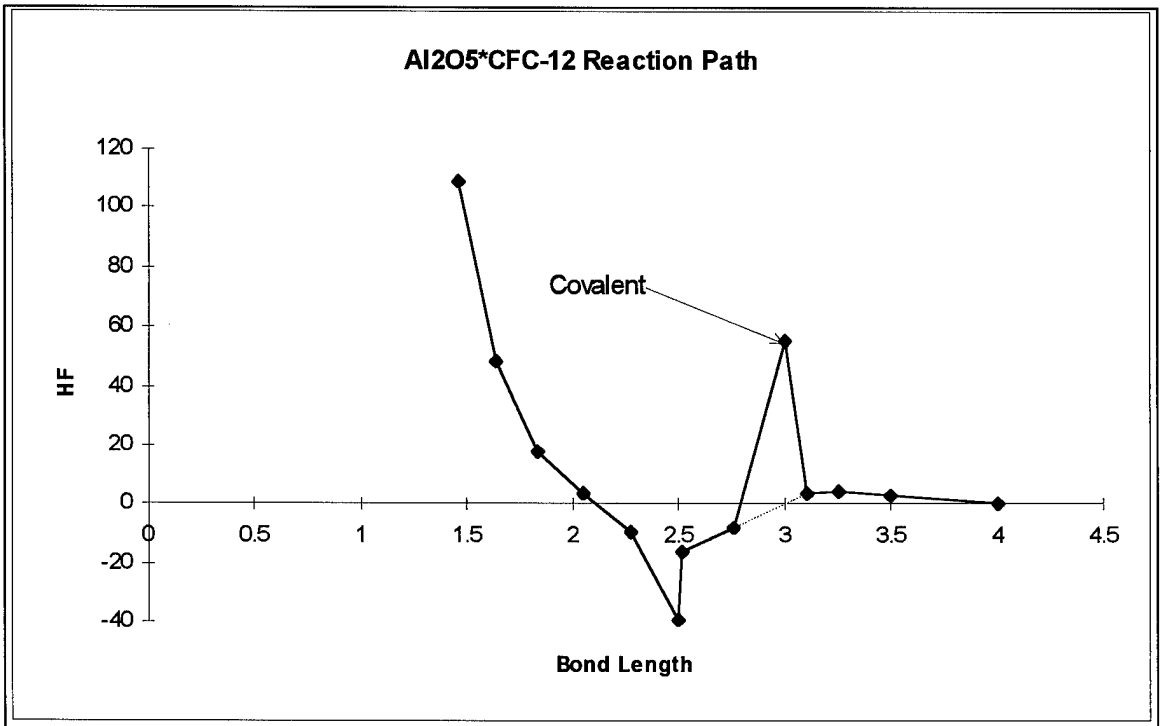

Figure 30: Reaction path for CFC-12 chemisorption on Al_2O_5

In the final reaction path determination as shown in Figure 30, one 'covalent' point appeared. Ignoring this, the chemisorption barrier was approximately 4.4 kcal/mol and the 'well' was approximately 43.7 kcal/mol deep. Note that minimum point obtained from an non-restrained optimization was well below the rest of the curve. This indicates that the other points had an artificially high energy due to energy input to the system through the restraints applied to the base cluster - CFC-12 distance.

With the exception of the unclear data on Al_2O_3, each reaction path indicated a small barrier to chemisorption for about 4 kcal/mol and that chemisorption could occur. The barriers to desorption of the chemisorbed CFC-12 varied from 20.9 - 43.7 kcal/mol

and appeared to increase as the number of coordinating oxygens to the Lewis acid site increased.

Small Cluster Summary

The following are the key items learned from the study of these smaller clusters:

1. Bond strength and thus Lewis acidity increases with increasing Al coordination to the add-atom/molecule.

2. Bond distance is indicative of bond strength. The shorter the bond, the stronger it is.

3. Heat of adsorption is indicative of bond strength. The larger the heat of adsorption, the stronger the bond.

4. O-H vibrations, where available and applicable, are indicative of bond strength.

5. The bond order conservation model, the single bridged series, the double bridged series and the increasing oxygen coordination series all indicated that the four oxygen coordinated aluminum is the strongest Lewis acid of the bond sites we investigated.

These results were then applied to design larger clusters that were intended to be more indicative of actual bonding conditions on the surface of alumina particles.

Large Clusters

The design of larger clusters were based on the results of the smaller clusters and past research, as mentioned in the previous chapter. Past research indicated that aluminums coordinated with three or four oxygens exist on the surface of reactive alumina

species.[68] Fortunately, the results of the smaller clusters tended to bear this out. In general, the smaller cluster results showed that stable structures could exist with various geometries and numbers of oxygen coordinating to each aluminum. Also, the initial geometry results showed that clusters with much more than about 15 atoms started to become time prohibitive. Thus, only a few larger clusters could be investigated.

We chose to examine two types of larger clusters with three and four coordinated Lewis acid sites by modeling chemisorption, dissociation and desorption of CFC-12 and HCl on those sites. The results from that effort were rather straight forward and are provided below. Note, however, that each calculation required anywhere from four to twenty four hours to complete.

Three Coordinate Sites

After the heat of formation of the base cluster was determined (-748.95 kcal/mol), CFC-12 was bonded to the surface in three different orientations (see Figure 12). The results are listed in Table 8 and the following discussion. The first orientation, one Cl bond to an acid site, formed a -6.81 kcal/mol lower energy structure than the base and CFC-12 separate, indicating a likely bonding condition. The second orientation, one Cl bond to an acid site and one C bond the central base site, formed a -3.36 kcal/mol lower energy structure, indicating a likely bonding condition. The third orientation, one Cl bond to each three oxygen coordinated acid site and one C bond to the central base site, formed a -19.73 kcal/mol lower energy structure, indicating a likely bonding condition.

With CFC-12 bonded to the surface in the third orientation, both C-Cl bonds on the CFC were broken and the structure was re-optimized. The new orientation was -0.42

kcal/mol less than before the bonds were broken, suggesting that dissociation of both Cls from CFC-12 ($CCl_2F_2 \rightarrow Cl^- + Cl^- + CF_2^{+2}$) was indeed quite possible if this was truly a new structure. However, the structure formed was virtually identical to the previous and for all intents and purposes, was the same cluster. Thus, we believe that CFC-12 does not actually dissociate into $Cl^- + Cl^- + CF_2^{+2}$ on the surface of this cluster.

With CFC-12 bonded to the surface in the third orientation, three different ionic desorption energies were calculated. First, 4.65 kcal/mol were required to desorb CF_2^{+2}, leaving two Cl^- on the cluster. Second, 30.5 kcal/mol were required to desorb $CClF^+$, leaving one Cl^- on the cluster. Third, 202.9 kcal/mole were required to desorb one Cl^- from the cluster, leaving $CClF^+$. Each desorption energy was positive, indicating that desorption was not probable, especially in the cases of desorbing the chloride ions. Thus, we believe chloride ion desorption is not very likely on these clusters. This makes perfect sense because we would not expect ions to easily desorb off the surface and completely escape the coulombic forces of the surface ions. This study should have been done with radicals rather than ion. We would expect the energies to dissociate and desorb radicals to be much less than that of the ions. Unfortunately, there is not time in this research effort to go back and re-run these calculations.

HCl was next bonded to the surface where the H bonded to the central base site and the Cl bonded to one of the acid sites. The heat of adsorption was -15.65 kcal/mol less, forming a lower energy structure than the base and CFC-12 separate, indicating a likely bonding condition. The H-Cl bond was then broken and the atoms moved apart by approximately one Angstrom, and the cluster was re-optimized. The new structure was

the same as the previous, leading us to believe that HCl dissociation on this surface is not likely. A second attempt was made to dissociate HCl on the surface by separating the atoms even further than before and forcing a bond between the Cl and one of the OH- groups on the octahedral Al that are found at either end of the structure (see Figure 10). The re-optimization indicated an additional 28.98 kcal/mol was required to force this dissociation. Again, this suggested that HCl dissociation on the surface was not likely.

The final calculation was placing OH^- on an acid site and optimizing. The new structure formed a -74.70 kcal/mol lower energy structure than the base and OH^- separate, indicating a highly likely bonding condition. We hoped to be able to compare this result directly with a similar calculation on the larger four coordinate cluster.

In each case, the lower energy structure indicates that the add-molecules will bond. The number value of the decrease not only relates to how tightly the add-molecule is bound but also relates directly to the energy required to desorb the add-molecule.

Table 8: Three Coordinated Cluster Results

Situation	Δ Heat (kcal/mol)	Comments
Three Coordinate Cluster	-748.95	Base cluster
w/CFC-12, single Cl bond	-6.81	First orientation - Chemisorbs
w/CFC-12, Cl and C bonds	-3.36	Second orientation - Chemisorbs
w/CFC-12, two Cl bonds	-19.73	Third orientation - Chemisorbs
w/CFC-12, third orientation, break both Cl bonds ?	-0.42	Cl bonds not broken
w/CFC-12, third orientation, desorb CF_2^{+2} ?	4.65	Does not desorb
w/CFC-12, third orientation, desorb $CClF_2^+$?	30.49	Does not desorb
w/CFC-12, third orientation, desorb Cl^- ?	202.92	Does not desorb
w/HCl on acid site	-15.65	Chemisorbs
HCl dissociation on surface?	28.98	Does not dissociate
w/OH^- ?	-74.70	Chemisorbs

Four Coordinate Sites

After the heat of formation of the base cluster was determined (-757.05 kcal/mol), CFC-12 was bonded to the surface in three different orientations (see Figure 12). The results are listed in Table 9 and the following discussion. The first orientation, one Cl bond to an acid site, formed a 12.00 kcal/mol higher energy structure than the base and CFC-12 separate, indicating an unlikely bonding condition. The second orientation, one Cl bond to an acid site and one C bond the central base site, formed a 36.33 kcal/mol higher energy structure, indicating a very unlikely bonding condition. The third orientation, one Cl bond to each three oxygen coordinated acid site and one C bond to the central base site, surprisingly formed a -14.54 kcal/mol lower energy structure, indicating a likely bonding condition.

With CFC-12 bonded to the surface in the third orientation, both C-Cl bonds on the CFC were broken and the structure was re-optimized. The new orientation was -1.50 kcal/mol less than before the bonds were broken, suggesting that dissociation of both Cls from CFC-12 ($CCl_2F_2 \rightarrow Cl^- + Cl^- + CF_2^{+2}$) was indeed quite possible if this was truly a new structure. However, when PM3 performs an optimization, it optimizes the positions of the atoms with respect to each other, regardless of whether or not there is a bond indicated on the display. So, although the orientation of the molecules changed slightly, they were still close enough to each other to be bonded, indicating that they were not actually dissociated. Thus, we believe that CFC-12 does not actually dissociate into $Cl^- + Cl^- + CF_2^{+2}$ on the surface of this cluster.

With CFC-12 bonded to the surface in the third orientation , three desorption energies were calculated. First, CF_2^{+2} was removed from the surface and re-optimized. The new structure was 20.46 kcal/mole higher in energy, suggesting that approximately 20.46 kcal/mol would be required to dissociate the CF_2^{+2}. Second, one of the two remaining Cl^-, was removed and the structure re-optimized. The calculations indicated that an additional 25.80 kcal/mol were necessary to desorb the Cl^-. The third calculation involved desorbing one Cl^- and leaving $CClF^{+2}$ on the surface. This required 192.5 kcal/mol. Thus, each dissociation energy was positive, indicating dissociation was not probable, especially in the cases of desorbing the chloride ions. Consequently, we believe chloride ion desorption is not very likely on these clusters. However, as mentioned previously, we should have investigated Cl radical desorption. We believe that radicals would more easily desorb than ions.

HCl was next bonded to the surface where the H bonded to the central base site and the Cl bonded to one of the acid sites. The heat of formation was -17.27 kcal/mol less, forming a lower energy structure than the base and CFC-12 separate, indicating a likely bonding condition. The H-Cl bond was then broken and the atoms moved apart by approximately one Angstrom, and the cluster was re-optimized. The new structure was 10.23 kcal/mole higher, leading us to believe that HCl dissociation on this surface is not likely.

The final calculation was placing OH^- on an acid site and optimizing. The new structure formed a 122.26 kcal/mol higher energy structure than the base and OH^- separate, indicating a highly unlikely bonding condition. However, this result was only

obtainable by changing the Hartree-Fock matrix from unrestricted (UHF) to restricted (RHF). This can affect the spin states of the electrons and potentially produce different results. We believe, that in this case, the RHF results were for a different state than the UHF would have produced, thus this result is not comparable to that obtained in the three coordinate cluster.

Only in one orientation did CFC-12 form, a lower energy structure with the base, indicating bonding without energy input. We preface that remark with the understanding that there could be an activation barrier to chemisorption similar to the approximate 4.0 kcal/mol in the increasing oxygen series. However, all attempts to duplicate the reaction path effort failed with these larger clusters. We were not able to optimize CFC-12 in the presence of the optimized base cluster without including the base cluster in the optimization. That is to say, that the method we pioneered with PM3 to develop reaction paths was previously somewhat successful, but was not successful with the large clusters. The number value of the decrease not only relates to how tightly the add-molecule is bound but also relates directly to the energy required to dissociate the add-molecule. Thus, the third CFC-12 orientation and the HCl that 'indicated' bonding could occur with little if any energy input. However, be do believe that the negative values of the bonded molecules do closely approximate the energy required to desorb the add-molecule from the surface.

Table 9: Four Coordinated Cluster Results

Situation	Δ Heat (kcal/mol)	Comments
Four Coordinate Cluster	-757.05	Base cluster
w/CFC-12, single Cl bond	12.00	First orientation - does not chemisorb
w/CFC-12, Cl and C bonds	36.33	Second orientation - does not chemisorb
w/CFC-12, two Cl bonds	-14.54	Third orientation - Chemisorbs
w/CFC-12, third orientation, break both Cl bonds ?	-1.50	Cl bonds probably not broken
w/CFC-12, third orientation, desorb CF_2^{+2} ?	20.46	Does not desorb
w/CFC-12, third orientation, desorb $CClF_2^+$?	25.80	Does not desorb
w/CFC-12, third orientation, desorb Cl^- ?	192.47	Does not desorb
w/HCl on acid site	-17.27	Chemisorbs
HCl dissociation on surface?	10.23	Does not dissociate
w/OH^- ?	122.26	Result suspect. See discussion

Summary

Past research and the results and experience obtained from modeling many different types of small clusters helped to develop the larger clusters on which the most important modeling of this research was to be done. CFC-12, HCl and OH^- optimized on larger clusters composed of adjacent acid and base sites. The results indicated that some instances chemisorption can occur with little or no energy input, that is to say, that the reaction is 'downhill.' Also CFC-12 dissociation on the surface seems unlikely because significant energy is required to dissociate all or part of the CFC. Again, instead of attempting to desorb ions, we should have also investigated the desorption of radicals. HCl did not appear to readily dissociate or desorb without significant energy input.

V. Conclusions and Recommendations

Overview

The main questions that this research effort hoped to answer were: 1) could a CFC chemisorb on the surface of an alumina particle?, 2) could a chemisorbed CFC dissociate on the surface?, 3) could parts of a dissociated CFC desorb off the surface?, and 4) if desorption could occur, could it happen in such a manner as to free up the initial bonding sites, thus allowing them to function as a surface site for catalytic destruction of CFCs? This research used PM3, a respected semi-empirical computational chemistry method, to model potential clusters of acid and base sites and their reactions with a representative CFC, CFC-12. Our conclusions give light to the research questions as well as inspire us to make recommendations for further research efforts in this field.

Chemisorption

CFC-12 chemisorption occurred freely in three orientations on the three coordinate cluster and in one orientation on the four coordinate structure. That is, lower energy structures were formed by bonding CFC-12 to the surface. We believe that this will occur with little or no energy barrier, although we were not able to explicitly demonstrate this on the larger clusters. Nonetheless our results clearly indicate CFC-12 can be chemisorbed on an alumina surface.

Dissociation

As discussed in the previous chapter, the larger clusters from our model indicated that CFC-12 dissociation was not likely due to the large energy inputs that would be

required. Recall that attempts were made to dissociate CFC-12 on the surface, but the PM3 optimization returned the non-joined CFC-12 atoms to molecular CFC-12 chemisorbed on the surface. So, dissociation requires an energy input, the extent of which we were not able to determine.

Further attempts were made to show CFC-12 dissociation by desorbing parts of the chemisorbed CFC-12. After all, we did not expect parts of CFC-12 to desorb without first dissociating on the surface. To do this parts of the CFC-12 molecule were removed from the alumina surface and then the remaining CFC-12/base cluster was reoptimized. Of the dissociation/desorption cases studied, the desorption of CF_2^{+2} required the least energy input, 4.65 kcal/mol. Thermally, a 4.65 kcal/mol barrier is to great to be overcome based on thermal energy in the stratosphere. To understand this, lets look at the temperature dependence of rate coefficients by using the Arrhenius expression (eq. 25):

$$k(T) = Ae^{(-Ea/RT)} \qquad (25)$$

where A is a collision frequency, Ea is the energy required for activation, R is the universal gas constant and T is the temperature of the surroundings. However, we also know that k_{eq} is proportional to the exponential (eq. 26).

$$k_{eq} \sim e^{(-Ea/RT)} \qquad (26)$$

So, in the case of desorbing CF_2^{+2} where Ea = 4.65 kcal/mol, R=1.987 kcal/mol*K and T=275K, (the approximate maximum temperature of the stratosphere), $k_{eq} \sim 2.02 \times 10^{-4}$. . Thus, we believe that ion dissociation does not occur thermally for our models. Had we investigated radicals, perhaps we would have seen dissociation.

Desorption

Free desorption of CFC-12 dissociation products, particularly Cl^- was not observed. The minimum energy required to desorb a Cl^- was 192.5 kcal/mol. Thus, we do not believe that Cl^- desorption occurs at stratospheric temperatures on our models. Again, had we investigated radicals, perhaps we would have seen desorption.

Catalytic

Dissociation and desorption were not observed in our calculations. Without the mechanisms of CFC-12 dissociation and then desorption of the dissociation products, catalytic activity could not occur. Thus, we believe that the catalytic destruction of ozone by the catalytic release of chlorine from CFC-12 on a SRM alumina exhaust particle in the stratosphere does not occur.

Good News

If the predictions of our models are representative of the true alumina surface - CFC reactions in the stratosphere, then perhaps alumina particles are sinks CFCs and other chlorinated compounds rather than a source for CFC breakdown and halogen release. If this were the case, CFCs and other chlorinated compounds would adsorb to the surface of the alumina particle and then eventually be washed out of the stratosphere.

Late Breaking News - Experimental Results

Aerodyne Research, Inc. has recently done some experiments regarding halomethane molecule reactions with γ-alumina. Their results that pertain to this work are as follows:[70]

1. Most CFC-12 fragments on γ-alumina desorb at temperatures < 130K
2. CFC-12 reacts with alumina at <180K, forming surface carbonate species
3. Al^{+3} sites are responsible for reactions
4. Formation of Al-X bond (X=F,Cl) promotes bond cleavage
5. γ-alumina surface reactivity decreases following repeated gas exposure.

Result #1 shows desorption that we did not experience. Result #2 shows a mechanism for CFC-12 dissociation that we did not consider. The oxygen in the carbonate specie must be liberated from the surface or provide by some other unidentified molecule. Again, we did not consider this mechanism. Result #3 agrees with our assumption that Lewis acid or Al^{+3} sites are reactive. Result #4 also agrees with our assumption that bonding to an acid site, especially in the presence of a base site, promotes the dissociation or cleavage of bond in CFC-12. Result #5 indicates that the surface is not catalytic and that the reactive sites are deactivated after repeated exposure. This agrees with our findings that the surface sites are not catalytic. The complete presentation slides can be found in appendix B.

It is clear that our model does not exactly parallel the experimental results. We believe the experimental results are more accurate than our modeling results, thus our

model is insufficient. We believe that this is mostly due to the limited size of our clusters. Our small 'larger clusters' probably did not accurately represent the ionic property of γ-alumina nor provide sufficient acid/base sites to represent the complexity of the alumina surface.

Recommendations

After our experience, we have recommendations for improving the research and for follow on research:

1. Build larger clusters, perhaps ten times the size of the ones we built. We believe that by their size alone, these clusters would be more representative of the alumina particle surface than the clusters we built. In order to do this one would need more powerful computing tools such as workstations or high performance computers.

2. Consider photo-energy inputs into dissociation and desorption instead of just thermal energy inputs. It is possible that photo-energy could be sufficient to for dissociation, desorption and catalytic activity to occur.

3. Look at radical desorption rather than ion desorption from the base clusters. Radical species might be more readily desorbed than ionic species.

4. Verify computed results against experimental results before proceeding with new research. This will lend greater validity to the model. Unfortunately, Aerodyne's results were not available when we started this research.

5. Provide dissociation/desorption scenarios that would allow for the formation of carbonates.

6. When doing Shustorovich bond order calculations/comparisons use a fluorine or chlorine radicals as the add-atom rather than water. We believe that PM3 results would be closer to Shustorovich predictions had we done this.

Summary

We observed CFC-12 chemisorption on the surface of our cluster models and we believe this to be a good result. For the alumina particle to be catalytic to CFC destruction, CFC dissociation and desorption of the dissociation products would need to occur. We did not observe CFC-12 dissociation or desorption of the dissociation products, thus the clusters we modeled do not indicate catalytic activity to CFC destruction. Recent experimental research suggest that dissociation and desorption of dissociation products occurs at stratospheric temperature. The experimental results do not show catalytic activity. We believe that our results did not show dissociation because the clusters we developed were too small and we did not fully investigate all the possible mechanisms for dissociation, like the formation of carbonates as experienced by Aerodyne.

References

[1] Brune, William H. In Air Pollution: Environmental Issues and Health Effects. Edited by S. K. Majumdar, E. W. Miller and John Cahir. The Pennsylvania Academy of Science, p. 136, 1991.

[2] Seinfled, John H. Atmospheric Chemistry and Physics of Air Pollution. New York: John Wiley and Sons, 1986.

[3] WMO, Scientific Assessment of Ozone Depletion: World Meteorological Organization Global Ozone Research and Monitoring Project, *Report No. 25.* World Meteorological Organization, Geneva, Switzerland, (1991).

[4] Husband, D. M. "Continuous Processing of Composite Solid Propellants," Chemical Engineering Progress, 55-61 (1989).

[5] Jackman, C. H. and others. In Scientific Assessment of Ozone Depletion: World Meteorological Organization Global Ozone Research and Monitoring Project, *Report No. 25*, Chapter 10. World Meteorological Organization, Geneva, Switzerland, (1991)

[6] Prather, M., M. M. Garcia, A. R. Douglass, C. H. Jackman, M. K. W. Ko, and N. D. Sze, "The Space Shuttles Impact on the Stratosphere," The Journal of Geophysical Research, 95(D11), 18,583 (1990).

[7] Hawkins, T. W. and B. E. Wilkerson, "Environmental Propellant: Current Issues and Assessment," 1992 JANNAF Propulsion Meeting, Indianapolis, Indiana

[8] Hauser, T. R. Class lecture, ENVR 505, Environmental Ethics. School of Engineering, Air Force Institute of Technology, Wright-Patterson AFB, OH, September 1995.

[9] TIM, Technical Interchange Meeting. Organized by Lt. Col. John J. Shirtz, USAF, SMC/SDZ, Los Angeles Air Force Base, CA. Meeting held 15-16 September 1994, NASA Headquarters, Washington DC.

[10] Lewis, Kerry L. 1Lt, USAF, SMC/SDZB, Los Angeles AFB, CA. Telephone Interview. 1 December 1994.

[11] Karol, I. L. et al. "Effect of Space Rocket Launches on Ozone," Annales Geophysicae 10, 810 (1992).

[12] Krüger, B. C. et al. "Effects of Solid-Fueled Rocket Exhausts on the Stratospheric Ozone Layer," Berichte der Bunsen-Gesellschaft fur Physikalisc 96, 268 (1992).

[13] AIAA. "Atmospheric Effects of Chemical Rocket Propulsion." Report of an AIAA Workshop, American Institute of Aeronautics and Astronautics, Washington, DC, October 1991.

[14] Danilin, M. Yu. "Local Stratospheric Effects of Solid-Fueled Rocket Emissions," Annales Geophysicae 11, 828 (1993).

[15] Denison, M. R.., et al. "Solid Rocket Exhaust in the Stratosphere: Plume Diffusion and Chemical Reactions," Journal of Spacecraft and Rockets, Vol. 31, 435 (1994).

[16] Krüger, B. C. "Ozone Depletion in the Plume of a Solid-Fueled Rocket," Annales Geophysciae 12, 409 (1994).

[17] Cofer, W. R. III, G. C. Purgold, E. L. Winstead, R. A. Edhal. "Space Shuttle Exhausted Aluminum Oxide: A Measured Particle Size Distribution," Journal of Geophysical Research, Vol. 96, NO. D9, 17,371-17,376 (1991).

[18] Robinson, G. N., A. Freedman, C. E. Kolb, and D. R. Worsnop. "Decomposition of Halomethanes on Alpha-Alumina at Stratospheric Temperatures." Geophysical Research Letters, Vol. 21, NO. 5: 377-380 (March 1994).

[19] Knözinger, H. and P. Ratnasamy. "Catalytic Aluminas: Surface Models and Characterization of Surface Sites," Catal. Rev.-Sci. Eng. 17(1): 31-70 (1978).

[20] Ballinger, T.H. and J.T. Yates. "Interaction and Catalytic Decomposition of 1,1,1-Trichloroethane on High Surface Area Alumina. An Infrared Spectroscopic Study," Journal of Physical Chemistry, Vol. 96, 1417 (1992).

[21] Ballinger, T.H., R.S. Smith, S.D. Colson, and J.T. Yates. "Thermal Decomposition of 1,1,1-Trichloroethane and 1,1-Dichloroethene over High surface Area Alumina," Langmuir, Vol. 8, 2473 (1992).

[22] Hegde, R.I., and M.A. Barteau. "Preparation, Characterization, and Activity of Fluorinated Aluminas for Halogen Exchange," Journal of Catalysis, Vol. 120, 387 (1989).

[23] Zolensky, M. E., D. S. McKay and L. A. Kaczor. "A Tenfold Increase in the Abundance of Large Solid Particles in the Stratosphere, as Measured Over the Period 1976- 1984." Journal of Geophysical Research, Vol. 94, NO. D1, 1047-1056 (1989).

[24] Datta, A. "Evidence for Cluster Sites on Catalytic Alumina," Journal of Physical Chemistry, Vol. 93, 7054 (1989).

[25] Stewart, J. J. P. "MOPAC: A Semiempirical Molecular Orbital Program," Journal of Computer-Aided Molecular Design 4, 1-105:1990

[26] Bennett, R. R. "'Clean' Propellants and the Environment," AIAA Report No. 92-3398, 1992.

[27] Toumi, R., B. J. Kerridge, and J. A. Pyle, "Highly Vibrational Excited Oxygen as a Potential Source of Ozone in the Upper Stratosphere and Mesosphere," Nature 351, 217 (1991).

[28] Schumann, U., and D. Wurzel. "Impact of Emissions from Aircraft and Spacecraft Upon the Atmosphere," Proceedings of an International Scientific Colloquium, Colonge, Germany, April 18-20. 1994.

[29] McElroy, M. B. and R. J. Salawitch, "Changing Composition of the Global Stratosphere," Science 243, 763 (1989).

[30] World Meterological Organization. "Scientific Assessment of Ozone Depletion: 1991." Global Ozone Research and Monitoring Project, Report NO. 25., p 1.3 Geneva, Switzerland, 1991.

[31] World Meterological Organization. "Scientific Assessment of Ozone Depletion: 1991." Global Ozone Research and Monitoring Project, Report NO. 25. , p 6.5, Geneva, Switzerland, 1991.

[32] Halverson, T., "Proposed Rocket Test Puts NASA on the Defensive," Florida Today, Oct. 28, 1991

[33] Bennett, R. R. Thiokol Corp. Telephone Interview. 19 September 1995.

[34] Cragun, B. C., "Hazards Properties of a Magnesium Neutralized Clean Propellant," paper presented a the 1992 JANNAF Propulsion Systems Hazards Subcommittee Conference, Silver Springs MD, April 1992

[35] Katzakian, A. Jr, "Alternate Clean Propellant Development," report prepared for the Astronautics Laboratory (AFSC), Report No. LHL-M-04, 20 October 1990

[36] Katzakian, A. Jr., G. M. Clark, C. E. Grix, R. L. Lou, and A. E. Oberth, "Development of a New High Performance Clean Solid Propellant," paper presented at the 1992 JANNAF Propellant Development and Characterization Subcommittee Meeting, Kennedy Space Center, Florida, 7-9 April, 1992.

[37] Katzakian, A. Jr, "Alternate Clean Propellant Development," report prepared for the Astronautics Laboratory (AFSC), Report No. LHL-M-04, 20 October 1990

[38] Katzakian, A. Jr., G. M. Clark, C. E. Grix, R. L. Lou, and A. E. Oberth, "Development of a New High Performance Clean Solid Propellant," paper presented at the 1992 JANNAF Propellant Development and Characterization Subcommittee Meeting, Kennedy Space Center, Florida, 7-9 April, 1992.

[39] Weyland, H. H. and R. R. Miller, "Clean Propellant for Large Solid Rocket Motors," Final report prepared for the Astronautics Laboratory (AFSC), Report No. AL-TR-90-016, 1990.

[40] Bradford, D. J., et al., "Clean Propellant Development Demonstration," report prepared for the Astronautics Laboratory (AFSC), Contract No. F04611-89-C-0082, Report Nos. 13 and 16, 1991

[41] Katzakian, A. Jr, "Alternate Clean Propellant Development," report prepared for the Astronautics Laboratory (AFSC), Report No. LHL-M-04, 20 October 1990

[42] Katzakian, A. Jr., G. M. Clark, C. E. Grix, R. L. Lou, and A. E. Oberth, "Development of a New High Performance Clean Solid Propellant," paper presented at the 1992 JANNAF Propellant Development and Characterization Subcommittee Meeting, Kennedy Space Center, Florida, 7-9 April, 1992.

[43] Lewis, Kerry L. 1Lt, USAF, SMC/SDZB, Los Angeles AFB, CA. Telephone Interview. 1 December 1994.

[44] Jackman, C. H. and others. In Scientific Assessment of Ozone Depletion: World Meteorological Organization Global Ozone Research and Monitoring Project, *Report No. 25*, Chapter 10. World Meteorological Organization, Geneva, Switzerland, (1991).

[45] Pyle, J. A., Report on the predicted effects of Arianne-V on the atmosphere using a two-dimensional model, submitted to ESA, (1991).

[46] Prather, M., M. M. Garcia, A. R. Douglass, C. H. Jackman, M. K. W. Ko, and N. D. Sze, "The Space Shuttles Impact on the Stratosphere," The Journal of Geophysical Research, 95(D11), 18,583 (1990)

[47] Molina, M. J., T-L Tso, L. T. Molina, and F. C-Y Wong. "Antarctic Stratospheric Chemistry of Chlorine Nitrate, Hydrogen Chloride, and Ice: Release of Active Chlorine," Science Vol. 238, 1253 (1987).

[48] Brasseur, G. P., Granier, C., and Walters, S., "Future Changes ins Stratospheric Ozone and the Role of Heterogeneous Chemistry", Nature 348, 626 (1990)

[49] Cofer, W. R. III, G. Garland Lala, and James P. Wightman. "Analysis of Mid-Tropospheric Space Shuttle Exhausted Aluminum Oxide Particles," Atmospheric Environment Vol. 21, No. 5, pp. 1187-1196, 1987.

[50] Dill, K. M., R. A. Reed, V. S. Calia, and R. J. Schultz. "Analysis of Crystalline Phase Aluminum Oxide Particles From Solid Propellant Exhaust," Journal of Propulsion, Sep-Oct, p 668-671, 1990.

[51] Peri, J. B., "A Model for the Surface of γ-Alumina," Journal of Physical Chemistry Vol 69 No 1, 220-230 (1965).

[52] Moeller, Therald and others. Chemistry With Inorganic Qualitative Analysis. Orlando: Academic Press, 1984.

[53] Wierschke, Scott G. A Computational Study of The Tensile and Compressive Properties of Ordered Polymers via The Austin Model 1 (AM1) Semi-Empirical Molecular Orbital Method. AFWAL-TR-88-4201. Wright-Patterson AFB, OH: Polymer Branch, October 1988.

[54] Hoffman, R. "An Extended Huckel Theory. I. Hydrocarbons," Journal of Chemical Physics, Vol 39, p. 1397 (1963).

[55] Hoffman, R. "Site Preferences and Bond Length Differences in $CaAl_2Si_2$-Type Zintl Compounds," Journal of the American Chemical Society, Vol 108, p. 1876 (1986).

[56] Parr, R. G., R. Pariser. "A Semi-Empirical Theory of the Electronic Spectra and Electronic Structure of Complex Unsaturated Molecules," Journal of Chemical Physics, Vol 21, p. 466, 767 (1953).

[57] Pople, J. A., D. P. Santry and G. A. Segal. "Approximate Self-Consistent Molecular Orbital Theory," Journal of Chemical Physics, Vol 43, p. 5129 (1965).

[58] Pople, J. A., and D. L. Beveridge, Approximate Molecular Orbital Theory, McGraw Hill, New York (1970).

[59] Hypercube, Inc. Computational Chemistry. HyperChem manual (HC40-00-03-00). Waterloo, Ontario, Canada, April 1994.

[60] Dewar, M. J. S. "Qunatum Organic Chemsitry," Science, Vol 187, p. 1037 (1975).

[61] Bingham, R. C., M. J. S. Dewar, and D. H. Lo. "Ground States of Molecules. XXV. MINDO/3. An Improved Version of the MINDO Semiempirical SCF-MO Method," Journal of the American Chemical Society, Vol 97, p. 1285 (1975).

[62] MOPAC 93. User Manual. First Edition, Fujitsu Limited. May 1993.

[63] Clark, T. A Handbook of Computational Chemistry, Wiley, New York, (1985).

[64] Dewar, M. J. S., and W. Thiel. "Ground States of Molecules. 38. The MNDO Method. Approximations and Parameters," Journal of the American Chemical Society, Vol 99, p. 4899 (1977).

[65] Dewar, M. J. S., E. G. Zoebisch, E. F. Healy, and J. J. P. Stewart. "AM1: A New General Purpose Qunatum Mechanical Molecular Model," Journal of the American Chemical Society, Vol 107, p. 3902 (1985).

[66] Stewart, J. J. P. In Reviews in Computational Chemistry: Semiempirical Molecular Orbital Methods, Edited by K. B. Lipkowitz and D. B. Boyd. HNC Publishers, p.45, (1990).

[67] Shustorovich, Evgeny. "Chemisorption Phenomena: Analytical Modeling Based on Perturbation Theory and Bond-Order Conservation," Surface Science Reports Vol. 6, p. 1-63, (1986).

[68] Kawakami H. and S. Yoshida. "Quantum Chemical Studies of Alumina: Part 3 - Acidity and Basicity of the Spinel-Type Crystal," Journal of the American Chemical Society, Faraday Transactions No. 2, Vol 82, p. 1385, (1986).

[69] Benzinger, J. B. In Metal surface Reaction Energetics: Theory and Applications to Heterogeneous Catalysis: Thermochemical Methods for Reaction Energetics on Metal Surfaces. Edited by Evgeny Shustorovich. New York: VCH (1991).

[70] Aerodyne Research, Inc. "Reaction of Halomethane Molecules With γ-Alumina." Results presented at AFOSR contractors meeting. Washington D. C. 22 October 1995.

Appendix A

SHUSTOROVICH / BOND ORDER CONSERVATION $ORIGIN \equiv 1$ $mole := henry$

Let index (n) for:
Maximum energy for On-Top site = 0
On-Top site = 1
Bridge site = 2
Hollow site = 3,4

NOTE: n=1: O-Al-OH2
n=2: Al2O2-OH2
n=3: Al3O3-OH2
n=4: Al4O4-OH2

Set-up index:

$n := 1..4$ This number could be higher, depending on the number of different bridge and hollow sites

The Speed of Light: $c := 2.9979 \cdot 10^{8} \cdot \frac{m}{sec}$

Mass of adatom (H20):

$$\mu := \begin{bmatrix} 18.01 \\ 18.01 \\ 18.01 \\ 18.01 \end{bmatrix} \cdot \frac{gm}{mole}$$ (Periodic Table)

Angle between M-A vector and the surface normal:

$\psi 4$ is the larger of the two possible angles. It comes from the shortest Al-OH2 bond.

$$\psi := \begin{bmatrix} 0 \\ 31.3 \\ 38.4 \\ 47.5 \end{bmatrix} \cdot deg$$ (PM3)

Determine the vibrational frequencies of the M-A bonds:

Observed Values:

$$wavenumber := \begin{bmatrix} 646.02 \\ 524.73 \\ 660.14 \\ 702.73 \end{bmatrix} \cdot \frac{1}{cm}$$ (PM3)

Convert Wavenumber to Wavelength: $\lambda_n := \frac{1}{wavenumber_n}$

Convert Wavelength w/Speed of Light to frequencies:

$$\omega_n := \frac{c}{\lambda_n}$$

The resulting frequencies:

$$\omega = \begin{bmatrix} 1.937 \cdot 10^{13} \\ 1.573 \cdot 10^{13} \\ 1.979 \cdot 10^{13} \\ 2.107 \cdot 10^{13} \end{bmatrix} \cdot \sec^{-1}$$

Now, calculate the Shustorovich values for Heat of Chemisorption, Q, and Bond Length, d:

Prime the equations with the initial, n=1, values:

$$Q_1 := 64.536 \cdot \frac{kcal}{mole} \qquad \text{(PM3)}$$

$$d_0 := 1.839 \cdot 10^{-10} \cdot m$$

Shustorvich Equation (5) for the maximum M-A bond energy:

$$Q_{shustor_n} := Q_1 \cdot \left(2 - \frac{1}{n}\right)$$

The resulting values:

$$Q_{shustor} = \begin{bmatrix} 64.536 \\ 96.804 \\ 107.56 \\ 112.938 \end{bmatrix} \cdot \frac{kcal}{mole}$$

In order to calculate the Bond Length, d, it is necessary to first determine the coefficient, a, from Shustorovich's Equaltion (16):

$$a_n := \frac{\cos(\psi_n)}{\omega_n} \cdot \left(\frac{2 \cdot Q_{shustor_n}}{\mu_n}\right)^{\frac{1}{2}}$$

The resulting "a" coefficients:

$$a = \begin{bmatrix} 2.828 \cdot 10^{-10} \\ 3.644 \cdot 10^{-10} \\ 2.8 \cdot 10^{-10} \\ 2.324 \cdot 10^{-10} \end{bmatrix} \cdot m$$

Shustorovich Bond Length Equation (15):

$$d_{shustor_n} := d_0 + a_n \cdot \ln(n)$$

The bond lengths:

$$d_{shustor} = \begin{bmatrix} 1.839 \cdot 10^{-10} \\ 4.365 \cdot 10^{-10} \\ 4.916 \cdot 10^{-10} \\ 5.06 \cdot 10^{-10} \end{bmatrix} \cdot m$$

Now compare the PM3 calculations against the Shustorovich model:

First use the Heats of Formation, HF, from the Hyperchem Log files to determine the Q's:

$$HF := \begin{bmatrix} -28.361 \\ -92.897 \\ -171.220 \\ -251.702 \\ -245.502 \\ -331.014 \\ -294.34 \\ -402.610 \end{bmatrix} \cdot \frac{kcal}{mole} \qquad \text{(PM3)} \qquad Q_{PM3} := \begin{bmatrix} HF_1 - HF_2 \\ HF_3 - HF_4 \\ HF_5 - HF_6 \\ HF_7 - HF_8 \end{bmatrix}$$

The resulting Q's:

$$Q_{PM3} = \begin{bmatrix} 64.536 \\ 80.482 \\ 85.512 \\ 108.27 \end{bmatrix} \cdot \frac{kcal}{mole}$$

Observed Bond Lengths:

"Muli-Coordinate"

$$d_{PM3} := \begin{bmatrix} 1.839 \cdot 10^{-10} \\ 2.086 \cdot 10^{-10} \\ 1.931 \cdot 10^{-10} \\ 1.670 \cdot 10^{-10} \end{bmatrix} \cdot m \qquad \text{(PM3)}$$

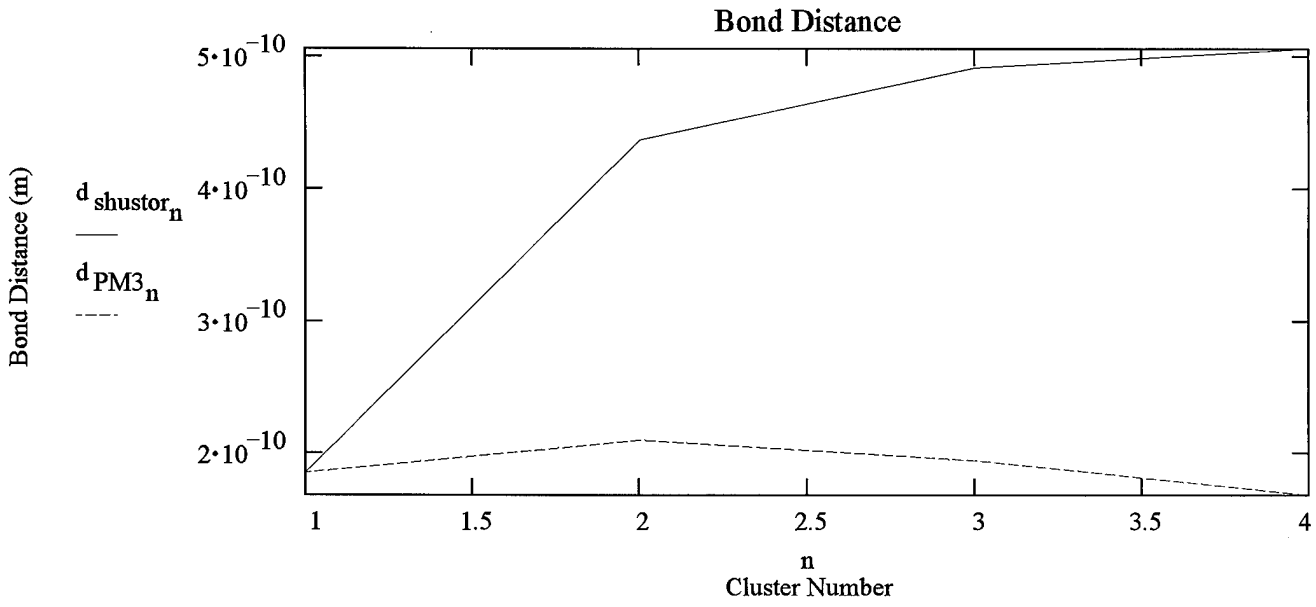

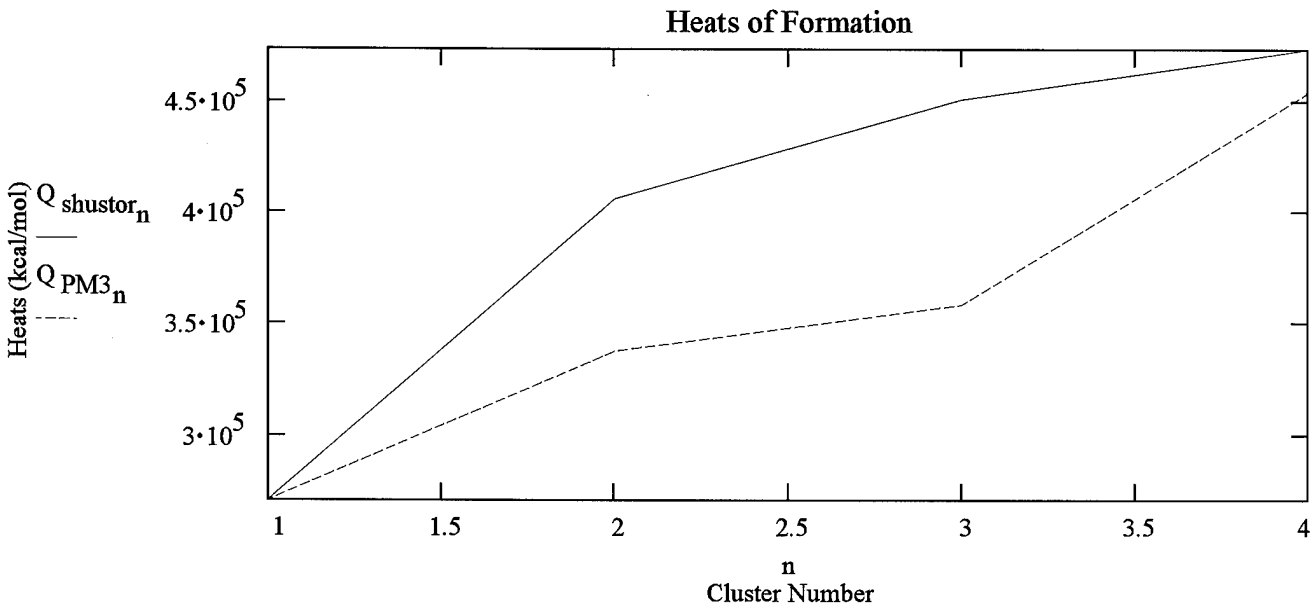
Heats of Formation
Heats (kcal/mol)
Q shustor_n
Q PM3_n
4.5·10^5
4·10^5
3.5·10^5
3·10^5
1
1.5
2
2.5
3
3.5
4
n
Cluster Number

Appendix B

AERODYNE RESEARCH, Inc.

REACTIONS OF HALOMETHANE MOLECULES WITH γ- ALUMINA

45 MANNING ROAD
BILLERICA, MA 01821
(508)663-9500; FAX:(508)663-4918

AERODYNE RESEARCH, Inc.

QING DAI, GARY ROBINSON and ANDREW FREEDMAN

CENTER FOR CHEMICAL and ENVIRONMENTAL PHYSICS

Research Supported by the Space and Missiles Systems Center and the Air Force Geophysics Directorate

45 MANNING ROAD

BILLERICA, MA 01821

(508)663-9500; FAX:(508)663-4918

HALOCARBON CHEMICAL LIFETIMES

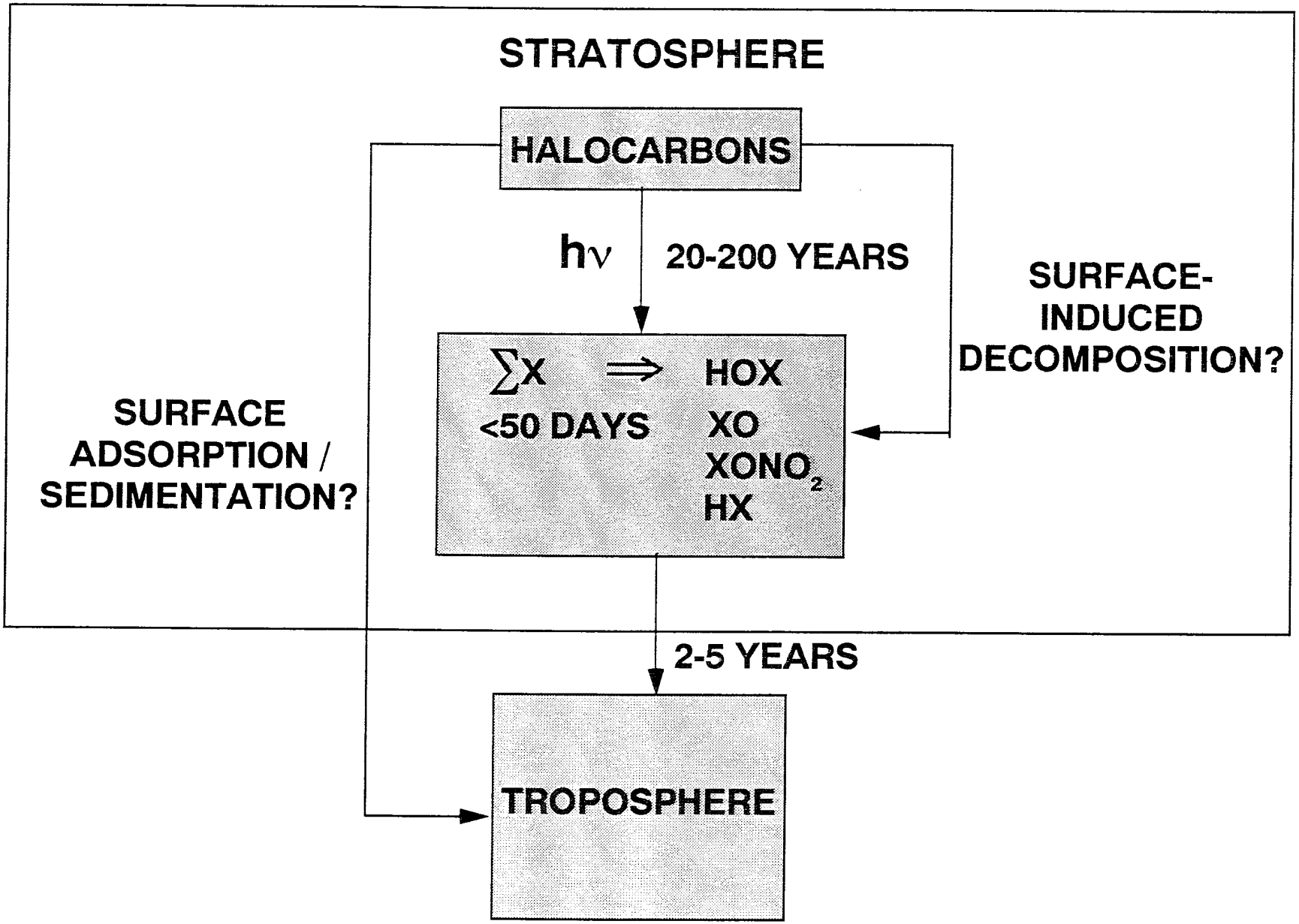

EXPERIMENTAL APPROACH

POWDER SAMPLES IN ULTRAHIGH VACUUM ENVIRONMENT

- γ- ALUMINA POWDER SAMPLES PREHEATED TO 1000K IN VACUUM BEFORE EXPOSURE
- TPD & FTIR EXPERIMENTS:
  SAMPLE EXPOSURE @ 100K
- XPS EXPERIMENTS:
  SAMPLE EXPOSURE @ 150K AND 200K
- FT-IR TRANSMISSION SPECTRA COLLECTED AT 100K AFTER SAMPLE IS HEATED TO SPECIFIED TEMPERATURE

XPS SPECTRA OF CF_3Cl

SIMILARITIES FOR ALL CFC's

- ORGANIC AND INORGANIC FLUORINE OBSERVED
- SURFACE Cl/F RATIOS SUB-STOICHIOMETRIC

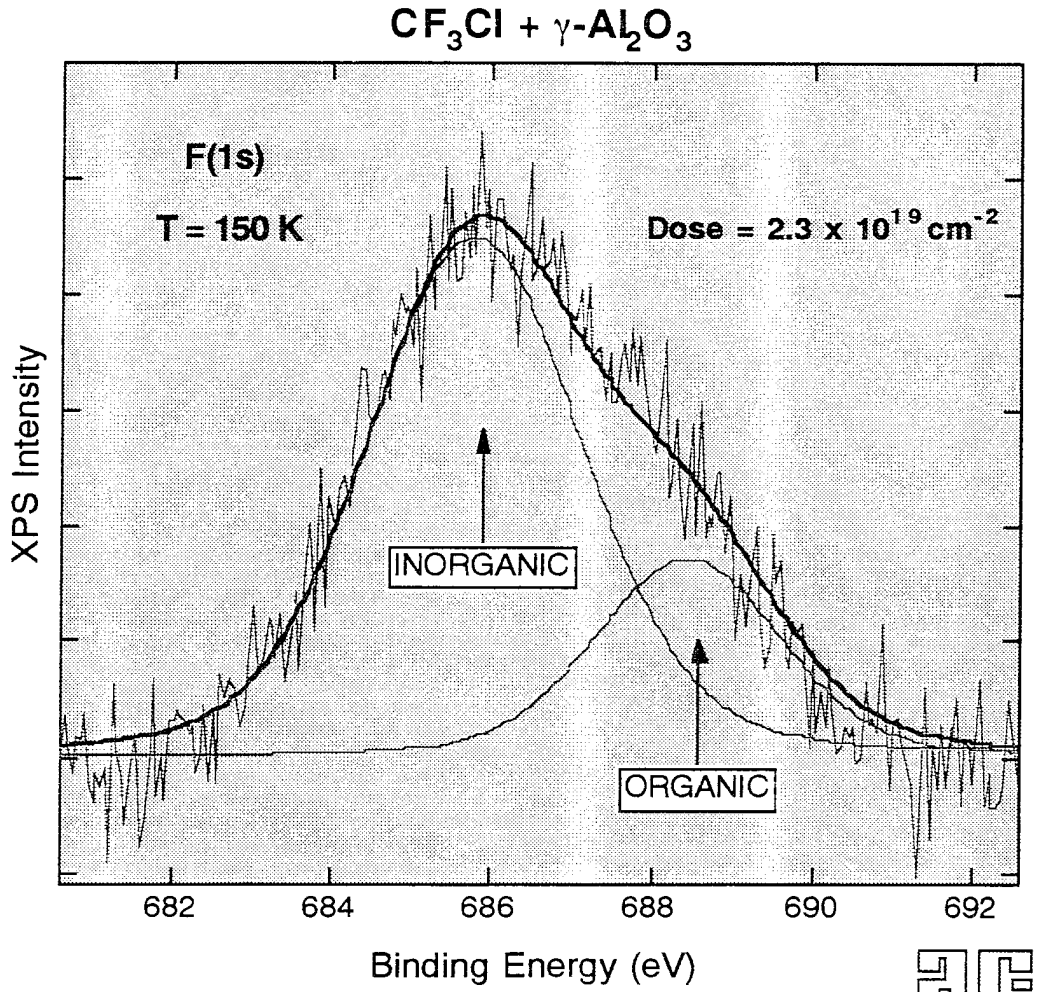

DEHYDROXYLATION OF ALUMINA

- HEATING TO 900K REMOVES WATER AND CONTAMINANTS
- HEATING ALSO REMOVES SURFACE OH GROUPS

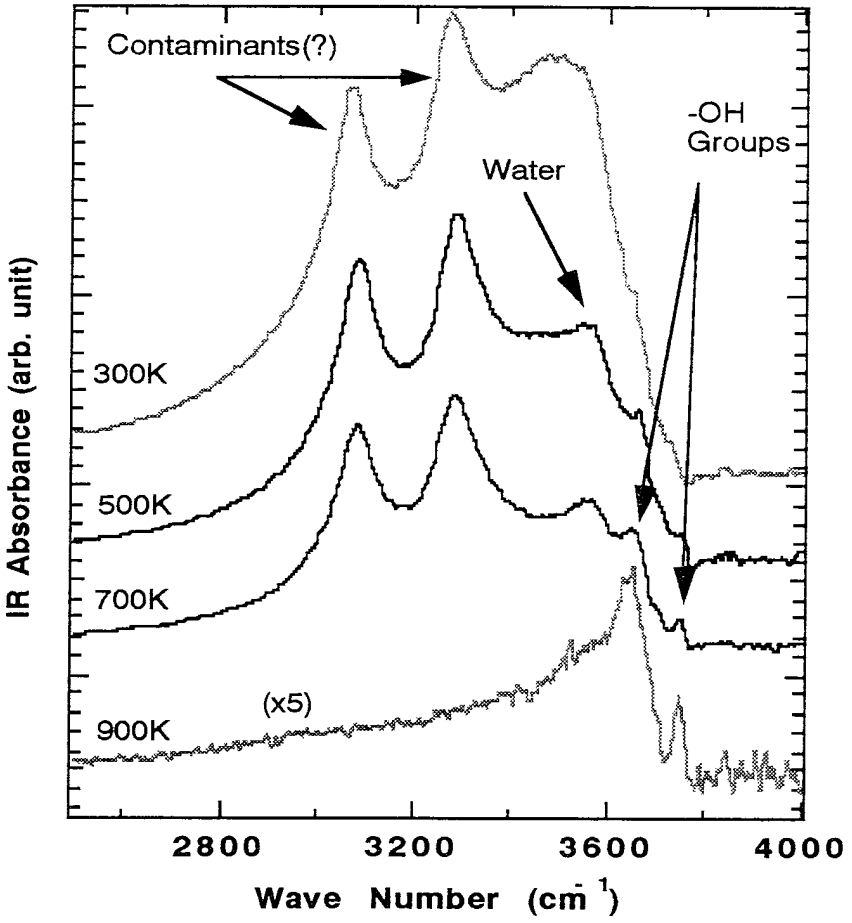

IR SPECTRA OF CCl_4

- SAME SURFACE INTERMEDIATE SPECIES OBSERVED
- SURFACE BI-CARBONATE FORMED AT LOWER TEMPERATURE COMPARED TO CF_2Cl_2

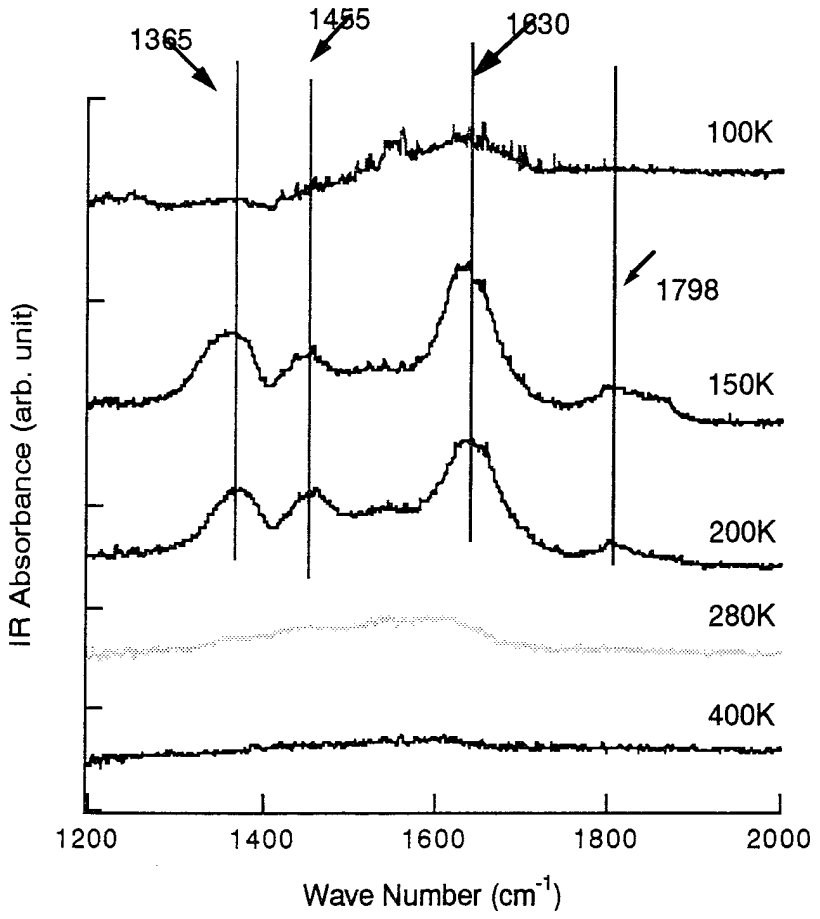

THERMAL DESORPTION SPECTRA OF CF_2Cl_2

- MOST CF_xCl_y FRAGMENTS DESORB BELOW 130K
- AT ELEVATED TEMPERATURES, CO_2 AND HCl DESORB

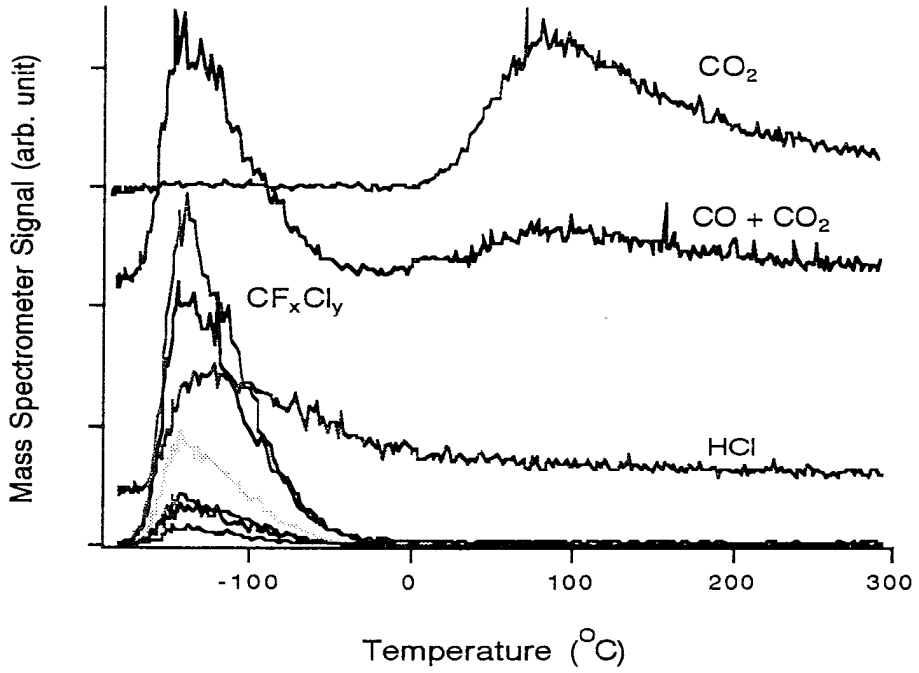

IR SPECTRA OF CF_2Cl_2

- EXPOSURE AT 100K FORMS HALOMETHANE 'ICE'
- CF_2Cl_2 REACTS WITH ALUMINA <180K FORMING SURFACE CARBONATE SPECIES
- SIMILAR CHEMISTRY OBSERVED FOR CF_3Cl, $CFCl_3$ AND CCl_4

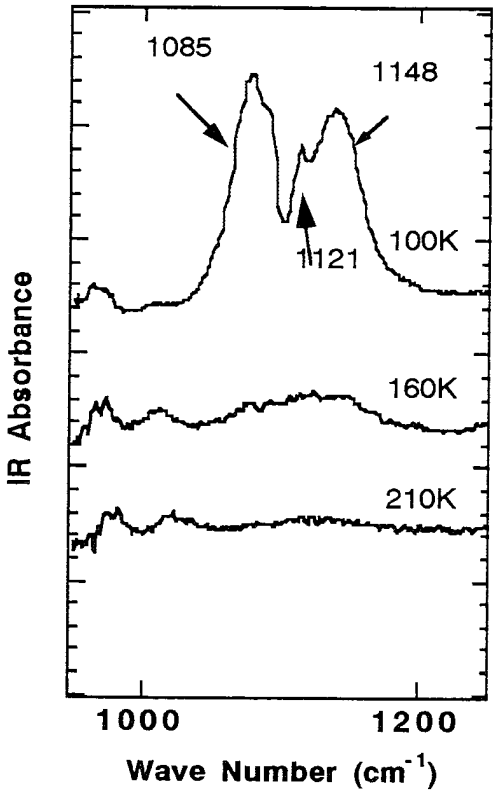

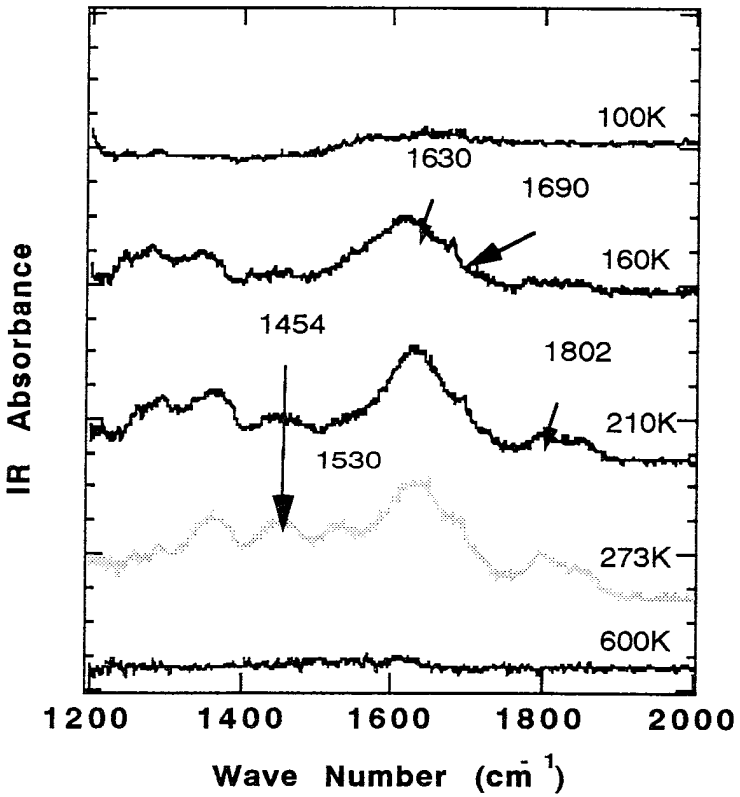

ARE SURFACE SITES POISONED AFTER REACTION?

REPEATED DOSING

CX_3 : ⇑

CO_2 : ⇓

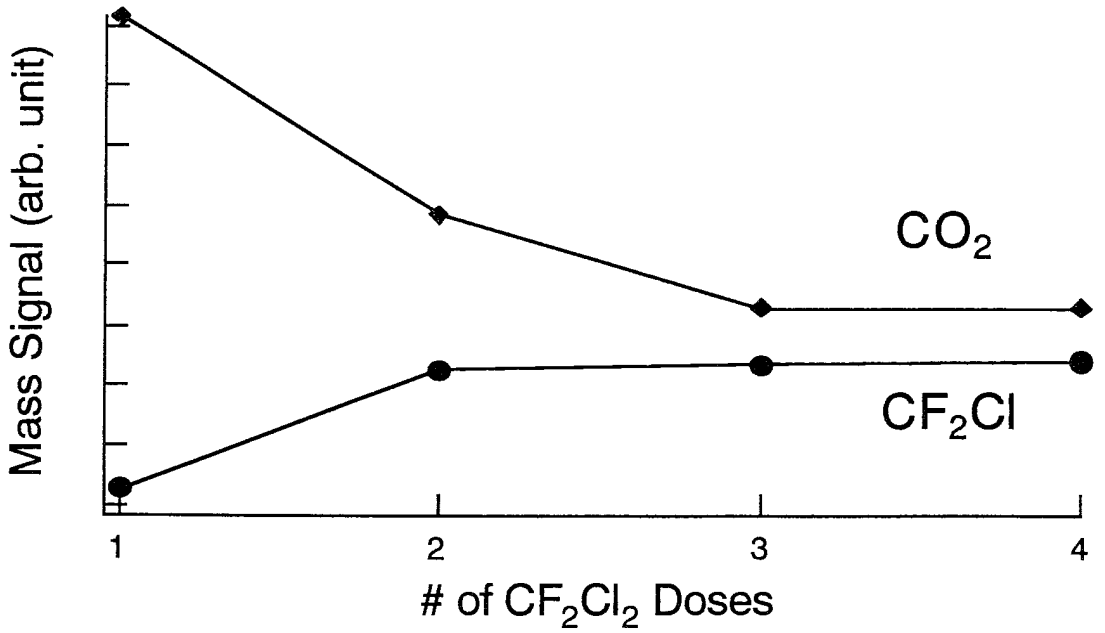

REACTION SITES

Al^{3+} SITES ARE RESPONSIBLE FOR REACTION
NO REACTION WHEN SITES ARE BLOCKED

OH- Covered Surface

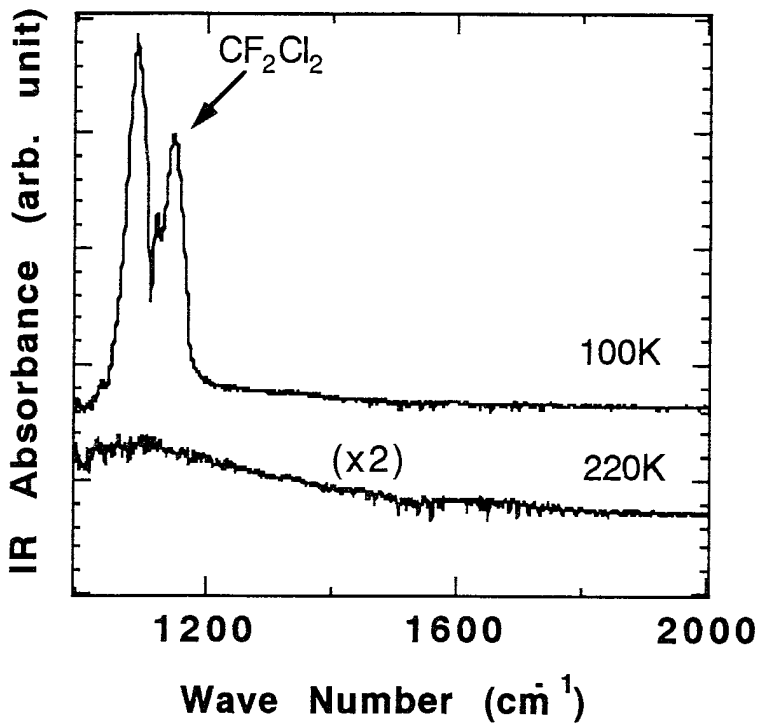

Pyridine- Covered Surface

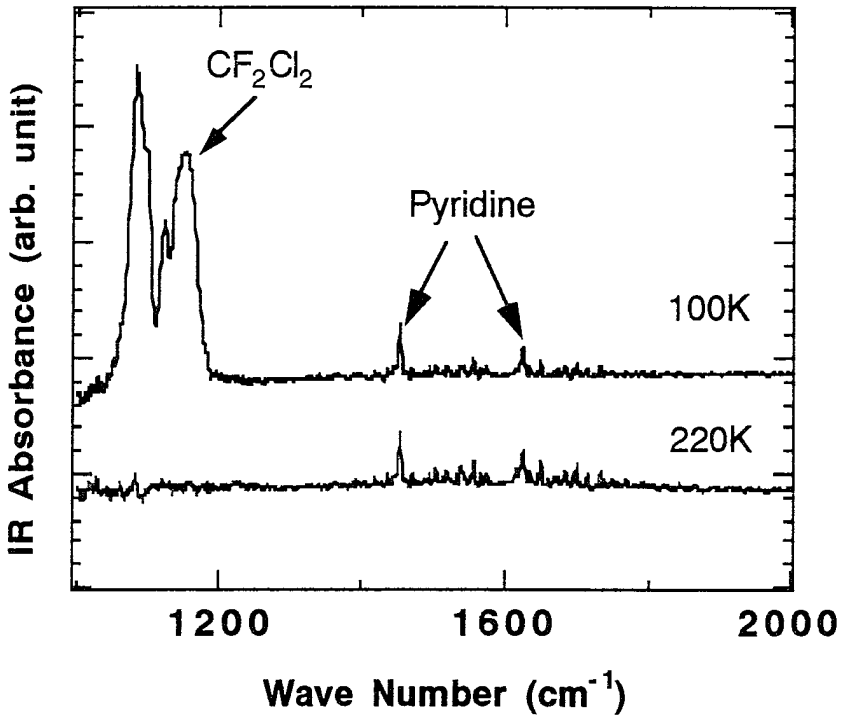

CONCLUSIONS

- HALOMETHANE MOLECULES DISSOCIATIVELY CHEMISORB ON DEHYDROXYLATED γ-ALUMINA BELOW 180 K
- INORGANIC AND ORGANIC HALIDE SURFACE SPECIES OBSERVED IN XPS, SURFACE CARBONATE IN IR
- FORMATION OF Al-X BONDS (X=F,Cl) PROMOTES BOND CLEAVAGE
- AT ELEVATED TEMPERATURES, PRODUCTS INCLUDE HCl, CO_2 AND POSSIBLY CF_XCl_Y FRAGMENTS
- REACTIVITY ORDER:

  $CCl_4 > CFCl_3 > CF_2Cl_2 > CF_3Cl$
- γ-ALUMINA SURFACE REACTIVITY DECREASES FOLLOWING REPEATED GAS EXPOSURE

QUESTIONS

- HOW DOES HCl EXPOSURE AFFECT SURFACE CHEMISTRY?
- DO ALUMINA PARTICLES REACT WITH PERFLUOROCARBONS?
- DO PHOTON-PROMOTED REACTIONS OCCUR?
- ARE THERE POSSIBLE CATALYTIC MECHANISMS?

Vita

Captain Gary E. Lund is from Provo, Utah. He graduated from Brigham Young University in 1991 with a Bachelor of Science degree in Mechanical Engineering. After graduation, Captain Lund was assigned to the 650th Civil Engineering Group at Edwards AFB, California.

During his tour at Edwards AFB, Captain Lund initially worked contract programming issues and later became the Chief of the Readiness Flight where he led Civil Engineering Prime BEEF and Disaster Preparedness. In January of 1993, Captain Lund was assigned as Lead Mechanical Engineer on a project design team deployed to Soto Cano AB, Honduras for 90 days. In January of 1994, Captain Lund was selected to attend the Air Force Institute of Technology.

In June of 1994, Captain Lund entered the Air Force Institute of Technology at Wright-Patterson AFB, Ohio. After completion of the required course work and this thesis, he graduated in December of 1995 with a Master of Science Environmental Engineering Management. He was subsequently assigned to the 18th Civil Engineering Group at Kadena AB, Okinawa, Japan.

REPORT DOCUMENTATION PAGE

Form Approved
OMB No. 0704-0188

1. AGENCY USE ONLY *(Leave blank)*	2. REPORT DATE	3. REPORT TYPE AND DATES COVERED
	December 1995	Master's Thesis

4. TITLE AND SUBTITLE

MODEL OF CHLOROCARBON (CFC-12) CHEMISORPTION ON SOLID ROCKET MOTOR ALUMINA EXHAUST PARTICLES

5. FUNDING NUMBERS

6. AUTHOR(S)

Gary E. Lund, Captain, USAF

7. PERFORMING ORGANIZATION NAME(S) AND ADDRESS(ES)

Air Force Institute of Technology,
WPAFB OH 45433-7765

8. PERFORMING ORGANIZATION REPORT NUMBER

AFIT/GEE/ENP/95D-6

9. SPONSORING / MONITORING AGENCY NAME(S) AND ADDRESS(ES)

10. SPONSORING / MONITORING AGENCY REPORT NUMBER

11. SUPPLEMENTARY NOTES

12a. DISTRIBUTION / AVAILABILITY STATEMENT

Approved for public release; distribution unlimited

12b. DISTRIBUTION CODE

13. ABSTRACT *(Maximum 200 words)*

Solid Rocket Motors (SRMs) that power Titan IV rockets and Space Shuttles, exhaust large quantities of potentially ozone damaging pollutants directly into the stratosphere, while in powered flight. In the past, studies on potential stratospheric impact of the exhaust products from aluminum/ammonium perchlorate based SRMs have focused on the effect of gaseous HCl from SRMs on the stratosphere. Until recently, the impact of heterogeneous chemistry on stratospheric ozone was believed to be relatively insignificant This research investigates the potential heterogeneous process of CFC-12 dissociative chemisorption on alumina surfaces and the release of reactive halogen species known to destroy ozone. Through a PM3 semi-empirical computational study of small alumina surface 'clusters,' dissociative chemisorption and desorption of CFC-12 was investigated. It was determined that CFC-12 does chemisorb but does not dissociate or desorb thermally based on our models. Follow-on work involving larger alumina structures should be investigated.

14. SUBJECT TERMS

Alumina, Solid Rocket Motors, Ozone, Computational Chemistry, PM3

15. NUMBER OF PAGES

140

16. PRICE CODE

17. SECURITY CLASSIFICATION OF REPORT	18. SECURITY CLASSIFICATION OF THIS PAGE	19. SECURITY CLASSIFICATION OF ABSTRACT	20. LIMITATION OF ABSTRACT
Unclassified	Unclassified	Unclassified	UL

GENERAL INSTRUCTIONS FOR COMPLETING SF 298

The Report Documentation Page (RDP) is used in announcing and cataloging reports. It is important that this information be consistent with the rest of the report, particularly the cover and title page. Instructions for filling in each block of the form follow. It is important to ***stay within the lines*** to meet ***optical scanning requirements***.

Block 1. Agency Use Only *(Leave blank)*.

Block 2. Report Date. Full publication date including day, month, and year, if available (e.g. 1 Jan 88). Must cite at least the year.

Block 3. Type of Report and Dates Covered. State whether report is interim, final, etc. If applicable, enter inclusive report dates (e.g. 10 Jun 87 - 30 Jun 88).

Block 4. Title and Subtitle. A title is taken from the part of the report that provides the most meaningful and complete information. When a report is prepared in more than one volume, repeat the primary title, add volume number, and include subtitle for the specific volume. On classified documents enter the title classification in parentheses.

Block 5. Funding Numbers. To include contract and grant numbers; may include program element number(s), project number(s), task number(s), and work unit number(s). Use the following labels:

C	- Contract	**PR**	- Project
G	- Grant	**TA**	- Task
PE	- Program Element	**WU**	- Work Unit Accession No.

Block 6. Author(s). Name(s) of person(s) responsible for writing the report, performing the research, or credited with the content of the report. If editor or compiler, this should follow the name(s).

Block 7. Performing Organization Name(s) and Address(es). Self-explanatory.

Block 8. Performing Organization Report Number. Enter the unique alphanumeric report number(s) assigned by the organization performing the report.

Block 9. Sponsoring/Monitoring Agency Name(s) and Address(es). Self-explanatory.

Block 10. Sponsoring/Monitoring Agency Report Number. *(If known)*

Block 11. Supplementary Notes. Enter information not included elsewhere such as: Prepared in cooperation with...; Trans. of...; To be published in.... When a report is revised, include a statement whether the new report supersedes or supplements the older report.

Block 12a. Distribution/Availability Statement. Denotes public availability or limitations. Cite any availability to the public. Enter additional limitations or special markings in all capitals (e.g. NOFORN, REL, ITAR).

DOD - See DoDD 5230.24, "Distribution Statements on Technical Documents."
DOE - See authorities.
NASA - See Handbook NHB 2200.2.
NTIS - Leave blank.

Block 12b. Distribution Code.

DOD - Leave blank.
DOE - Enter DOE distribution categories from the Standard Distribution for Unclassified Scientific and Technical Reports.
NASA - Leave blank.
NTIS - Leave blank.

Block 13. Abstract. Include a brief *(Maximum 200 words)* factual summary of the most significant information contained in the report.

Block 14. Subject Terms. Keywords or phrases identifying major subjects in the report.

Block 15. Number of Pages. Enter the total number of pages.

Block 16. Price Code. Enter appropriate price code *(NTIS only)*.

Blocks 17. - 19. Security Classifications. Self-explanatory. Enter U.S. Security Classification in accordance with U.S. Security Regulations (i.e., UNCLASSIFIED). If form contains classified information, stamp classification on the top and bottom of the page.

Block 20. Limitation of Abstract. This block must be completed to assign a limitation to the abstract. Enter either UL (unlimited) or SAR (same as report). An entry in this block is necessary if the abstract is to be limited. If blank, the abstract is assumed to be unlimited.